IEA
SOLAR R&D

The Characterization and Testing of Solar Collector Thermal Performance

A report of Task III: Performance Testing of Solar Collectors

April 1993

IEA
INTERNATIONAL ENERGY AGENCY
Solar Heating & Cooling Programme

The Characterization and Testing of Solar Collector Thermal Performance

A Report of TASK III:

Performance Testing of Solar Collectors

April 1993

S.J. Harrison
Solar Calorimetry Laboratory
Queen's University, Kingston, Ontario, Canada

B.A. Rogers
Department of Mechanical Engineering & Energy Studies
University College, Cardiff, U.K.

H. Soltau
Sektion Physik, Ludwig-Maximilians-Universitat
Munchen, Germany

B.D. Wood
Center for Energy Systems Research
Arizona State University, Tempe, Arizona, USA

NOTICE

This report was prepared for the International Energy Agency by the Solar Calorimetry Laboratory, Queen's University at Kingston and sponsored by CANMET, Natural Resources Canada. Neither Queen's University nor CANMET nor the International Energy Agency, nor any of their employees, nor any of their contractors, subcontractors, or their employees makes any warranty, express or implied, or assumes any legal liability or responsibility for the accuracy, completeness or usefulness of any information apparatus, product or process disclosed, or represents that its use would not infringe on privately owned rights.

Distribution Classification: Unrestricted
Additional copies Available from:

Dr. S.J. Harrison,
Solar Calorimetry Laboratory
Queen's University
McLaughlin Hall,
Kingston, Ontario
K7L 3N6
Canada

This report has been compiled as part of the work within the IEA Solar Heating and Cooling Programme,
Task III: Performance Testing of Solar Collectors
Subtask D: Characterization of the Thermal Performance of Solar Collectors
Contributions were provided by the Subtask D participants:

CANADA
Dr. S.J. Harrison
Solar Calorimetry laboratory
Department of Mechanical Engineering
Queen's University
Kingston, Ontario
Canada K7L 3N6

DENMARK
Mr. T. Vest Hansen
Danish Solar Energy Testing Laboratory
Department for Energy Technology
Technological Institute
PO Box 141
DK-2630 Tastrup
Denmark

Mr. P. Vejsig Pedersen
Thermal Insulation Laboratory
Building 118
Technical University of Denmark
DK-2800 Lyngby
Denmark

Mr. J.E. Nielsen
Danish Solar Energy Testing Laboratory
Department for Energy Technology
Technological Institute
PO Box 141
DK-2630 Tastrup
Denmark

GERMANY
Dr. H. Soltau
Sektion Physik
Universität München
Amalienstr. 54
D-8000 München 40
F. R. Germany

Mr. W. Schoelkopf
Sektion Physik, Universität München
Amalienstr. 54/IV
D-8000 München 40
F. R. Germany

ITALY
Mr. F. Aleo
Part. IVA 00611460874
Via G Leopardi 148
95127 Catania
Italy

Dr. F. Vivona, Consiglio Nazionale Ricerche
Progetto Finalizzato Energetica
Via Nizza 128
00198 Roma
Italy

THE NETHERLANDS
Ir E.M. Keizer-Boogh
Institute of Applied Physics, TNO-TH
PO Box 155
2600 AD Delft
The Netherlands

Ir J. Havinga
Institute of Applied Physics, TNO-TH
PO Box 155
2600 AD Delft
The Netherlands

Ir A.C. de Geus
Institute of Applied Physics, TNO-TH
PO Box 155
2600 AD Delft
The Netherlands

SPAIN
Dr. Ing. E. Mezquida
Departamento de Motopropulsion y Energia
Instituto Nacional de Tecnica Aeroespacial
Torrejon de Ardoz
Madrid
Spain

Dr. Ing. A Gozalez Garcia-Conde
Departamento de Motopropulsion y Energia
Instituto Nacional de Tecnica Aeroespacial
Torrejon de Ardoz
Madrid, Spain

SWEDEN
Mr. B.O. Perers
Energy Technology Division
Studsvik Energy
S-611 82 Nykoping
Sweden

Dr. H.E.B. Andersson
Swedish Council for Building Research
Sankt Goransgatan 66
S-112 33 Stockholm
Sweden

Mr. H. Walletun
Energy Technology Division
Studsvik Energy
S-611 82 Nykoping
Sweden

SWITZERLAND
Dr. J. Keller
Paul Scherrer Institute
Wurenlingen and Villigen
CH-5232 Villigen PSI
Switzerland

Dr. J.M. Suter
Paul Scherrer Institute
Wurenlingen and Villigen
CH-5232 Villigen PSI
Switzerland

Dr. Nguyen Dinh Lan
Swiss Institute of Technology, Lausanne
Laboratoire de Thermodynamique
CH-1015 Lausanne
Switzerland

UK
Dr. B.A. Rogers
Department of Mechanical & Energy Studies
University College
Newport Road
Cardiff
UK CF2 1T

Dr. B.J. Brinkworth
Department of Mechanical & Energy Studies
University College
Newport Road
Cardiff
UK CF2 1T

USA
Dr. B.D. Wood
Center for Energy Systems Research
College of Engineering & Applied Sciences
Arizona State University
Tempe Arizona 85287
USA

EUROPEAN COMMISSION
Dr. E. Aranovitch
Joint Research Centre, Euratom
I-21020 Ispra
Italy

Dr. G. Riesch
Joint Research Centre, Euratom
I-21020 Ispra
Italy

Mr. D. Gilliaert
Joint Research Centre, Euratom
I-21020 Ispra
Italy

Introduction to the International Energy Agency
Solar Heating And Cooling Programme

International Energy Agency

The International Energy Agency, headquartered in Paris, was formed in November 1974 as an autonomous body within the framework of the Organization for Economic Cooperation and Development to establish cooperation in the area of energy policy. Twenty-one countries are presently members, with the Commission of the European Communities participating under a special arrangement.

Collaboration in the research, development and demonstration of new energy technologies to help reduce dependence on oil and to increase long-term energy security has been an important part of the Agency's programme. The IEA R&D activities are headed by the Committee on Research and Development (CRD) which is supported by a small Secretariat staff. In addition, four Working Parties (in Conservation, Fossil Fuels, Renewable Energy and Fusion) are charged with monitoring the various collaborative energy Agreements, identifying new areas for cooperation and advising the CRD on policy matters.

Solar Heating and Cooling Programme

One of the first collaborative R&D agreements was the IEA Solar Heating and Cooling Programme which was initiated in 1977 to conduct joint projects in active and passive solar technologies, primarily for building applications. The eighteen members of the Programme are:

Australia
Austria
Belgium
Canada
Denmark
European Community
France (observer)
Finland
Germany
Italy
Japan
The Netherlands
New Zealand
Norway
Spain
Sweden
Switzerland
United Kingdom
United States

A total of eighteen projects or "Tasks" have been undertaken since the beginning of the Programme. The overall programme is managed by an Executive Committee composed of one representative from each of the member countries, while the leadership and management of the individual Tasks is the responsibility of Operating Agents. These Tasks and their respective Operating Agents are:

IEA Tasks

*Task 1:	Investigation of the Performance of Solar Heating and Cooling Systems - Denmark
*Task 2:	Coordination of Research and Development on Solar Heating and Cooling - Japan
*Task 3:	Performance Testing of Solar Collectors - United Kingdom
*Task 4:	Development of an Insulation Handbook and Instrument Package - United States
*Task 5:	Use of Existing Meteorological Information for Solar Energy Application - Sweden
*Task 6:	Solar Heating, Cooling and Hot Water Systems Using Evacuated Collectors -United States
*Task 7:	Central Solar Heating Plants with Seasonal Storage - Sweden
*Task 8:	Passive and Hybrid Solar Low Energy Buildings - United States
*Task 9:	Solar Radiation and Pyranometry Studies - Federal Republic of Germany
*Task 10:	Material Research and Testing - Japan
*Task 11:	Passive and Hybrid Solar Commercial Buildings - Switzerland
Task 12:	Building Energy Analysis and Design Tools for Solar Applications - United States
Task 13:	Advanced Solar Low Energy Buildings - Norway
Task 14:	Advanced Active Solar Systems - Canada
Task 15:	Advanced Central Solar Heating Plants (In Planning Stage)
Task 16:	Photovoltaics in Buildings - Germany
Task 17:	Measuring and Modeling Spectral Radiation - Germany
Task 18:	Advanced Glazing Materials - United Kingdom

*Completed Task

Task III

Performance Testing of Solar Collectors

The overall goal of Task III was by international cooperation to develop and validate common test procedures for rating the performance of solar thermal collectors and solar domestic hot water heating systems.

Task III was initiated in 1977 with three subtasks:

Subtask A: Standard Test Procedures to Determine Thermal Performance
Subtask B: Development of Reliability and Durability Test Procedures
Subtask D: Investigation of the Potential of Solar Simulators

Upon the completion of these subtasks at the end of 1982, the Executive Committee approved an extension of the Task with the following three subtasks:

Subtask D: Characterization of the Thermal Performance of Solar Collectors.
Subtask E: Development of a Capability to Evaluate Domestic Hot Water System Performance using Short-Term Test Methods.

Subtask F: Development of a Basis for Identifying the Performance Requirements and for Predicting the Service Life of Solar Collector System Components.

At the end of 1985 a further extension was approved, with a completion date at the end of 1987.

Participants in Task III (those marked * until the end of 1985 only) were:

Australia*, Austria*, Belgium*, Canada, Denmark, F.R. Germany, Italy, Japan*, the Netherlands, Spain, Sweden, Switzerland, United Kingdom, United States and the Commission of the European Communities.

During the period from 1977-83 Germany (KFA Julich) acted as the Operating Agent and from 1983-1987 the U.K. (University College - Cardiff) acted as Operating Agent.

Executive Summary

This report documents the work of IEA Task III participants completed in support of Subtask D: The Characterization of the Thermal Performance of Solar Collectors. IEA work conducted towards the establishment of standardized test methods for solar collectors was initiated in 1977 under Subtask A. As a result of this early collaboration within Task III and other international programmes, a large measure of agreement was reached about the standard of instrumentation and laboratory practice necessary to achieve reliable test data.

For conventional, glazed flat-plate collectors, standard thermal-performance test methods were established and produced results that were repeatable and comparable within accepted experimental tolerances. However, these test procedures were found to have two significant limitations: 1) they were not adequate for many new collector designs that did not respond with the same sensitivities to environmental conditions as traditional flat-plate solar collectors, and 2) they often produced a "snap shot" of performance derived under standard test conditions rather than a characterization of how the collector will perform under a range of meteorological conditions.

Many new products were sensitive to factors not evaluated in previous test standards and consequently test results derived according to these requirements did not adequately predict their performance over the full range of environmental conditions. As a result of these limitations, the focus of attention among Task participants was directed toward the development of thermal performance test procedures for the wider range of collector types, including unglazed collectors, evacuated-tube, heat-pipe and boiling/condensing collectors, and low- or medium-power concentrators.

This report summarizes the progress that was made by the Task participants in developing characterization equations and test methods for a variety of collector types. In particular, it shows how a simple generic model can be used to describe a variety of collector types (including conventional flat-plate collectors) operating over a wider range of conditions than is normally covered in standard tests. For each of these collector types, simple models were developed to describe the sensitivities of the thermal performance to operating conditions. Among the variables treated were irradiance levels, thermal radiation, and ambient and fluid temperatures. For unglazed solar collectors, the effects of wind-induced convection losses were also considered.

The models developed are all simple generalizations of the Hottel-Whillier-Bliss equation for flat-plate collectors with extra terms included to describe the additional effects. These models form the basis both for performance testing and for predicting collector performance in operation. In classifying the sensitivities of solar collectors to environmental factors, different solar collector types were seen to be dependent on differing factors. For example, the performance of concentrating collectors and evacuated tube type collectors was significantly affected by optical factors related to the incident angle and nature of the solar flux (e.g. diffuse fraction). Other collector types such as conventional flat-plates were strongly dependent on the top heat loss coefficient which was dependent on the ambient environmental conditions.

Throughout the Task's duration, a major goal was the identification of a generalized performance representation that would accommodate virtually all classes of solar collectors and to identify test sequences that may be used to quantify these dependencies. To arrive at the form of an equation that will adequately predict the performance of a variety of collector types operating under a range of environmental conditions, an analysis of the heat loss mechanisms in various solar collectors was conducted to identify significant dependencies and characterize their effects.

The selection of a suitable performance characteristic for a particular solar collector type must be a compromise between testing complexity, time, and cost relative to the accuracy required. The selection of suitable conditions for conducting a characterizing test for a particular collector depends to a large degree on the range of environmental conditions anticipated during normal use of the collector and should be determined by the location of use and the climatic conditions.

As a result of this work, recommendations for the testing of a variety of glazed solar collectors are presented and a test procedure for unglazed liquid based collectors is outlined. It is shown that generic models can account for a number of these effects and that conventional collector testing can be extended to a wider range of collectors and test conditions. The performance of collectors operating in different localities and under different weather conditions can be predicted more accurately.

TABLE OF CONTENTS

Subtask D participants i
Introduction to the International Energy Agency Solar Heating and Cooling Programme iii
IEA Tasks iv
Task III: Performance Testing of Solar Collectors v
Executive Summary vii
Table of Contents ix
Nomenclature xi

Chapter 1 **Introduction** 1

1.1 Thermal Performance Testing 1
1.2 Basic Thermal Models of Solar Collectors 2
1.3 References 10

Chapter 2 **Review of Test Methods and Procedures** 13

2.1 Survey of Thermal Performance Test Standards 13
2.2 Problems Related to Thermal Performance Testing 18
2.3 References 21

Chapter 3 **The Effects of Atmospheric Factors on Collector Heat Loss** 23

3.1 Theory 23
3.2 Collector Heat Losses 24
3.3 The Effects of Atmospheric Factors on Heat Loss 28
3.4 Wind Effects 31
3.5 Sky Temperature Effects 33
3.6 References 34

Chapter 4 **Unglazed Collectors** 37

4.1 Introduction 37
4.2 Review of Recent Work 38
4.3 Characterization Equations 42
4.4 Validation of Proposed Test Method 47
4.5 References 48

Chapter 5 **Evacuated-tubular, Heat-pipe and Boiling/condensing Collectors** 51

5.1 Evacuated Tube Collectors 51
5.2 Evacuated Tube With Heat-pipe 55
5.3 Boiling/Condensing Flat Plate Solar Collectors 59
5.4 References 64

Chapter 6 **Low-concentration Concentrating Collectors** 67

6.1 Characterizing Equations 67
6.2 Recommendations for Thermal Performance Testing 68
6.3 Example Test Results 69
6.4 References 69

Chapter 7 **Generalized Model of Solar Collector Thermal Performance** 71

7.1 Introduction 71
7.2 Glazed Solar Collectors 72
7.3 Collector Models for Glazed Solar Collectors 76
7.4 Generalized Characterization Equation for Glazed Solar Collectors 79
7.5 Unglazed Collectors 80

7.6 Low-concentration Ratio Concentrating Collectors 82
7.7 Selection of Test Conditions 82
7.8 References 82

Appendix A **A Recommended Test Procedure for Determining the Thermal Performance of Unglazed Flat-Plate Liquid-Type Solar collectors** 83
1.0 Introduction 83
2.0 Scope 83
3.0 Thermal-performance Model 84
4.0 Instrumentation and Measurement 86
5.0 Test Conditions 87
6.0 Analysis of Data 89
7.0 Representation of the Test Results 89
8.0 References 90

Appendix B **Recommendations for the Testing of Glazed Solar Collectors** 91
1.0 Introduction 91
2.0 Generalized Characterization Equation for Glazed Solar Collectors 91
3.0 Test conditions 92
4.0 References 93

NOMENCLATURE

a	thermal diffusivity, (m^2/s)
a_1, a_2	experimentally derived performance coefficients, eq. 4.37, (dimensionless)
A	coefficient used in characterization equations, (dimensionless)
A_a	collector aperture area, (m^2)
A_c	collector cover area, (m^2)
A_{ab}	absorber plate surface area, (m^2)
A_g	collector gross area, (m^2)
A_r	collector receiver area, (m^2)
A_R	collector reference area, (m^2)
A_{top}	collector top surface area, (m^2)
b_o	slope of the correlating straight line, (dimensionless)
b_1, b_2	experimentally derived performance coefficients, eq. 4.37, (dimensionless)
B	coefficient used in characterization equations, (dimensionless)
C_p	specific heat capacity of heat transfer fluid, (J/(Kg • K))
C_{pa}	specific heat capacity of absorber, (J/(Kg • K))
C	coefficient used in characterization equations, (dimensionless)
d	thickness of back insulation, (m)
D	coefficient used in characterization equations, (dimensionless)
E	coefficient used in characterization equations, (dimensionless)
e	partial water-vapour pressure, (Pa)
F'	collector efficiency factor, (dimensionless)
F''	collector flow factor, (dimensionless)
F_g	ground shape factor in collector field of view, (dimensionless)
F_R	collector heat removal factor, (dimensionless)
F_s	sky shape factor in collector field of view, (dimensionless)
G_{dn}	effective normal solar irradiance on collector aperture, (W/m^2)
$G^{\#}$	threshold irradiance for boiling/condensing collectors, (W/m^2)
G_b	direct solar irradiance in plane of collector, (W/m^2)
G_{bt}	beam irradiance in the plane of the collector aperture, (W/m^2)
G_c	critical radiation level, (W/m^2)
G_{dt}	diffuse solar irradiance in plane of collector, (W/m^2)
G_{gt}	solar radiation reflected from the ground, (W/m^2)
G_T	rate of incident solar radiation on the solar collector per unit area, (W/m^2)
$h_{c,b\text{-}a}$	convection heat-transfer coefficient from absorber back surface to ambient air, ($W/(m^2 • K)$)
$h_{c,m\text{-}p}$	convective heat transfer coefficient from fluid to the absorber plate, ($W/(m^2 • K)$)
$h_{c,p\text{-}a}$	convection heat transfer coefficient from absorber to ambient air, ($W/(m^2 • K)$)
$h_{c,p\text{-}c}$	convection heat-transfer coefficient from absorber plate to cover, ($W/(m^2 • K)$)
$h_{r,b\text{-}a}$	radiant heat-transfer coefficient from absorber back surface to the ambient, ($W/(m^2 • K)$)
$h_{r,c\text{-}s}$	radiant heat-transfer coefficient from cover to sky, ($W/(m^2 • K)$)
$h_{r,p\text{-}a}$	radiant heat-transfer coefficient from absorber plate to ambient air, ($W/(m^2 • K)$)
$h_{r,p\text{-}c}$	radiant heat-transfer coefficient from absorber plate to cover, ($W/(m^2 • K)$)
$h_{r,p\text{-}e}$	radiant heat-transfer coefficient from absorber plate to the surrounding environment, ($W/(m^2 • K)$)

$h_{r,p-s}$	radiant heat-transfer coefficient from absorber plate to sky, (W/(m^2 • K))
h_{top}	heat loss coefficient from top of collector, (W/(m^2 • K))
h_w	wind induced heat transfer coefficient, (W/(m^2 • K))
$h_{w,c-a}$	wind induced heat transfer coefficient from cover to ambient air, (W/(m^2 • K))
k	thermal conductivity, (W/(m • K))
k_a	thermal conductivity of air, (W/(m • K))
K_1	constant used in equation 2.6 (dimensionless)
K_2	constant used in equation 2.6 (dimensionless)
K_b	incidence angle modifier for beam irradiance, (dimensionless)
$K_{\alpha\tau}$	incidence-angle modifier, (dimensionless)
K_d	diffuse-irradiance incidence-angle modifier, (dimensionless)
L	L_p+L_b (for a collector with $\varepsilon_b = \varepsilon_p$), (W/m^2)
L_b	net thermal irradiance on back of collector as measured by a radiometer at the ambient temperature, (W/m^2)
L_c	characteristic length for convective heat losses, (m)
L_p	net thermal irradiance in plane of collector as measured by a radiometer at the ambient temperature, (W/m^2)
L_{p-c}	distance between absorber plate and cover in a flat-plate solar collector, (m)
$\dot{m}$	mass flowrate, (kg/s)
Nu	Nusselt number, (dimensionless)
q_{c-a}	heat loss from cover to ambient air, (W/m^2)
q_{c-s}	heat loss from cover to sky, (W/m^2)
q_{p-c}	heat transfer from the absorber plate to the cover, (W)
$q_{rad,p-s}$	heat transfer by radiative exchange between the absorber plate and the sky, (W)
$\dot{q}_u$	useful output power per unit reference area, (W/m^2)
Q_L	overall rate of heat loss, (W)
Q_S	rate of absorption of solar energy, (W)
Q_U	useful output power, (W)
S	rate of absorption of solar energy per unit absorber area, (W/m^2)
T_a	ambient air temperature, (K)
T_{bm}	mean absorber back surface temperature, (K)
T_{boil}	temperature at onset of boiling in boiling condensing collectors, (K)
T_c	mean collector cover temperature, (K)
T_d	dew point temperature, (K)
T_e	effective field-of-view temperature including the sky and ground, (K)
T_{fe}	exit temperature of the fluid, (K or ^{o}C)
T_{fi}	inlet temperature of the fluid, (K or ^{o}C)
T_{fm}	average temperature of fluid in the collector, i.e. arithmetic mean of inlet and outlet temperature, (K)
T_{fo}	outlet temperature of the fluid, (K or ^{o}C)
T_g	effective background temperature, (K)
Tm	mean temperature of absorber and surrounding air temperature, (K)
T_p	absorber-plate temperature, (K)
T_{pm}	mean absorber-plate temperature, (K)
T_s	effective sky temperature, (K)
T_{sat}	saturation temperature, (K)

T_v	effective field-of-view temperature, (K)
u	air speed, (m/s)
$U_{c\text{-}a}$	heat loss coefficient from cover to ambient air, (W/(m^2 • K))
U_{back}	heat loss coefficient from back of collector, (W/(m^2 • K))
U_L	collector overall heat-loss coefficient, (W/(m^2 • K))
$U_{p\text{-}c}$	heat loss coefficient from absorber-plate to cover, (W/(m^2 • K))
U_{top}	top loss coefficient, (W/(m^2 • K))
V_w	wind velocity, (m/s)
α	solar absorptance, (dimensionless)
γ	fraction of specularly reflected radiation from the reflector or refracted radiation which is intercepted by the solar collector receiving area, (dimensionless)
ΔT	$T_{fi} - T_a$ {or $T_{fm}-T_a$, or $T_{pm}-T_a$}, (K)
ΔT_{ex}	excess temperature, (K)
ε_c	thermal emittance of cover, (dimensionless)
ε_b	thermal emittance of absorber back, (dimensionless)
ε_{bg}	$1/[(1/\varepsilon_b)+(1/\varepsilon_g)-1]$, (dimensionless)
ε_g	thermal emittance of ground, (dimensionless)
ε_p	thermal emittance of absorber plate, (dimensionless)
η	collector efficiency, (dimensionless)
θ	angle of incidence, (° from normal)
ρ	solar reflectance, (dimensionless)
σ	Stefan-Boltzmann constant, (W/(m^2 • K^4))
τ	transmittance of cover, (dimensionless)
τ_{LW}	transmittance of the cover to long-wave radiation, (dimensionless)
$(\tau\alpha)_{b,\theta}$	effective transmittance-absorptance product for the beam solar radiation, (dimensionless)
$(\tau\alpha)_d$	effective transmittance-absorptance product for diffuse irradiance (dimensionless)
$(\tau\alpha)_e$	effective transmittance-absorptance product, (dimensionless)
$(\tau\alpha)_{e,n}$	effective transmittance-absorptance product for normal incidence, (dimensionless)
$\Gamma, \psi, \varphi, \Omega$	angles in Figure 10, (°)

[NOTE: Because certain equations for radiative heat exchange are only valid for thermodynamic temperatures, the unit of temperature specified in the above list is the Kelvin (K). However, all the equations in this document that do not contain the Stefan-Boltzmann constant σ are equally valid with temperatures expressed in degrees Celsius (° C).]

Chapter 1

Introduction

1.1 Thermal Performance Testing

Test methods for determining the thermal performance of solar collectors are intended to provide objective information that can help 1) manufacturers to optimize the design of collectors, 2) designers of solar heating systems to select components and to optimize system performance for a particular application, and 3) consumers to compare the performance and cost-effectiveness of competing products.

To investigate the suitability of proposed test methods, IEA Task III participants undertook a number of round robin test programs involving flat-plate and vacuum tube collectors [1,2]. As a result of the collaboration within Task III and other international programmes, a large measure of agreement was reached about the standard of instrumentation and laboratory practice necessary to achieve reliable test data. For conventional, glazed flat-plate collectors, standard thermal-performance test methods have been established in many of the countries participating in the IEA Solar Heating and Cooling Programme and in general, these test procedures produce results which are repeatable and comparable within accepted experimental tolerances.

1.1.1 The Need for Improved Testing Methods

These test procedures were found to have two significant limitations: 1) they are not adequate for many new collector designs which do not respond with the same sensitivities to environmental conditions as traditional flat-plate solar collectors, and 2) they often produce a "snap shot" of performance derived under standard test conditions rather than a characterization of how the collector will perform under a range of meteorological conditions. Many factors considered of "second order" effect are significant and must be accounted for if accurate predictions of performance are to be established or reliable comparisons or ratings of products made.

As a result of these limitations, a focus of attention among Task participants in recent years has been the development of thermal performance test procedures for the wider range of collector types, including unglazed collectors, evacuated-tube, heat-pipe and boiling/condensing collectors, and low- or medium-power concentrators.

1.1.2 The Scope of This Report

The thermal performance of solar collectors may be determined by an analysis of the optical and thermal properties of the solar collector components or by analysis and thermal performance testing of the complete collector under controlled conditions.

In practice, due to uncertainties in the material properties, construction details and heat transfer modeling, testing of complete collectors according to standardized procedures is usually undertaken. Values of collector thermal performance are measured experimentally under specified and controlled conditions and the performance coefficients for a specified characterizing equation determined by "least-squares" regression of the experimental data.

These performance coefficients, along with the general characterizing equation, can then be used to predict the performance of that collector type under typical operating conditions.

This report summarizes the progress that was made by the Task participants in developing characterization equations and test methods for a variety of collector types. In particular it shows how a simple generic model can be used to describe a variety of collector types (including conventional flat-plate collectors) operating over a wider range of conditions than is normally covered in standard tests. Recommendations for new or improved test procedures are included in this report.

1.2 Basic Thermal Models of Solar Collectors

The theoretical basis of thermal performance testing is provided by a general model of the thermal processes governing solar collector operation. Fundamental thermal models of solar collectors are based on the analysis provided by Hottel, Whillier, and Bliss (HWB) [3,4]. This representation is a simplified model of the thermal performance and a number of parameters are not taken into account. These factors are often thought to represent only second-order effects.

The following sections give a brief summary of standard thermal models for solar collectors. Their primary purpose is to introduce the notation and terminology which is used in the report, and the assumptions upon which the previous test methods are based. Further details of the models can be obtained from texts such as that by Duffie and Beckman [5].

1.2.1 Energy Balance for Flat-plate Solar Collectors

A typical flat-plate solar collector consists of an insulated box with a transparent cover, Figure 1. Heat is removed from an internal absorber surface by a heat transfer medium, (e.g. air, water, or glycol etc.), which is circulated through flow channels.

Figure 1 Typical flat-plate solar collector.

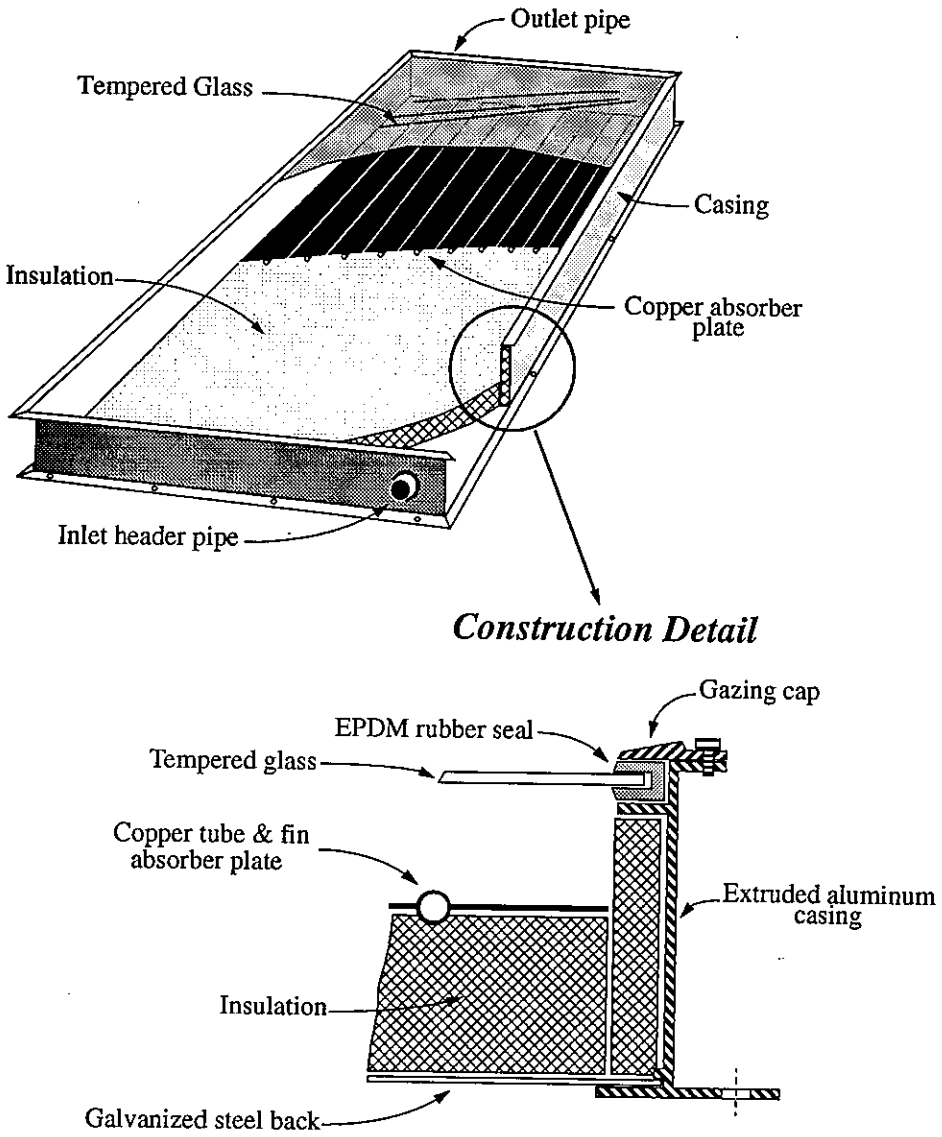

The rate of extraction of solar energy by the heat transfer fluid circulating through a solar collector, Q_U, may be described in terms of the rate of solar energy absorption, S; the rate of energy storage in the collector, Q_S; and the thermal losses from the collector enclosure to the surroundings, Q_L, i.e.

$$Q_U = S - Q_L - Q_S \tag{1.1}$$

Each of the terms in this simple heat balance is influenced by complex heat transfer mechanisms including conduction, convection, and radiation heat transfer. Detailed heat transfer models have been developed in the past to describe both the transient and steady-state performance of various solar collector types, (see Chapter 3).

However, it is generally accepted that transient effects tend to be small and that over the course of a day their net effect is negligible [5]. Consequently, for the purpose of design and rating purposes, solar collector models have been developed based on steady-state performance where Q_S is effectively considered to be zero.

1.2.2 The Hottel, Whillier, Bliss Model of Performance

The Hottel, Whillier, Bliss model of performance is a simplified representation of thermal performance and a number of parameters are not taken into account. These factors are often thought to represent only second-order effects.

The theoretical performance of flat-plate solar collectors is described for steady-state conditions, where the rate of energy extracted from the collector per unit of collector area, Q_U/A_a, is equal to the rate of radiative energy absorbed, minus the rate of heat loss to the surroundings, (i.e., Q_S=0):

$$Q_U/A_a = G_T(\tau\alpha)_e - U_L(T_p-T_a) \tag{1.2}$$

where

G_T = rate of incident solar radiation on the solar collector per unit area, W/m^2,
$(\tau\alpha)_e$ = effective transmittance-absorptance product of the cover and absorber plate,
A_a = aperture area of the solar collector, m^2,
Q_U = rate of energy extraction from the collector by the heat transfer fluid, W,
U_L = heat loss coefficient for the collector, W/m^2 K,
T_p = average temperature of the collector absorber surface, ^{o}C,
T_a = ambient air temperature,^{o}C.

1.2.2.1 Collector Efficiency Factors

For the purpose of system design, it is convenient to relate the performance of the solar collectors to the temperature of the heat transfer fluid, as the plate temperature is usually not known. Bliss [4] derived two collector efficiency factors, F' and F_R, to allow the use of either the mean or inlet fluid temperature in the collector equation, i.e.

$$Q_U/A_a = F'[G_T(\tau\alpha)_e - U_L(T_{fm}-T_a)] \tag{1.3}$$

$$Q_U/A_a = F_R[G_T(\tau\alpha)_e - U_L(T_{fi}-T_a)] \tag{1.4}$$

where

F' = collector efficiency factor,
F_R = collector heat removal factor,
T_{fm} = average temperature of fluid in the collector, ^{o}C (i.e. mean of inlet and outlet temperature),
T_{fi} = temperature of the fluid at the inlet to the collector, ^{o}C.

The heat removal factor accounts for the fact that the fluid entering the collector is heated in the direction of flow and consequently is not all at the same temperature as the inlet fluid. It is derived according to [4] as

$$F_R = F'F'' \tag{1.5}$$

F'' the collector flow factor, is given by Duffie and Beckman [5]

$$F'' = \left[\frac{\dot{m} \cdot C_p}{A_a U_L F'}\right]\left[1 - e^{-(A_a U_L F') / (\dot{m} \cdot C_p)}\right] \tag{1.6}$$

where $(\dot{m} \cdot C_P) / (A_a U_L F')$ is the dimensionless collector capacitance rate and

$\dot{m}$ = mass flow rate of the heat transfer fluid, kg/s,
C_P = specific heat of the heat transfer fluid, J/(kg K).

A typical plot of F_R versus collector flow rate is given in Figure 2. The collector efficiency factor, F', is a function of the physical dimensions and construction details of the absorber plate and accounts for the fact that the surface of the absorber plate may not all be at the local fluid temperature of the heat transfer fluid. It represents the ratio of the actual useful energy gain to the useful energy gain that would result if the collector absorber surface had all been at the local fluid temperature [4].

Figure 2 Effect of collector flow rate on F_R for a typical flat-plate solar collector.

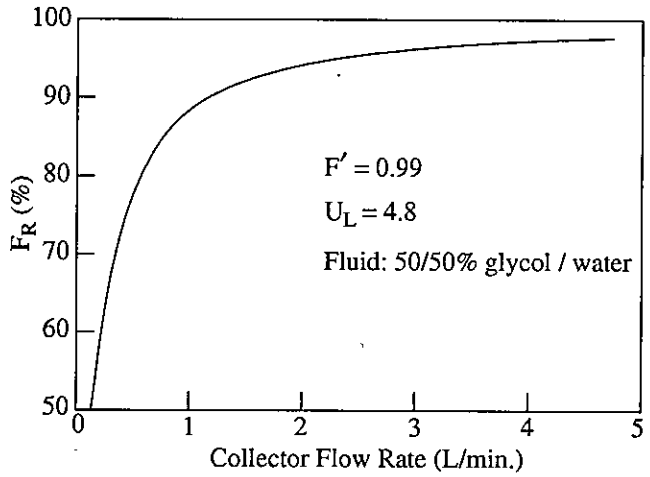

1.2.3 Collector Efficiency

The ratio of collected useful energy to solar energy incident on the collector is the collection efficiency, η,

$$\eta = \frac{Q_U}{G_T \cdot A_a} = F_R(\tau\alpha)_e - F_R U_L\left(\frac{T_{fi} - T_a}{G_T}\right) \tag{1.7}$$

or in terms of mean fluid temperature

$$\eta = \frac{Q_U}{G_T \cdot A_a} = F'(\tau\alpha)_e - F'U_L\left(\frac{T_{fm} - T_a}{G_T}\right) \tag{1.8}$$

If values of η are plotted versus corresponding values of $(T_{fm}-T_a)/G_T$ {or $(T_{fi}-T_a)/G_T$} a straight line with an intercept $F'(\tau\alpha)_e$ {or $F_R(\tau\alpha)_e$} and slope $F'U_L$ {or F_RU_L} will result, Figure 3. The values of $F'(\tau\alpha)_e$ and $F'U_L$ are indicative of the optical efficiency and the heat loss from the collector, respectively.

Figure 3 The Hottel-Whillier-Bliss representation of solar collector performance, based on T_{fi}.

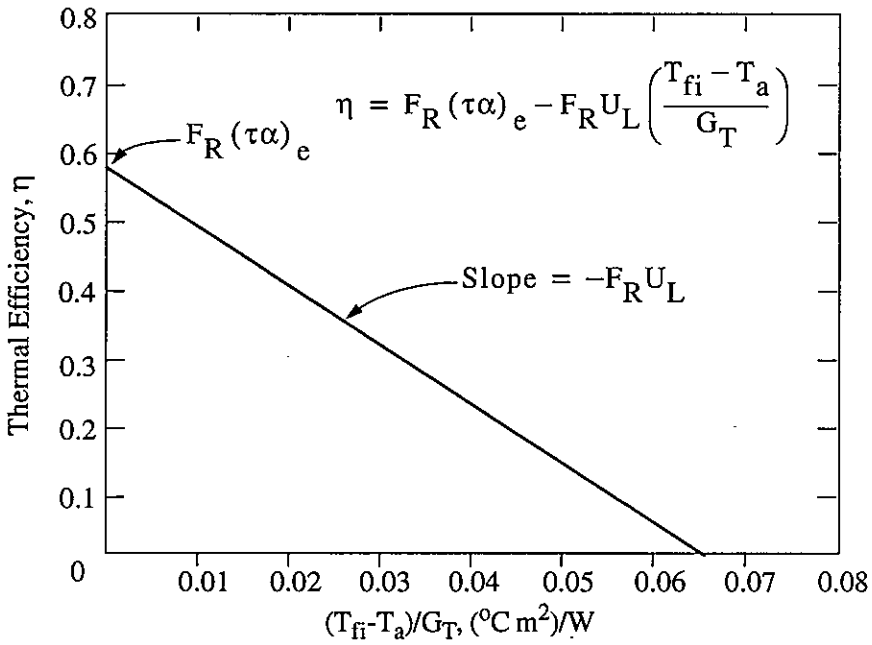

Task members have utilized an alternative representation of collector performance in the development of the characterizing equations [6,7]. When values of Q_U/A_a are plotted against G_T for values of ΔT, {i.e. $(T_{fi}-T_a)$ or $(T_{fm}-T_a)$}, series of parallel straight lines result, Figure 4.

Figure 4 "Input/output" representation of characteristic plot shown in Figure 3.

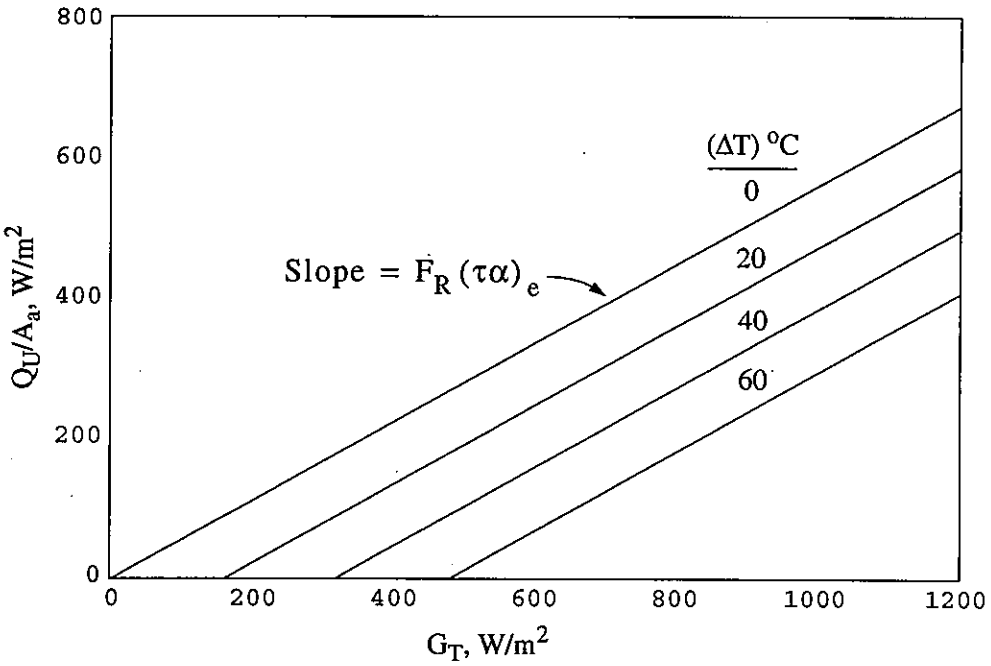

Plots of this type ("input/output curves") have been used successfully within IEA Task VI to relate the average daily output of solar heating systems to the average daily solar irradiance [8]. Figure 4 shows a "power input/output curve" for a theoretical solar collector where the power output of the collector is plotted relative to the incident solar irradiance. The slope of the lines is seen to be equal to the optical conversion efficiency $F_R(\tau\alpha)_e$ and the value of solar irradiance at which $Q_U/A_a = 0$, for a particular value of ΔT, may be considered to equal the "critical radiation level", G_c, for that value of ΔT [9], e.g.

$$G_c = \frac{U_L(\Delta T)}{(\tau\alpha)_e} \tag{1.9}$$

Thus, the performance of a solar collector may be given as;

$$Q_U/A_a = F_R(\tau\alpha)_e(G_T - G_c) \tag{1.10}$$

1.2.4 Absorbed Solar Radiation

When predicting the performance of solar collectors, the effects of diffuse irradiance and the incident angle of beam irradiance occurring throughout the day should be accounted for. The total irradiance measured in the plane of the collector aperture is the summation of: the solar radiation that is received directly from the sun, the component of the beam irradiance in the plane of the collector aperture, G_{bt}; the component of the diffuse irradiance, G_{dt}; and G_{gt}, the component of the solar radiation that is reflected from the ground adjacent to the solar collector, i.e.

$$G_T = G_{bt} + G_{dt} + G_{gt} \tag{1.11}$$

Solar collector tests are usually performed outdoors on sun-tracking test frames during clear sky periods when most of the absorbed solar irradiance is beam irradiance, or indoors with a solar simulator at near normal incident angles. In such cases the value of the effective transmittance-absorptance product is the value at normal incidence, i.e. $(\tau\alpha)_{e,n}$.

When predicting the performance of solar collectors under real sky conditions, the effects of other incident angles which occur throughout the day, and overcast conditions are accounted for by correcting the value of the absorbed solar radiation that occurs at normal incidence by, $K_{\alpha\tau}$, given by (for $G_{gt} = 0$)[1]

$$K_{\alpha\tau} = \frac{(\tau\alpha)_e}{(\tau\alpha)_{e,n}} = \frac{G_{bt}}{G_T}\frac{(\tau\alpha)_{b,\theta}}{(\tau\alpha)_{e,n}} + \frac{G_{dt}}{G_T}\frac{(\tau\alpha)_d}{(\tau\alpha)_{e,n}} \tag{1.12}$$

where $(\tau\alpha)_{b,\theta}$, $(\tau\alpha)_d$ are the effective transmittance-absorptance products for the beam and diffuse components of the solar radiation. The value of $(\tau\alpha)_{b,\theta}/(\tau\alpha)_{e,n}$ is referred to as the "beam-irradiance incidence-angle modifier", K_b, i.e.

$$K_b = (\tau\alpha)_{b,\theta} / (\tau\alpha)_{e,n} \tag{1.13}$$

and

$$K_d = (\tau\alpha)_d / (\tau\alpha)_{e,n} \tag{1.14}$$

is known as the "diffuse-irradiance incidence-angle modifier".

In principle, the incidence-angle modifier can be calculated from the geometry and optical properties of the collector [10]. In calculating $(\tau\alpha)_e$ the angular dependence of the plate absorptance can usually be neglected, since the absorptance of most absorber surfaces is insensitive to incidence angle. However, the transmittance of even flat-sheet cover materials normally decreases strongly when the angle of incidence is greater than about 60°, and this dependence must be taken into account.

[1] This equation neglects the ground component of the reflected solar radiation. A discussion of methods for accounting for ground reflected solar radiation is given in reference [5].

The transmittance of a flat homogeneous sheet can in principle be calculated directly from values of the refractive index and the extinction coefficient of the material, using Fresnel's formulae for the reflectance of the polarized components of radiation, Snell's law for refraction, and Bouguer's law for absorption [10]. Calculated results for a single pane of glass are shown, Figure 5. Edwards has also presented a method for calculating the transmission through multiple glazing systems [11].

In real collectors the effects of shading of the absorber surface by the sides of the collector housing may be significant and the incidence-angle modifier will have to take this into account [12]. Typical results of three flat-plate solar collectors are shown in figure 6 [13].

Figure 5 Transmission of a single sheet of glass versus beam radiation incident angle.

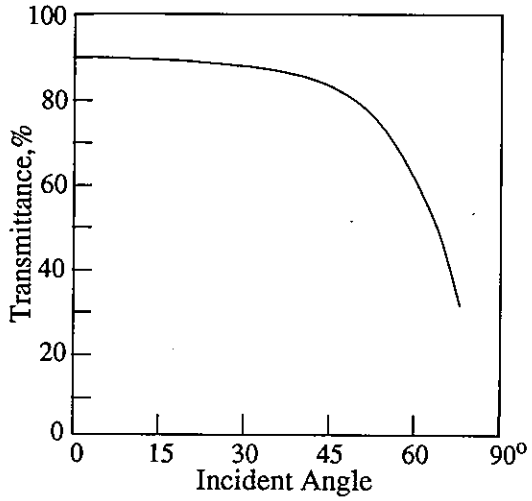

1.2.4.1 Diffuse Incidence-angle Modifier

For most flat-plate solar collectors [14], values of K_d may be estimated from

$$K_d = \int_{0°}^{90°} (K_{\alpha\tau}(\theta) \cdot \sin(2\theta))\, d\theta \qquad (1.15)$$

Under the usual assumption of isotropic diffuse radiation, the diffuse modifier is the weighted average of the beam incidence-angle modifier over a hemisphere. For collectors with essentially planar glazings and absorber surfaces; the value of K_d can be approximated by the value of $K_{\alpha\tau}(60°)$ [14], i.e.

$$K_d \cong K_{\alpha\tau}(60°) \qquad (1.16)$$

Figure 6 Typical Incident Angle Modifiers for Three Collectors (Adapted from reference 13).

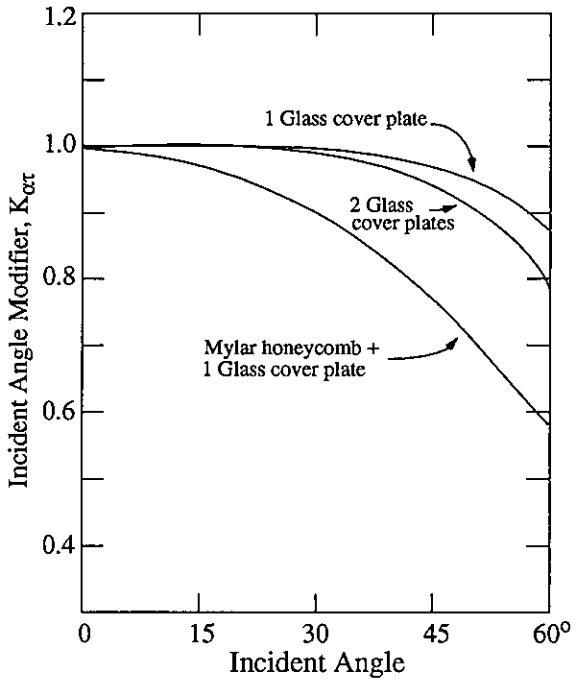

For systems that use collectors in which the value of $K_{\alpha\tau}$ is not symmetrical, i.e. may vary depending on which axis it is evaluated in, (e.g. horizontal versus vertical incidence angles), it may be necessary to complete a more complex calculation of $K_{\alpha\tau}$. These effects may be most significant for collectors employing tubular covers or collectors employing trough structures, mirrors, or lenses such that the geometries are characterized by biaxial symmetry. In these cases the use of biaxial incident angle modifiers may be required, see ref. 13 and Chapter 2.

1.3 References

1 **Results and Analyses of IEA Round Robin Testing**, Report of the IEA Solar Heating and Cooling Program, Task III - Performance Testing of Solar Collectors, prepared by H.D. Talarek, IKP - Kernforschungsanlage, Jülich, GmbH, Germany (1979)

2 **Survey of Solar Simulator Test Facilities and Initial Results of IEA Round Robin Tests Using Solar Simulators**, Report of the IEA Solar Heating and Cooling Program, Task III - Performance Testing of Solar Collectors, prepared by W. Ley, Deutsche Forschungs - und Versuchsanstalt für Luft- und Raumfahrt e.v., Cologne, Germany (1979)

3 Hottel, H.C. and A. Whillier.: **Evaluation of Flat-Plate Solar Collector Performance**. Transactions of the Conference on the Use of Solar Energy. Vol.3, Thermal Processes, Tucson (1955)

4 Bliss, R.W.: **The Derivation of Several Plate-Efficiency Factors Useful in the Design of Flat Plate Solar Heat Collectors**. Solar Energy, 3, No.4 (1959)

5 Duffie, J.A. and W. A. Beckman: **Solar Engineering of Thermal Processes**. Wiley-interscience, (1980)

6 Harrison, S.J.: **The Effects of Irradiance Level on Thermal Performance Tests of Solar Collectors.** Proceedings of the ISES world Congress, Intersol 85, Montreal (1985)

7 Rogers, B.A. and S.J.Harrison: **Collector Characterization and Collector Thermal Performance testing in Task III of the IEA Solar Heating and Cooling Programme.** Proceedings of the ISES Solar World Congress, Hamburg, F.R. Germany (1987)

8 **Eight Evacuated Collector Installations**, Interim Report for the IEA Task on the performance of solar heating, cooling and hot water heating systems using evacuated collectors: W.S. Duff, Editor, International Energy Agency, Solar Heating and Cooling Programme, Task VI (1982)

9 Lui, B.Y.H. and R.C. Jordan: paper in **Applications of Solar Energy for Heating and Cooling of Buildings**. ASHRAE, New York, (1977)

10 Mitalas, G.P. and D.G. Stephenson: **Absorption and Transmission of Thermal Radiation by Single and Double Glazed Windows**. NRC Division of Building Research, Research Paper No. 173, Ottawa (1962)

11 Edwards, D.K.: **Solar Absorption by Each Element in an Absorber-Cover Glass Array**. Solar Energy, Vol. 19, pp. 401-402 (1977)

12 Thomas, W.C., Dawson, III, A.G., Waksman, D. and E.R. Streed: **Incident Angle Modifiers for Flat-Plate Solar Collectors: Analysis of Measurement and Calculation Procedures**. Transactions of the ASME, Vol. 104, pp. 349-357 (1982)

13 **ASHRAE: Methods of Testing to Determine the Thermal Performance of Solar Collectors.** ASHRAE Standard 93-1986, Atlanta (1986)

14 Simon, F. and E.H. Buyco: **Outdoor Flat-Plate Collector Performance Prediction from Solar Simulator Test Data**. AIAA 10th Thermophysics Conference, Denver, Colorado (1975)

Chapter 2

Review of Test Methods and Procedures

2.1 Survey of Thermal Performance Test Standards

Thermal performance test methods were reviewed during 1974 by The National Bureau of Standards [1]. This lead to the drafting of a formalized test method including the testing procedure and facility to be used, and the required accuracy of the measurement instruments [2]. The NBS procedure was later adopted (with minor modifications) by The American Society of Heating, Refrigerating, and Air-Conditioning Engineers, Inc., (ASHRAE) as ASHRAE Standard 93-77 [3].

The ASHRAE Standard included additional tests for determining the transient response of the collector and the variation in performance due to the increasing angle of incidence of solar irradiance. It subsequently formed the basis for National Standards in a variety of countries. It requires that steady-state tests be performed over a range of collector inlet fluid temperatures under clear sky and steady radiation conditions, at times near solar noon. Values of experimental efficiency, "η" are determined by measuring simultaneously, the mass flow rate, inlet and outlet fluid temperatures and the solar insolation. The instantaneous efficiency is determined by the ratio of energy collected by the heat transfer fluid to the solar energy incident on the collector. This is given by:

$$\eta = \frac{Q_U}{G_T A_R} = \frac{\dot{m} \cdot C_P (T_{fo} - T_{fi})}{G_T A_R} \qquad (2.1)$$

where A_R = reference area of the collector (may be the aperture area, A_a; the absorber plate area, A_{ab}, or the gross area of the collector, A_g, [4],

T_{fo} = outlet temperature of the fluid, °C.

Experimentally derived values of collection efficiency may then be plotted against the appropriate parameter, i.e., $(T_{fi}-T_a)/G_T$, and the values of $F_R(\tau\alpha)_e$ and F_RU_L determined by the intercept and the slope of the performance curve, Figure 7.

Figure 7 Typical test results as determined by the ASHRAE procedure [5].

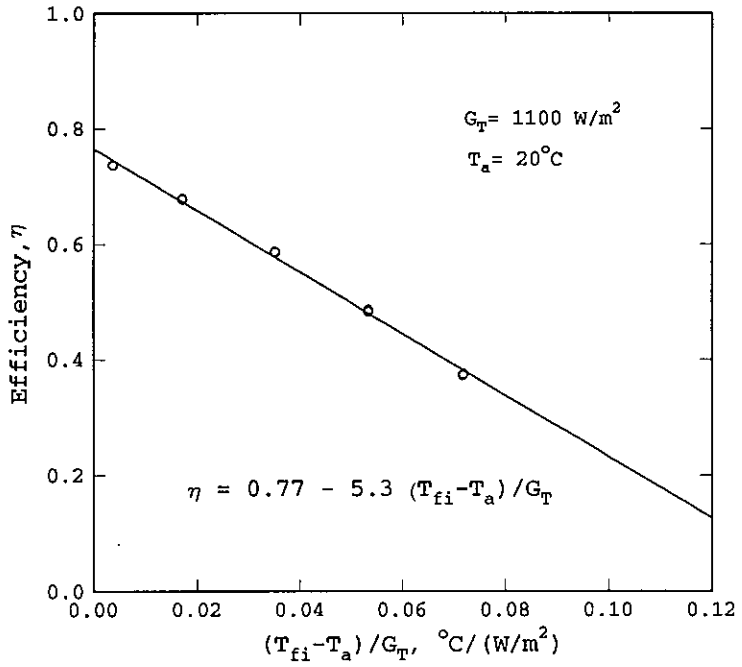

A later revision to the ASHRAE Standard [5] added test methods and requirements for conducting tests indoors in a solar simulator test facility, and outlined methods for determining "bi-axial incident angle modifiers". The revision also added recommendations for additional test sequences for certain collector types.

Other test procedures have been developed in the past, including that published by the Bundesverband Solarenergie (BSE) [6] and which was later adopted as a German Industrial Standard, DIN 4757 [7]. This test method specifies tests to separately determine the optical performance and the heat loss characteristics of solar collectors. While allowing higher order representations for the heat loss characteristics of solar collectors, it is not suitable for certain collector types (especially those where the heat transfer processes are not similar for heat gain and heat loss) [8]. Recently the Commission of the European Community (CEC) has also published a standard based on the ASHRAE test procedure [9].

2.1.1 Measurement of $K_{\alpha\tau}(\theta)$

A method of determining the incidence-angle modifier is specified in the ANSI/ASHRAE Standard 93-1986 [5]. The values of $K_{\alpha\tau}$ for irradiance incident at angles of 0°, 30°, 45°, and 60° to the aperture normal are determined by measuring the collector efficiency $F_R(\tau\alpha)_e$ with the inlet temperature equal to the ambient temperature. On the assumption that F_R is independent of incidence angle, $K_{\alpha\tau}$ is given by the ratio of

the measured efficiency occurring at the evaluated incident angle θ, relative to the efficiency measured at normal incidence

$$K_{\alpha\tau} = \frac{F_R(\tau\alpha)_{e,\theta}}{F_R(\tau\alpha)_{e,n}} = \frac{\eta_\theta}{\eta_n} \tag{2.2}$$

Experimentally determined values of $K_{\alpha\tau}$ are given in Figure 8 for a flat-plate solar collector with a single, textured glass cover (one side only). Results are shown for the transverse (east-west) and vertical (north-south) directions for the case of the textured pattern upwards facing and the case of the textured pattern downward facing.

To allow for interpolation of experimental test points when predicting a collector's performance, Simon and Buyco [10] correlated experimental data by plotting empirical values of $K_{\alpha\tau}$ against $(1/\cos\theta) - 1$, where θ is the angle of incidence. For conventional flat-plate collectors the plot should approximate a straight line, Figure 9; the slope of which can be found by a least-squares fit [5]. The dependence of incidence-angle modifier on θ is thus characterized by the equation

$$K_{\alpha\tau} = 1 - b_o\left(\frac{1}{(\cos\theta)} - 1\right) \tag{2.3}$$

where b_o is the slope of the correlating straight line.

Figure 8 Incidence angle modifier for a single glazed flat plate collector with single, textured glass cover (one side only) as measured according to [5].

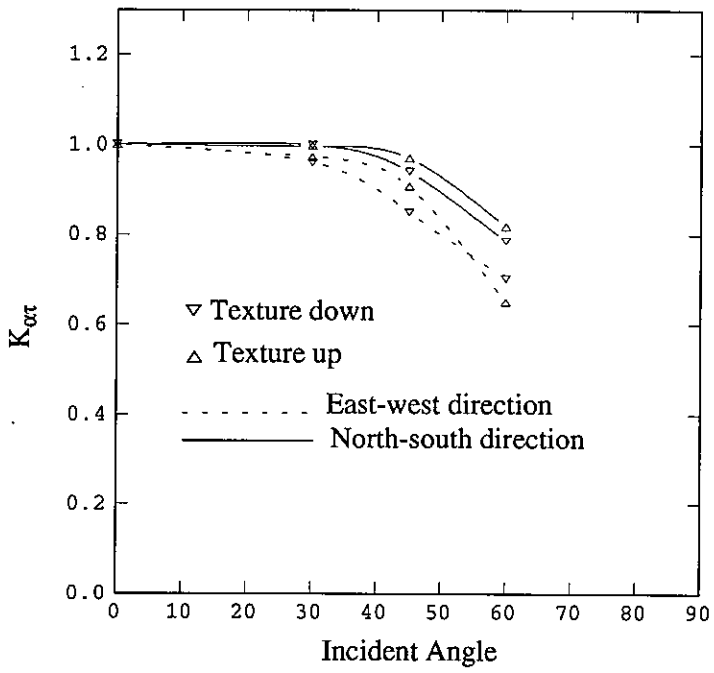

This linear equation is applicable only for collectors with flat, parallel cover and absorber surfaces, and even then is incorrect for grazing incidence (i.e. $\theta \approx 90°$). It does not account for shading of the absorber surface by the collector housing.

If beam irradiance only is considered, then the thermal performance of an irradiated solar collector operating under quasi-steady-state conditions can be described as;

$$Q_U/A_g = F_R [K_{\alpha\tau} (\tau\alpha)_{e,n} G_T - U_L (T_{fi} - T_a)] \quad (2.4)$$

or letting $T_{fm} = (T_{fi} - T_{fe})/2$ then

$$Q_U/A_g = F' [K_{\alpha\tau} (\tau\alpha)_{e,n} G_T - U_L (T_{fm} - T_a)] \quad (2.5)$$

While this will provide reasonable predictions of performance under clear sky conditions with small amounts of diffuse irradiance, in many cases the effects of diffuse solar irradiance must be accounted for.

Figure 9 Incident Angle Modifier As A Function Of Angle Of Incidence For Three Collectors (Adapted From ASHRAE Standard 93-77 (1977) [3]).

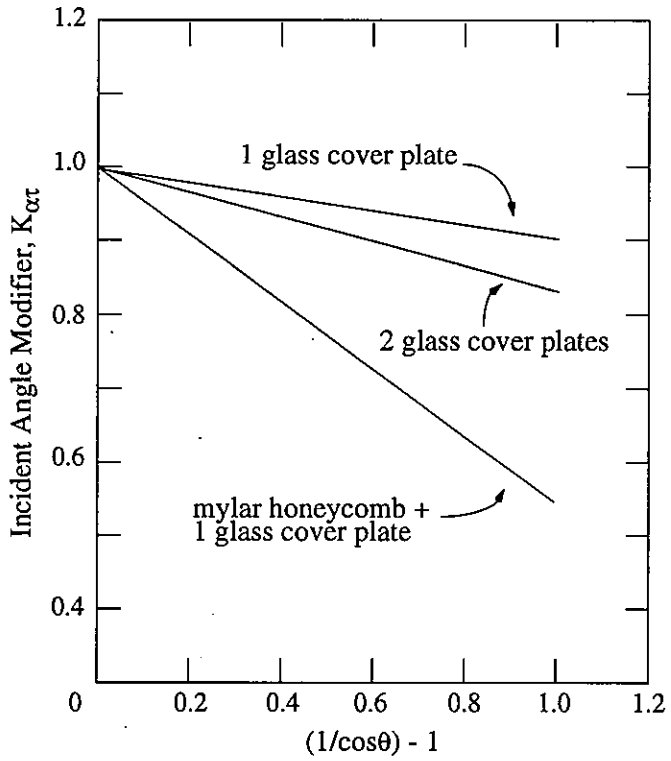

2.1.2 Biaxial Incidence-angle Modifiers

For those collectors (e.g., evacuated tube collectors, CPC concentrators and linear "one-axis-tracking "concentrators) for which the incidence angle effects are not symmetrical with direction of incidence, it is necessary to measure the incident angle effects from more than one direction to fully characterize the incident angle modifier [5].

The complex individual incident angle modifier can be estimated by considering it to be the product of the separate incident angle modifiers, K_1 and K_2, for two perpendicular symmetry planes that characterize the collector geometry [11] as shown in Figure 10. In general terms, the value of $K_{\alpha\tau}$ may be approximated by

$$K_{\alpha\tau}(\theta) = K_1(\Omega) \bullet K_2(\Gamma) \tag{2.6}$$

or in the case of tubular collectors, one set of incident angle modifier data is taken in the plane containing the normal to the collector aperture and all other normals to the tube axis; the other set is taken in the plane containing the aperture normal and the tube axis. The combined incident angle modifier is then estimated by:

$$K_{\alpha\tau}(\theta) = K_1(\Omega) \bullet K_2(\psi) \tag{2.7}$$

Figure 10 Angles used to define directions for Bi-axial Incident angle modifiers [5].

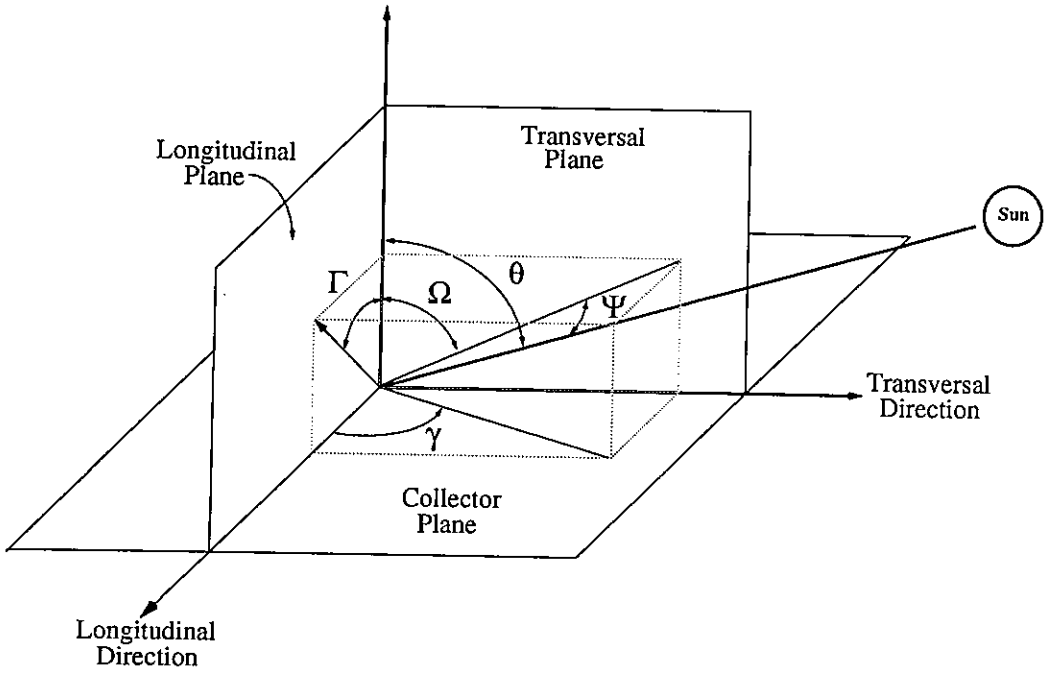

2.2 Problems Related To Thermal Performance Testing

Previous performance standards where based on established technologies and consequently are not suitable for the wide range of new products that have been developed. In certain cases testing procedures are biased against new products and tend to under-predict their performance. Similarly, new collector designs have been developed which incorporate a variety of design features not previously used. These include evacuated envelopes around absorber plates to minimize thermal losses, as is the case with evacuated tube type collectors [12]; the use of heat pipes or two-phase thermosiphones in absorber plates to enhance heat transfer or to produce "thermal diode" operation [13] or combinations of both [14].

These collectors are often sensitive to factors not evaluated in previous test standards and consequently test results derived according to these requirements may not adequately predict their performance over the full range of environmental conditions. To fully characterize these new collector types, test methods are required that evaluate the factors that significantly affect performance.

Current test procedures were intended to provide standardized test procedures to enable the characterization of the thermal performance of solar collectors in universal plots. These plots could then be compared in order to rate products and predict system performance. However, because they are based on the simplified Hottel-Whillier-Bliss model for thermal performance, a number of parameters are not accounted for, including wind speed and direction, absolute ambient air temperature, ground reflectance, collector tilt, the percentage of diffuse radiation, and the intensity of solar radiation.

These factors have in the past been considered to account for only second-order effects and it was thought satisfactory to just limit the extreme values during data selection. Consequently, the test procedures set ranges of acceptable values for wind-speed, solar radiation, and ground reflectance. Outdoor test periods are limited to clear sky periods when the diffuse solar radiation level is low or testing must be conducted in an artificial solar irradiance simulator [10]. Current test methods attempt to compromise between available test periods and variability in the test results.

A number of analytical studies have been conducted to quantify the effect of operational factors on collector performance. Lumisdane [15] cites collector tilt angle, wind velocity, and ratio of direct to diffuse solar radiation as factors causing variations in test results. Bruck [16] showed the effects of atmospheric conditions experienced during a test by computer analysis but did not verify the results by experimental means.

The effects of environmental factors was demonstrated by Harrison [17] for a single glazed, selective absorber surface, flat-plate solar collector and compared with experimental measurements. Results show that a large variability in test results was possible even under the restricted range of test conditions allowed for in the ASHRAE Standard. This spread in test results could have been reduced by further restricting test conditions or conducting tests under controlled conditions in an environmental simulator.

While this would produce highly repeatable test results, the data would represent an evaluation of the product under the test conditions and would not guarantee that performance in the field would be accurately predicted. Other studies and papers have been published identifying the problems of applying current test procedures to other collector types, i.e. evacuated tube type collectors. In certain cases, the effects of environmental factors are more significant than with conventional flat-plate solar collectors.

As a result, the classical performance plot is not a universal plot for a given collector, but dependent on the values of the meteorological conditions experienced during its determination. The HWB model of collector performance implicitly assumes that the value of $F_R(\tau\alpha)_e$ and F_RU_L are effectively constant. Bowen [18], and Shewen and Hollands [19] have elaborated on the problems of utilizing a constant value for the heat loss coefficient of solar collectors. Not accounting for environmental and operational conditions, may result in an under- or over-prediction of collector performance. This makes comparisons between collector types and accurate performance predictions impossible.

While normalization of test results to standard test conditions has been suggested as one approach to direct comparison, another possibility is to modify the basic Hottel-Whillier-Bliss model to account for more of the environmental parameters experienced during normal operation. Modifications of this type have been suggested by Proctor [20], Shewen and Hollands [19], Tabor [21,22], Cooper [23], Phillips [24], and Harrison [25].

2.2.1 Incidence Angle Modifiers

Experimentally measured values of Incident Angle Modifier are shown in Figure 8 for a flat plate solar collector. These results do not fit equation (2.3) exactly and when transformed only approximate the linear

Figure 11 Experimental data for evacuated tube and reflector combinations as measured in the transverse and longitudinal planes according to [5].

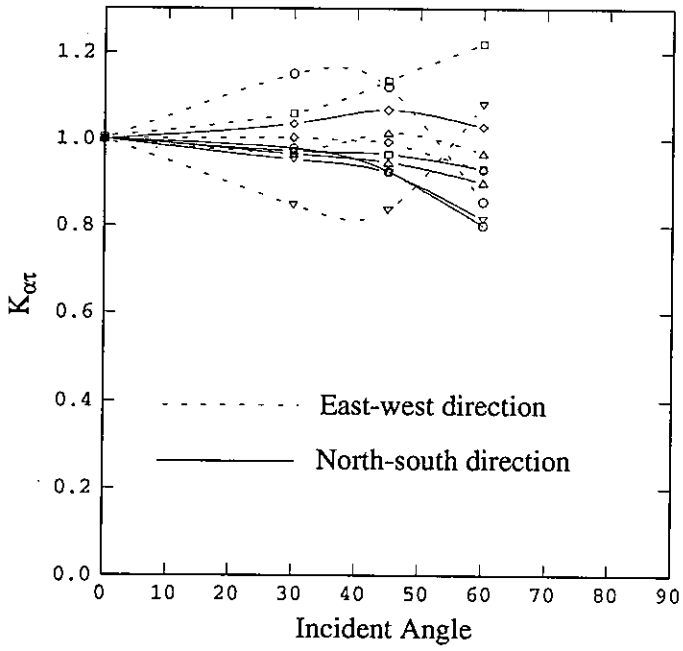

LEDEND:
- ▽ Owens-Illinois ETC with white flat reflector
- △ Phillips' ETC with ripple reflector
- □ Phillips' ETC with black flat reflector
- ○ Solartech with involute reflector
- ◇ Sanyo ETC, (east-west) axis

response shown in Figure. 9. This effect is largely due to shading of the collector absorber by the collector housing at large incident angles.

Equation (2.3) is even less suited for collectors with complex optical geometries e.g. evacuated tube collectors. Experimental data for a variety of evacuated tube and reflector combinations is shown in Figure 11 as measured in the transverse and longitudinal planes. This figure shows the wide range of optical response possible with evacuated tube and reflector designs. It is also apparent that the response of many collectors is different in the bi-axial planes. The results of Figure 11 when plotted against (1/cosθ) - 1 show the inability of this relationship to linearly correlate the experimental data, Figure 12.

In addition, a recent study [26] has indicated that the average of the bi-axial incident angle modifiers (i.e. K_1 and K_2) produces a better representation of optical performance at compound angles than eqs. 2.6 and 2.7, in particular for evacuated tube collectors where the incident angle modifier may be greater than 1 at significant incident angles.

An alternative representation of the incidence-angle modifier that has been suggested by Widder [27], is

$$K_{\alpha\tau} = 1 - (\tan\frac{\theta}{2})^{n} \tag{2.8}$$

where n is an empirical constant.

Figure 12 Data of Figure 11 plotted against (1/cosθ) - 1 as recommended [5].

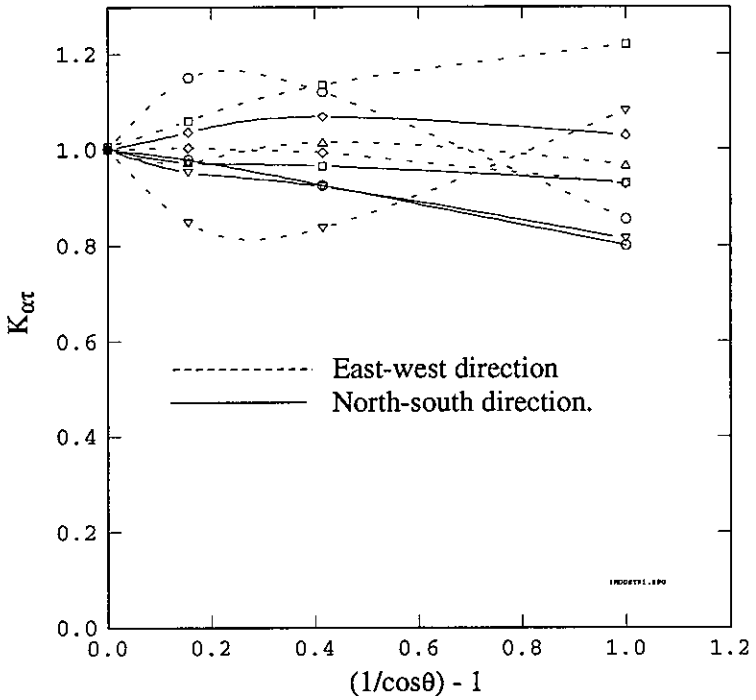

This model has been validated for single-and double-glazed flat-plate collectors, however the relationship is not defined for values of $K_{\alpha\tau}$ greater than one, making it unsuitable for most evacuated tubular collector designs.

Finally, for data which do not fit a simple analytical model, a cubic spline fit has been recommended as a simple and general method of interpolation.

2.3 References

1 Hill, J.E., et al.: **Development of Proposed Standards for Testing Solar Collectors and Thermal Storage Devices**. NBS Technical Note 899 (1976)

2 Hill, J.E. and T. Kusuda: **Method of Testing for Rating Solar Collectors Based on Thermal Performance**. National Bureau of Standards Report NBSIR 74-635 (1974)

3 **Methods of Testing to Determine the Thermal Performance of Solar Collectors**. ASHRAE Standard 93-77, ASHRAE, 345 East 47th St. New York, New York, 10017 (1977)

4 **Canadian Standards Association: Solar Collectors**. CSA Standard 378-M1982, Toronto (1982)

5 **ASHRAE: Methods of Testing to Determine the Thermal Performance of Solar Collectors.** ASHRAE Standard 93-86, Atlanta (1986)

6 Bundesvervan Solarenergie: Guidelines and Directions for Determining the Usability of Solar collectors. **Solar Collector Efficiency Test**. BSE, Essen, F.R.G. (1978)

7 Deutsches Institute Für Normung: Solar Heating Plants - Solar Collectors - Determination of Efficiency, Heat Capacity and Pressure Drop. **DIN Standard 4757, Part 4**, DIN, Postfach 1107, Berlin 30, F.R.G. (1982)

8 Jenkings, J.P., Hill, J.E.: A Comparison of Test Results for Flat-Plate Water-Heating Solar Collectors Using the BSE and ASHRAE Procedures. **ASME Journal of Solar Energy Engineering, Vol. 102**, 2 (1980)

9 **CEC, Recommendations for Performance and Durability Tests of Solar Collectors and Water Heating Systems: Non Nuclear Energies**. European Solar Collector and Systems Testing Group, Ispra, Italy (1989)

10 Simon, F.F. and Buyco, E.H.: **Outdoor Flat-plate Collector Performance Prediction from Solar Simulator Test Data**. American Institute of Aeronautics and Astronautics, AIAA 10th Thermal Physics Conference, Paper No. 75-741, Denver, Colo. (1975)

11 McIntire, W.R.: **Factored Approximations for Biaxial Incident Angle Modifiers.** Solar Energy, Vol. 29. No. 4, pp.315-322 (1982)

12 Saltiel, C.J. and M. Soholov: **Thermal and Optical Analysis of Evacuated Circular Cylindrical Concentrating Collectors**. Solar Energy, 29, 391 (1982)

13 Rush, C.K.,and R.F.Sendall: **Performance of a Boiling Condensing Flat-Plate Collector**. Proceedings of 1977 SESCI National Conference, Edmonton, Alberta (1977)

14 **Philips Corporation: An Evacuated Tubular Solar Collector incorporating a Heat Pipe**. Philips Technical Review, Volume 40 (1982)

15 Lumsdaine, E.: **On the Testing of Solar Collectors to Determine Thermal Performance.** Proceedings of the 1978 Annual Meeting of the American Section of the International Solar Energy Society, Inc., Denver (1978)

16 Bruck, M., et al: **Collector Test Methods, Analysis Of Test Methods For the Determination Of The Thermal Efficiency Of Flat-plate Collectors,** Austrian Solar And Space Agency, (ASSA), A-1090 Vienna (1979)

17 Harrison, S.J.: **The Effects of Operational and Meteorological Factors on Solar Collector Thermal Performance Test Results.** SESCI 84 Conference, Calgary (1984)

18 Bowen, J.C.: **The Problem of Treating U_L as a Constant.** Proceedings of the 1980 Annual Meeting of the American Section of the International Solar Energy Society Inc., Phoenix (1980)

19 Shewen, E.C. and K.G.T. Hollands: **Equations for Representing the Ul Dependence in Collector Test Procedures.** Proceedings of the International Solar Energy Society, Atlanta (1979)

20 Proctor, D.: **A Generalized Method For Testing All Classes of Solar Collector-II, Evaluation of Collector Thermal Constants.** Solar Energy, 32, 387 (1984)

21 Tabor, H.: **Testing of Solar Collectors.** Solar Energy, 20, 293 (1978)

22 Tabor, H.: **Letter to the Editor.** Solar Energy, 24, 113 (1980)

23 Cooper, P.I.: **The Testing of Flat Plate Solar Collectors.** The Institution of Engineers' Annual Engineering Conference, Townsville, Australia (1976)

24 Phillips, W.F.: **A Simplified Nonlinear Model for Solar Collectors.** Solar Energy, 29, 77 (1982)

25 Harrison, S.J.: **Improved Characterization for the Thermal Performance of Solar Collectors.** Ph.D Thesis, Dept. of Mechanical Engineering, Queen's University, Canada (1992)

26 Knappmiller, K., and Duff, W.: **Computing Incidence Angle Modifiers for Advanced Solar Collectors.** Proceedings of the Biennial Congress of the International Solar Energy Society, Denver Colo. (1991)

27 Widder, F.: **Unterlagen zur Bestimmung des Wermeertrages von sonnenkollektoren für charakteristische limazonen der Schwei.** EIR-Bericht Nr. 427, Eidg. Institut für Reaktorforschung Würenlingen, Schweiz (1981)

Chapter

3

The Effects of Atmospheric Factors on Collector Heat Loss

3.1 Theory

The Hottel, Whillier, Bliss (HWB) representation of thermal performance assumes solar collectors can be fully characterized by a linear relationship between efficiency, η, and $(T_{fi}-T_a)/G_T$, {or $(T_{fm}-T_a)/G_T$}. In this simplified model of thermal performance, many environmental factors are considered to have only minimal affects on operation. However, as the requirements for accuracy and repeatability increase, the influence of these factors becomes more significant.

Solar collectors are subjected to a range of environmental conditions during normal use. These may include: solar radiation, G_T, ranging from 0 to 1200 W/m^2; ambient air temperatures, T_a, from -30 to +30°C; effective sky temperatures, T_s, from values equivalent to the air temperature to values 30 K colder; and wind speeds normally ranging from 0 to 15 m/s. As well, inlet fluid temperatures, T_{fi}, of up to 120°C are typical of applications suitable for flat-plate solar collectors working with water or glycol based heat transfer fluids.

Previous studies [1,2,3] have indicated that environmental factors cause variations in the performance of solar collectors and have shown their effects on thermal performance test results. McMurrin and Buchburg [4] point out that there are at least twelve variables, not related to specific collector design that affect collector performance. These include:

(i) solar factors: the rate of incident solar radiation on the collector, the fraction that is diffuse solar irradiance, the angle of incidence between the sun's rays and the solar collector surface;

(ii) collector ambient: air temperatures surrounding the collector, the rate of exchange of long-wave thermal radiation (often represented by an effective sky temperature); and

(iii) operating conditions: fluid inlet temperature, mass flow rate of the coolant and its properties (e.g. specific heat), and collector slope or tilt angle.

This report addresses primarily the effects of (i) solar factors, (ii) collector surroundings or ambient, and the inlet fluid temperature effects of (iii). These represent items usually outside the control of the user, whereas flow rate, collector slope and coolant fluid properties may be specified or set at standard conditions for the purpose of rating testing.

In classifying the sensitivities of solar collectors to environmental factors, different solar collector types can be seen to be dependent on differing factors. For example, the performance of concentrating collectors and evacuated tube type collectors may be significantly affected by optical factors related to the incident angle and nature of the solar flux (e.g. diffuse fraction). Other collector types such as conventional flat-plates are strongly dependent on the top heat loss coefficient which is dependent on ambient environmental conditions.

Recent developments in solar collector technology have resulted in collectors in which the performance is also dependent on the heat removal processes occurring within the absorber plate. This is the case with collectors incorporating intermediate heat transfer fluids that change phase within the absorber plate in order to enhance heat transfer. Their performance may be dependent on a number of factors that are inter-related.

In most instances the major problem is related to identifying a generalized performance representation that will accommodate virtually all classes of solar collectors and to identify test sequences that may be used to quantify these dependencies. This is most easily accomplished by analyzing the factors that affect the heat loss mechanisms in solar collectors and evaluating correlations for representing the effects of the most significant factors.

This chapter investigates the heat loss characteristics of glazed solar collectors (i.e. those with transparent covers over the absorber) and demonstrates the effects of environmental factors on their performance. Because of the high sensitivity of unglazed solar collectors to wind and atmospheric radiation effects these are separately dealt with in Chapter 4.

3.2 Collector Heat Losses

For the purpose of defining an "efficiency expression" Proctor [5] has stated that the thermal losses from solar collectors can be classified as:

i) apparently independent of temperature,

ii) dependent on temperature difference,

iii) due to radiation heat exchange alone,

iv) due to air movement over the collector.

In each case, it is possible to identify generic collector types that may fall into the above classifications. To arrive at the form of an equation that will adequately predict the performance of a variety of collector types operating under a range of environmental conditions, an analysis of the heat loss mechanisms in various solar collectors must be conducted to identify significant dependencies and characterize their effects. To accomplish this objective, an analytical study was conducted [6] to evaluated the effects of atmospheric factors on the heat loss of a typical flat-plate solar collector with selective absorber surface (SGSEL collector), a collector with a non-selective absorber (SGNS collector) and a collector with a vacuum envelope surrounding the absorber plate (VAC collector). In each case, the factors that significantly affect heat losses from the absorber were identified.

3.2.1 Heat Transfer Analysis

From equation (1.1), for steady state operation, the rate of energy extracted from a solar collector, Q_U, may be simply represented as the difference between the rate of solar energy absorbed by the absorber plate, $A_aG_T(\tau\alpha)_e$, and the rate of thermal energy loss to the surroundings, Q_L, i.e.

$$Q_U = A_aG_T(\tau\alpha)_e - Q_L \tag{3.1}$$

where

$$Q_L = U_LA_a(T_p-T_a) \tag{3.2}$$

U_L is the overall heat loss coefficient from the absorber plate (at a temperature T_p) to the surroundings at a temperature T_a. Both the optical and heat transfer properties of the solar collector (given by the values of $(\tau\alpha)_e$ and U_L) are affected by meteorological conditions.

Thermal losses from the collector consist of conduction losses through the back and edge of the collector to the surrounding environment, and conduction, convection and radiation losses through the front of the collector.

In order to assist in the identification of suitable characterizing relationships, the basic heat transfer mechanisms involved in solar collectors are described and the effects of variation in environmental factors indicated. This Chapter and Chapter 7 should develop an understanding of the mechanisms involved in the heat loss and thus the conditions under which the HWB model and the assumption of constant U_L are valid.

3.2.2 Heat Loss Coefficient, U_L.

For a solar collector with a cover, the heat loss from the absorber plate consists of heat losses through the collector glazing and the back and edge of the collector casing. For most collectors, back and edge losses are small compared with the losses through the collector's front cover. Consequently U_L can be approximated by U_{top}, the heat loss coefficient through the top cover of the solar collector.

3.2.2.1 Top Heat Loss Coefficient, U_{top}.

Heat loss through the top of the solar collector results from both convection and radiation heat transfer. Heat is transferred from the absorber plate to the cover plate by convection across an inclined air layer and also by radiative exchange between the plate and the cover.

Some long-wave radiation is transmitted through the glass from the absorber plate to the atmosphere but as the glass is almost totally opaque to long-wave radiation, this accounts for only a small amount of the heat loss[1]. The energy transferred to the cover from the absorber plate is lost to the atmosphere by convection to the ambient air (often enhanced by wind), and by radiation exchange from the cover plate to the sky and the surroundings.

1. This is not always the case for some thin films and plastics that may be significantly transparent to long-wave radiation, i.e. τ_{LW}=0.3 for TEFLON™ film. In these cases the effects of long-wave solar radiation transmitted through the cover should be considered.

The cover plate is usually assumed to radiate to a black-body source for infrared radiation which is at an effective sky temperature, T_s. A heat transfer network for U_{top}, Figure 13, shows the radiative and convective heat loss paths. U_{top} is a function of both: T_a, T_p and T_s; and the values of $h_{w,c-a}$, $h_{r,c-s}$, $h_{c,p-c}$, and $h_{r,p-c}$

where $h_{w,c-a}$ is the wind heat transfer coefficient between the cover and the ambient air
$h_{r,c-s}$ is the radiation heat transfer coefficient between the cover and the sky
$h_{c,p-c}$ is the convection heat transfer coefficient between the absorber plate and the cover
$h_{r,p-c}$ is the radiation heat transfer coefficient between the absorber plate and the cover

These heat transfer coefficients vary with, among other parameters, the collector orientation and wind velocity. Following the general analysis of reference [7], we may summarize the expressions for the heat loss through the cover of a solar collector.

The heat transfer from the absorber plate to the cover can be expressed as

$$q_{p-c} = A_{ab} U_{p-c} (T_{pm} - T_c) \tag{3.3}$$

where

$$U_{p-c} = h_{c,p-c} + h_{r,p-c} \tag{3.4}$$

The radiation heat transfer coefficient is calculated from

$$h_{r,\,p-c} = \frac{\sigma (T_p^2 + T_c^2) \cdot (T_p + T_c)}{(1/\varepsilon_p) + (1/\varepsilon_c) - 1} \tag{3.5}$$

Figure 13 Thermal network for heat-loss from the top of a solar collector showing convective and radiative components.

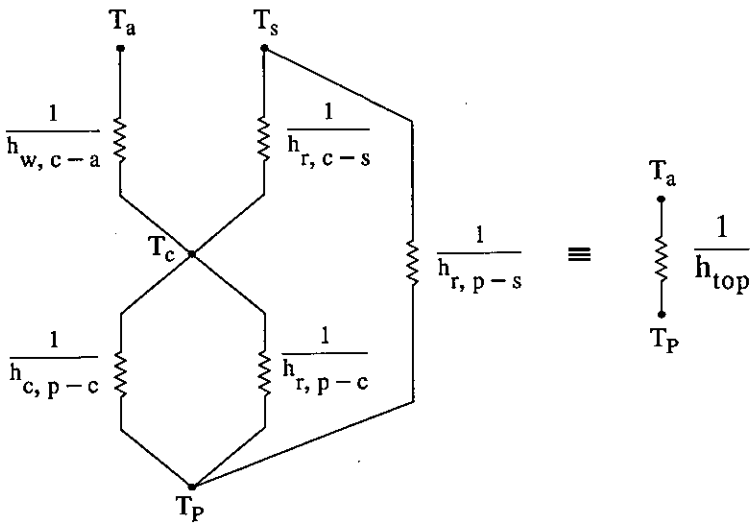

and the value of the convective heat transfer coefficient, $h_{c,p-c}$, determined by the relationship

$$h_{c,p-c} = Nu\ (k_a/L_{p-c}) \tag{3.6}$$

Values for Nu, the Nusselt number and k_a, the thermal conductivity of air are dependant on collector slope, temperature difference between surfaces and fluid properties which are generally related to a representative temperature for the enclosed air layer [8].

The heat loss from the absorber plate to the cover glass is equivalent to the heat transferred from the cover glass to the atmosphere, i.e. $q_{p-c} = q_{c-s}$. Heat is lost from the cover to the atmosphere by convection to the surrounding air and by radiation to the sky. The resultant heat loss is given by:

$$q_{c-a} = A_c\ U_{c-a}(T_c - T_a) \tag{3.7}$$

where

$$U_{c-a} = h_w + h_{r,c-s} \tag{3.8}$$

and h_w is the wind induced heat transfer coefficient. The heat transfer coefficient for radiation exchange between the cover and the sky is

$$h_{r,\,c-s} = \frac{\varepsilon_c \sigma (T_c^4 - T_s^4)}{(T_c - T_a)} \tag{3.9}$$

where T_s is the effective sky temperature "seen" by the solar collector. Heat transfer by radiative exchange between the absorber plate and the sky is given by

$$q_{rad,\,p-s} = A_{top} \cdot \tau_{LW} \cdot \varepsilon_p \cdot \sigma \cdot (T_p^4 - T_s^4) \tag{3.10}$$

where τ_{LW} is the transmittance of the cover to long-wave radiation. This may be represented by a radiation heat transfer coefficient:

$$h_{r,\,p-s} = \frac{\tau_{LW} \varepsilon_c \sigma (T_p^4 - T_s^4)}{(T_p - T_a)} \tag{3.11}$$

and the overall heat transfer coefficient for top heat loss expressed as

$$U_{top} = \left[\frac{1}{U_{p-c}} + \frac{1}{U_{c-a}}\right]^{-1} + h_{r,\,p-s} \tag{3.12}$$

3.3 The Effects of Atmospheric Factors on Heat Loss

3.3.1 Temperature effects:

Experimental test results for a single glazed solar collector with selective surface are shown in Figures 14 and 15 as measured in a solar simulator at a range of solar irradiance levels [6]. These results clearly indicate that the performance of the solar collector is not well represented by a single characteristic curve but is seen to depend on the irradiance level used during the tests.

These results are due to the dependance of the heat loss coefficient, U_L, on the temperatures of the absorber plate and surrounding ambient. By iteratively solving the expressions presented in section 3.2.2.1, values of U_{top} can be determined which correspond to specific environmental conditions [6]. From this analysis, the effects of variations in the environmental factors can be determined.

In Figure 16, values of top loss heat transfer coefficient, U_{top}, are shown as a function of the mean absorber plate temperature, T_{pm}, for values of ambient air temperature, T_a. These results show that in fact U_{top} is not constant but is seen to vary with both the value of T_{pm} and T_a. Referring to Table 1, the significance of the problem may be illustrated where values of constant $(T_{fi}-T_a)/G_T$ are shown for various values of T_{fi}, T_a, G_T and $(T_{fi}-T_a)$. Considering that the value of T_{pm} is very close to T_{fi} for most solar collectors, it is apparent that a range of absorber plate temperatures and ambient temperatures are possible for a particular value of $(T_{fi}-T_a)/G_T$. This results in higher efficiency values being observed at lower values of irradiance (for fixed values of $(T_{fi}-T_a)/G$), as shown in Figure 14. The same results plotted as "input vs. output" in Figure 15 also clearly differ from the ideal HWB case in that the performance characteristics are not evenly spaced with respect to the temperature difference ΔT, i.e. $(T_{fi}-T_a)$.

While it has been common practice in the past to assume that collector efficiency, η, is only a function of the parameter $(T_{fi}-T_a)/G_T$, it is apparent from Table 1 and Figure 16 that variations in the rate of heat loss from this type of solar collector may occur for the same value of $(T_{fi}-T_a)/G_T$ if different values of T_{fi} (and T_{pm}) are experienced.

Table 1 Varying Factors For Fixed $(T_{fi}-T_a)/G_T$

$(T_{fi}-T_a)/G_T$	T_{fi}	T_a	G_T	$T_{fi}-T_a$
0.1	30°C	20°C	100 W/m^2	10°C
0.1	-20	-30	100	10
0.1	100	0	1000	100
0.1	70	-30	1000	100

Figure 14 Experimental results for single glazed flat-plate collector with selective absorber surface [6].

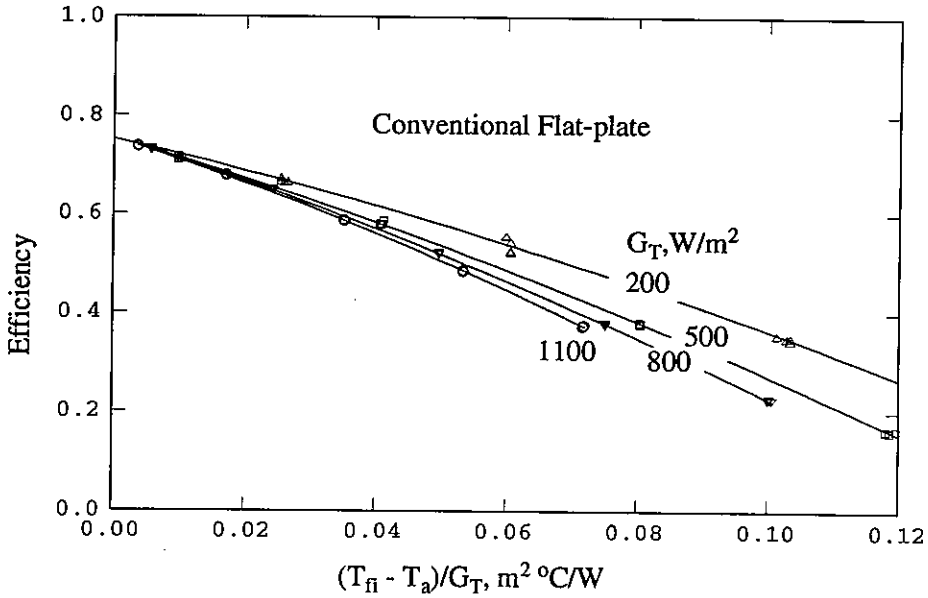

Figure 15 Input/output curve of the experimental results for the single glazed flat-plate collector with selective absorber surface [6].

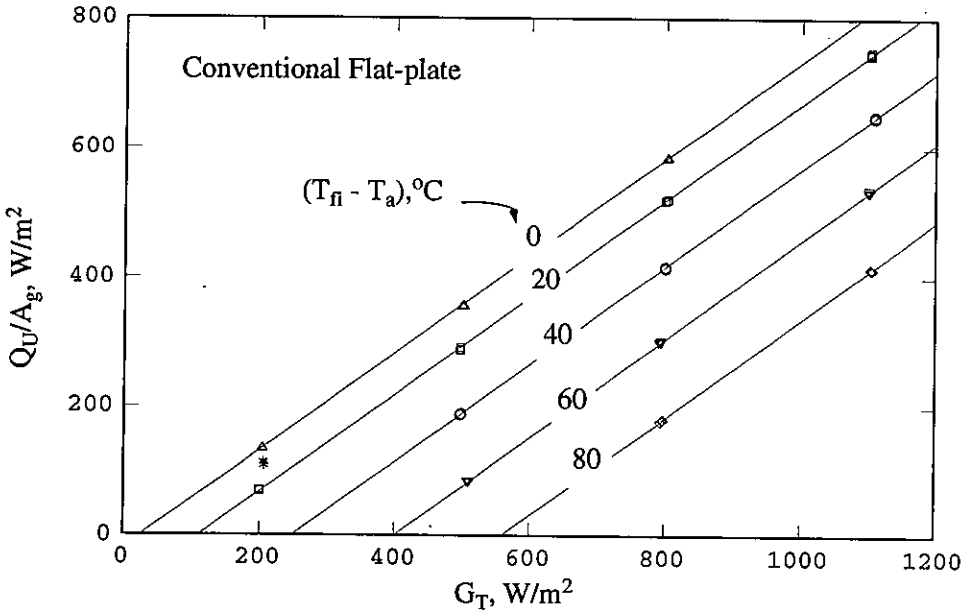

Figure 16 Variation of U_{top} with T_{pm} for a range of T_a ("selective absorber collector").

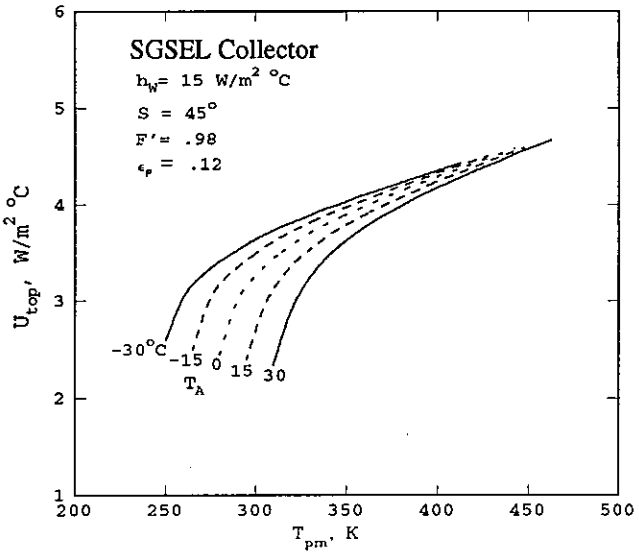

Figure 17 Variation in U_{top} with T_{pm} for a solar collector with "non-selective" absorber plate.

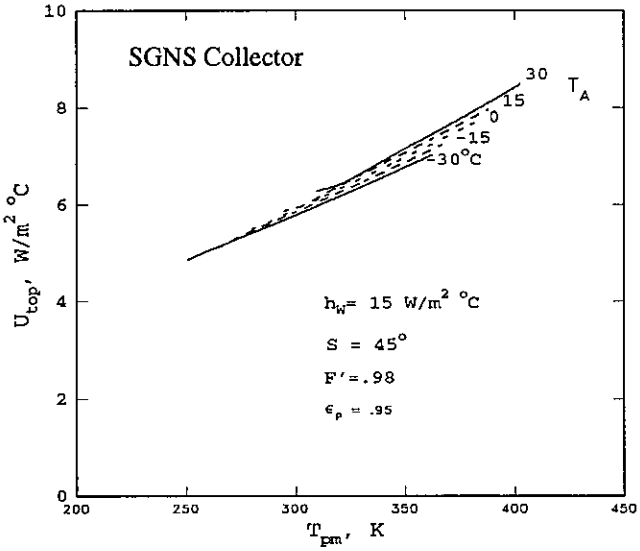

Figure 18 The effects of absorber plate emissivity and air temperature on U_{top} for a collector dominated by radiation heat losses.

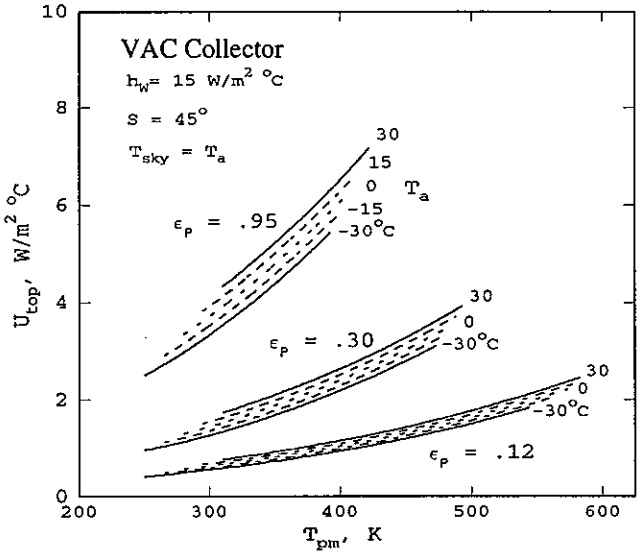

The results shown in Figure 16 are for a single glazed solar collector with a "selective" absorber plate (designated SGSEL) with emissivity to thermal radiation, ε_p, equal to 0.12. Many collectors are constructed with "non-selective" absorbers with much higher, ε_p, (i.e. ε_p=0.95). In this case a larger percentage of the heat transfer is due to radiation exchange between the absorber surface and glazings. The radiative heat loss coefficients, $h_{r,p-c}$ and $h_{r,p-s}$, were shown in section 3.2.2.1 to depend on the difference of the fourth powers of the absolute temperatures, contrary to the assumption of being constant for a given solar collector. Consequently, the variation in U_{top} becomes even more significant as absolute plate and ambient temperature increase. Values of U_{top} are shown in Figure 17 for a single glazed collector with non-selective absorber plate (designated SGNS) where the variation with ambient air temperature, T_a, is seen to be greater than the case for the SGSEL collector.

In the case of collectors in which the absorber housings are evacuated (as is the case with vacuum tube type solar collectors), pressures between the absorber and glazing are reduced to the point were convection heat transfer no longer takes place and conduction is reduced to very low values [9]. Heat loss from the absorber is almost completely due to radiative heat exchange between the absorber plate and the collector glazing. Because the radiative heat loss coefficients dominate the heat loss, U_{top} is seen to vary in a convex-upward manner; significantly different from those of the previous cases. Values of U_{top} are shown in Figure 18 for a solar collector in which the heat loss due to conduction and convection is effectively zero (i.e. heat loss is by radiation heat transfer). Results for this type of collector (designated VAC) are given for three values of absorber plate emissivity. It may be noted that in the case of ε_p =.12, the values of U_{top} are very low even at very high temperatures.[2]

3.4 Wind effects

The value of U_{p-c} represents only one component of the heat loss from the absorber; another major contribution to heat transfer is due to the wind enhanced heat transfer from the outer surface of the glass cover. The heat transfer may be that of natural convection if the wind velocity is very low, e.g. h_w = 4 or 5 W/m^{2}K; but as wind velocity increases, natural convection is dominated by forced convection, increasing h_w. This offers less resistance to heat loss from the absorber plate and consequently, U_{top} increases until h_w no longer represents the limiting factor, i.e. h_{p-c} dominates.

The effects of wind induced heat transfer have been investigated [10,11,12]. Considerable controversy still exists on an accurate method of quantifying h_w and it is convenient to investigate the effects of the magnitude of wind induced heat transfer coefficient rather than the effects of wind speed or direction. For reference, the relationship proposed by McAdams [13] is generally assumed to give reasonable estimates of h_w

$$h_w = 5.7 + 3.8V_w \tag{3.13}$$

where V_w is the wind speed in m/s, and h_w is in W/(m^{2}K).

The effects of varying h_w are shown in Figure 19 for the SGSEL collector, Figure 20 for SGNS collector, and Figure 21 for the VAC collector. In the latter case, wind effects are small for the collectors with low ε_p.

2. Data shown in Fig. 18 assumes that the value of the absorber plate emissivity, ε_p, does not change with temperature. This is not always the case for certain coatings which will increase in emissivity at high temperatures. This usually only occurs at temperatures significantly greater than those considered as typical operating conditions.

Figure 19 The effects of wind heat transfer coefficient on U_{top} for a collector with "selective Absorber".

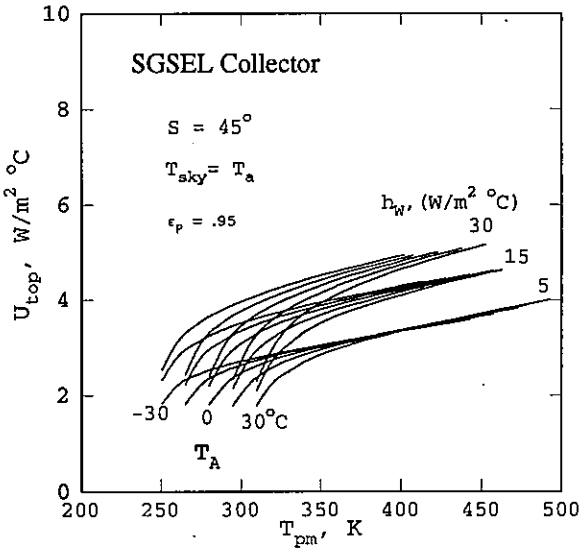

Figure 20 The effects of wind heat transfer coefficient for a collector with "non-selective" absorber.

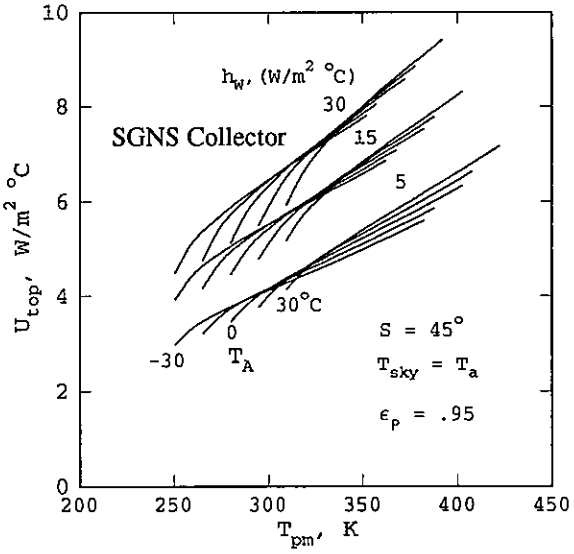

Figure 21 The effects of wind heat transfer coefficient on U_{top} for "vacuum" collectors.

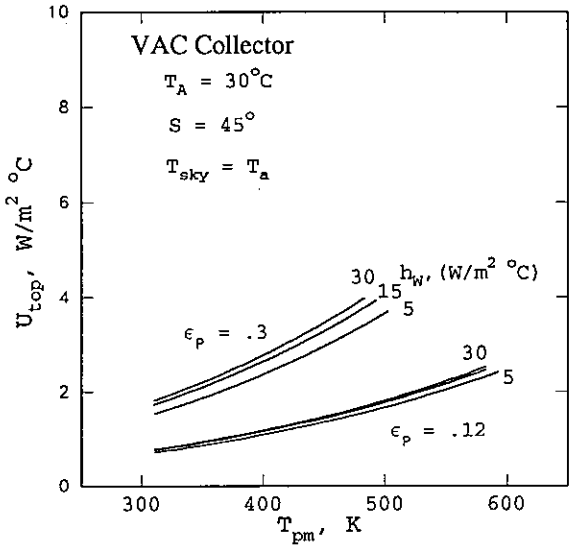

Wind effects are a dominating factor in the performance of unglazed solar collectors and as such are separately investigated in Chapter 4.

3.5 Sky temperature effect

To evaluate the radiation exchange between the cover of a solar collector and the sky, the sky can be considered as a blackbody at an effective sky temperature T_s. In Figures 19 to 21 it was assumed that the cover glass radiated energy to the atmosphere at a temperature equivalent to T_a. This is not the case for clear days where the effective sky temperature may be significantly lower than T_a [14,15].

Cloud cover results in higher effective sky temperatures as compared to the clear sky case where the net radiative exchange is to the much colder upper atmosphere. The value of T_s depends on the air temperature and the portion of the sky that the collector sees, as shown in Figure 22, (values calculated according to Cole, [16]).

At high tilt angles, the collector "sees" the ground which is usually at a temperature close to T_a. At low values of h_w and $(T_{pm}-T_a)$, lower sky temperatures significantly increases the value of U_{top} as shown in Figure 23 for a "worst case" situation. The worst case situation occurs at high ambient air temperatures and low wind speeds, i.e. low values of h_w. This effect is reduced at higher values of h_w and $(T_{pm}-T_a)$, where $h_{r,p-c}$ is less significant in the overall heat transfer.

Figure 22 Effective sky temperatures for inclined surfaces and clear sky conditions, (calculated according to [16]).

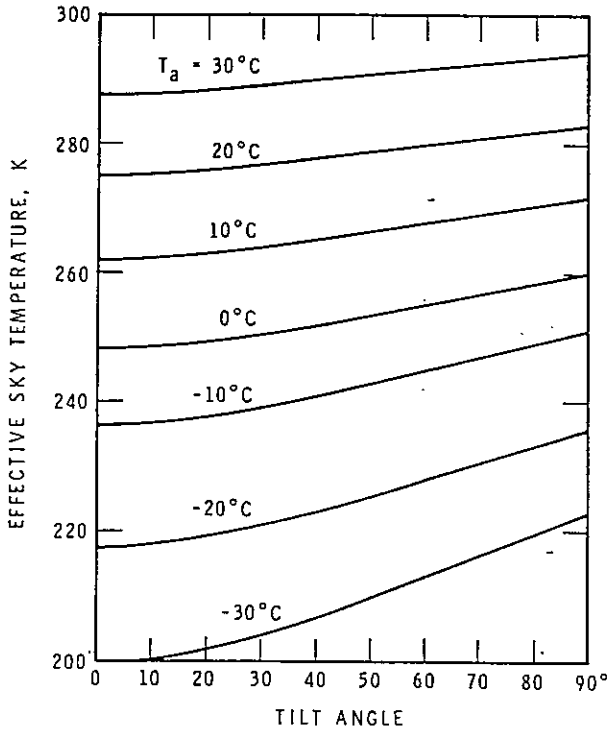

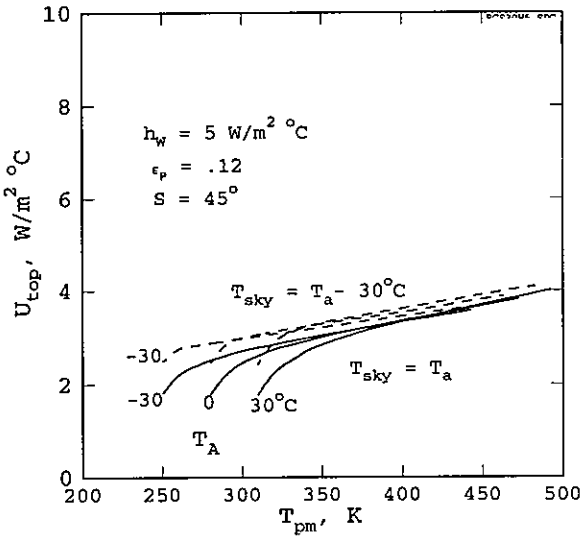

Figure 23 The effects of sky temperature on U_{top} for a collector with "selective" absorber during low wind speed conditions

3.6 References

1. Bruck, M., et al: **Collector Test Methods, Analysis Of Test Methods For the Determination Of The Thermal Efficiency Of Flat-plate Collectors**, Austrian Solar And Space Agency, (ASSA), A-1090 Vienna (1979)

2 Green, A.A.: **The Influence of Operating Conditions on the Thermal Performance of Non-Concentrating Solar Collectors, Ph.D. Thesis**, University of Wales, Cardiff, UK (1984)

3 Harrison, S.J.: **The Effects of Operational and Meteorological Factors on Solar Collector Thermal Performance Test Results**. SESCI 84 Conference, Calgary, Canada (1984)

4 McMurrin, J.C. and Buchberg H.: **Effects of Operating Conditions on the Performance of Honeycomb and Conventional Flat Plate Solar Collectors**. Proceedings of the Biennial Congress of the International Solar Energy Society, Atlanta, Ga. (1979)

5 Proctor, D.: **A Generalized Method For Testing All Classes of Solar Collector-II, Evaluation of Collector Thermal Constants**. Solar Energy, 32, 387 (1984)

6 Harrison, S.J.: **Improved Characterization of the Thermal Performance of Solar Collectors**. Ph.D Thesis, Department of Mechanical Engineering, Queen's University, Kingston, Canada (1992)

7 Duffie, J.A. and Beckman, W.A.: **Solar Engineering of Thermal Processes**, Wiley-interscience, (1980)

8 Hollands, K.G.T., T.E. Unny, G.D. Raithby and L. Konicek: **Free Convective Heat Transfer across Inclined Air Layers**. Journal of Heat Transfer, Vol. 98, No. 2 (1976)

9 de Grijs, J.C. et al.: **Evacuated Tubular Collector with Two Phase Heat Transfer into the System**. Development Department for Solar Collectors, Philips Corporation, The Netherlands (1982)

10 Green, A.A., Kenna, J.P., Rawcliffe, R.W.: **The Dependance of Wind Speed on Flat-Plate Solar Collector Performance**. IEF Conference, Future Energy Concepts, London (1981)

11 Sparrow, E.M., Nelson, J.W.: **Wind-related Heat Transfer Coefficients for Leeward-Facing Solar Collectors**. ASHRAE Transactions, Vol.87, Pt. 1 (1981)

12 Hewitt Jr., H.C., Griggs, E.I.: **Wind Effects on Collectors**, U.S. Department of Energy Report. D.O.-E./CS/35364-TI (1979)

13 McAdams, W.H.: **Heat Transmission**. McGraw Hill (1933)

14 Swinbank, W.C., Quart, J.: **Longwave Radiation from Clear Skies**. Royal Meteorological Society, no. 89 (1963)

15 Unsworth, M.J., J.L. Monteith: **Longwave Radiation at the Ground (I) and Angular Distribution of Incoming Radiation.** Royal Meteorological Society Vol. 101, pp.1-13 (1971)

16 Cole, P.J.: **The Longwave Radiation Incident Upon the External Surface of Buildings**, B.S.E., Vol. 44 (1976)

Chapter

4

Unglazed Collectors

4.1 Introduction

Unglazed collectors represent a substantial proportion of the commercial market for solar thermal collectors. Usually made of a plastic material, they are widely used for the heating of swimming pools, for which they can provide relatively inexpensive low-grade heat. Without the optical losses due to glazing they can have high thermal efficiencies at operating temperatures near to the ambient temperature. At higher temperatures however, substantial losses occur by wind-induced convection and thermal radiation exchange with the field of view. Hence the performance of unglazed collectors is generally sensitive to meteorological conditions.

A standard procedure for testing unglazed collectors is provided by ANSI/ASHRAE Standard 96-1980. To provide a single, repeatable thermal characteristic for the collector performance, this procedure imposes a restricted set of test conditions. Thus the average wind speed for each test point is limited to a maximum of 1.3 m/s, while the ambient temperatures for the test points must be within the range 15-38°C and not differ from each other by more than 10°C.

Much work has taken place in recent years to characterize the performance of unglazed collectors under a wide range of operating conditions and to develop test procedures which can measure the sensitivities of the performance to variations in these conditions. This chapter describes the work done within Task III and how it formed the basis for a new test procedure that was developed jointly by the Task participants. It is included in this report as Appendix A.

4.2 Review of recent work

A series of contributions to the Task's understanding of unglazed collectors was provided by a long-term project undertaken at the Institute of Applied Physics TNO-TH in the Netherlands [1-7]. Havinga and Wijsman [1] reported sensitivity studies on the influence of wind speed and temperature using both computer modelling and experimental measurements in a solar simulator, and showed the influence of the different thermal-radiation regimes indoors and outdoors. Further computer simulations were reported in reference [2], where performance characteristics were plotted as diagrams of energy output versus incident solar irradiation for fixed values of $(T_{fi} - T_a)$. The scatter that occurred in these results was greatly reduced by limiting the wind speed variation.

Outdoor measurements were also made [3] with a forced wind speed of 5 m/s imposed on the natural wind and with the difference between the collector inlet temperature and the ambient temperature held within 1 K of a nominal value of 5 K. These results showed that this approach could be used to measure thermal performance characteristics. However, the scatter that remained was considered unacceptable, and further work was recommended to take into account the additional influence of wind speed fluctuations and variations in effective sky temperature.

To account for effective sky temperature effects, Keizer-Boogh [5] included a radiative exchange term in the Hottel-Whillier-Bliss equation. Effective sky temperatures were measured using a pyrgeometer, however, it was concluded that significant errors occurred in these measurements [6] [1].

The characterization of the thermal performance of unglazed collectors was also investigated by Keller [8] at the Swiss Federal Institute for Reactor Research (now the Paul Scherrer Institute). In this study Keller developed a model for the contributions to the thermal losses by natural and wind-induced convection, thermal radiation exchange, and condensation (which has an important influence on the performance of collectors used as low-temperature sources for heat pumps).

The model was based on correlations for the heat-transfer coefficients, with the sky treated as a grey body emitter at the ambient temperature.[2] Computer simulations based on this model were used by Keller to show the sensitivities of the loss coefficients to meteorological variables and collector parameters.

The work was supported by an experimental program in which $F'U_L$ was measured from night-time collector heat losses. By selecting data for which $V_w > 0.7$ m/s (forced convection), $T_{pm} > T_a$ (no condensation) and $T_{pm} = T_s = T_a$ (no net thermal radiation exchange), and by calculating T_{pm} as the log-mean fluid temperature, Keller was able to determine empirical values for $h_{c,m-p}$ and $h_{c,p-a}$. Using a standard test procedure [9] he also measured the optical efficiencies $F'(\tau\alpha)_{c,n}$ and $F'(\tau\alpha)_d$, and showed that within the errors of measurement they were identical. Since $\tau \equiv 1$ for an unglazed collector, this confirmed the insensitivity of α to the angle of incidence.

---

1. Cooling of the pyrgeometer may be possible to remove this effect. The influence of effective sky temperature on the test results was further discussed in [7].

2. Note that the emittance of the sky ('$\varepsilon\alpha$' in Keller's notation) is equivalent to T_s^4 / T_a^4 here. Although this quantity is usually ≤ 1, Keller noted that it could sometimes have a value > 1.

However, a plot of Keller's data for the dependence of the heat loss to wind speed, showed significant scatter around the curve predicted by the correlation even with five-minute averaged values. This was attributed to the poor correlation between the meteorological wind speed and the air currents over the front and back of the collector, and in a subsequent report [10] it was shown that the same degree of scatter could be seen on a comparison between the measurements made by two anemometers mounted 1m apart. To reduce this problem Keller proposed that rather than the meteorological wind speed, the air speed over the collector aperture "u" be measured, using an anemometer mounted immediately above and parallel to the collector surface.

The model developed by Keller provided a good basis on which to develop a new test method for the thermal performance of unglazed collectors, but, as Task III was concerned with purely solar applications, two simplifications were adopted. Only plate temperatures above the dew point would be considered, eliminating condensation losses and in view of the large uncertainties in the air-speed dependence of losses, only conditions of forced convection would be considered, allowing a simpler correlation for the dependence on air speed to be adopted.

The CEC Collector and System Testing Group, coordinated by the Joint Research Centre at Ispra was also pursuing a program of work on unglazed collectors, and their work was made available to participants of the Task III. Among the studies commissioned, one was undertaken by Svendsen [11] at the Thermal Insulation Laboratory of the Technical University of Denmark.

Svendsen proposed the use of the absorber temperature as a characteristic collector temperature, which he measured directly using a radiation thermometer. Thus the model developed by Svendsen for a freestanding, rack-mounted collector with no back insulation was (in the notation of the present document)

$$\dot{q}_u = \alpha G_T - h_{c,p-a}\,(T_{pm} - T_a) - \varepsilon_p\,\sigma\,(T_{pm}^4 - T_e^4) - h_{c,b-a}\,(T_{bm} - T_a) - \varepsilon_{bg}\,\sigma\,(T_{bm}^4 - T_g^4) \qquad (4.1)$$

with

$$\varepsilon_{bg} = 1/[(1/\varepsilon_b) + (1/\varepsilon_g) - 1] \qquad (4.2)$$

Of the terms on the right-hand side of equation (4.1), the first represents the solar energy absorbed by the absorber plate, the second, the convective and conductive losses from the front surface of the collector to the ambient air ($h_{c,p-a}$ being wind speed dependent), the third, the radiative losses from the front surface to its field of view (including the sky and the ground), modelled as a perfect emitter with an effective temperature T_e, the fourth, the convective and conductive losses from the back of the collector to the ambient air behind the collector, and the fifth, the grey-body radiative exchange between the back of the collector and the background field of view. For a collector insulated at the back, the fifth term was dropped and $h_{c,b-a}$ was replaced by the heat-transfer coefficient for conduction through the thermal insulation.

Svendsen proposed a performance test in which the optical parameters α and ε_p and the heat transfer coefficients were determined by separate laboratory measurements. For the air-speed dependence of the convective heat-loss coefficient it was assumed, based on observation,

$$h_{c,p\text{-}a} = [u/(0.0458\ m/s)]^{0.75} \quad (4.3)$$

The effective temperatures T_e and T_g were obtained by measuring the thermal radiation on the collector surfaces using a pyrgeometer. Finally, in order to relate the absorber temperature to the operating fluid temperature, a separate heat loss measurement was used to determine $h_{c,m\text{-}p}$, the heat-transfer coefficient between the fluid in the collector and the absorber surface. Svendsen's method thus offered simple models for the convective and radiative thermal losses experienced by the collector but a less convenient characterization in terms of the absorber plate temperature.

In June 1987, the results of a study of the outdoor convective heat losses from unglazed solar collectors by Soltau and Angermier at the Ludwig-Maximilians-Universitat in Munich were presented to the Task III participants by Soltau [12]. From measured values of the overall heat-loss coefficient U_L made on an unglazed collector, the radiative heat-transfer coefficient $h_{r,p\text{-}a}$ was subtracted to yield empirical values for the convective heat-transfer coefficient $h_{c,p\text{-}a}$ [13].

The resulting data are plotted against average wind speed and compared with a number of models in Figure 4.1. Curve (1) on the plot shows the linear model [14] due to Jurges:

$$h_{c,p\text{-}a} = 5.7 + 3.8u \quad (4.4)$$

Curve (2) shows a correlation due to Krischer [15] for laminar parallel flow over a rectangular plate:

$$h_{c,p\text{-}a} = 6.8\ L_c^{-0.25}\ u^{0.75} \quad (4.5)$$

where L_c is a characteristic length. Curve (3) is Svendsen's model, equation (4.3), and curve (4) a linear fit to data measured by Test and Lessmann [16] for turbulent flow:

$$h_{c,p\text{-}a} = (8.55 \pm 0.86) + (2.56 \pm 0.32)u \quad (4.6)$$

The inconsistencies in the models and the broad scatter in the data show that the average wind speed is not a sufficient parameter to characterize the convective heat-transfer coefficient. Other variables that influence the value of $h_{c,p\text{-}a}$ were identified by Soltau and Angermeier [17, 18] as the wind direction relative to the collector surface, the rate of change of wind direction, and the free-stream turbulence caused by these wind fluctuations.

Unfortunately these variables cannot easily be measured in a routine collector test, and they are not available in the meteorological data used to predict the performance of collectors in operation. However, if a single air-speed measurement had to suffice for collector testing, it appeared that the value best correlated with the losses would be the free-stream value just above the collector boundary layer - as measured by Keller [19]. Also, in view of the uncertainties, the dependence of the heat-transfer coefficient on air speed in the region of forced convection could be as accurately represented by a straight-line fit as by any other form of correlation.

Perers [20] also showed that a linear dependence of the convective heat-transfer coefficient on airspeed could be fitted to experimental data. In the model used by Perers, the thermal radiation field seen by the collector was also represented by the effective black-body temperature T_e ('T_b' in his notation).

Figure 24 Experimentally measured values of wind induced heat transfer coefficient compared with the models of Jurges (1), Krischer (2), Svendson (3), and Test et al (4) from Ref. 17.

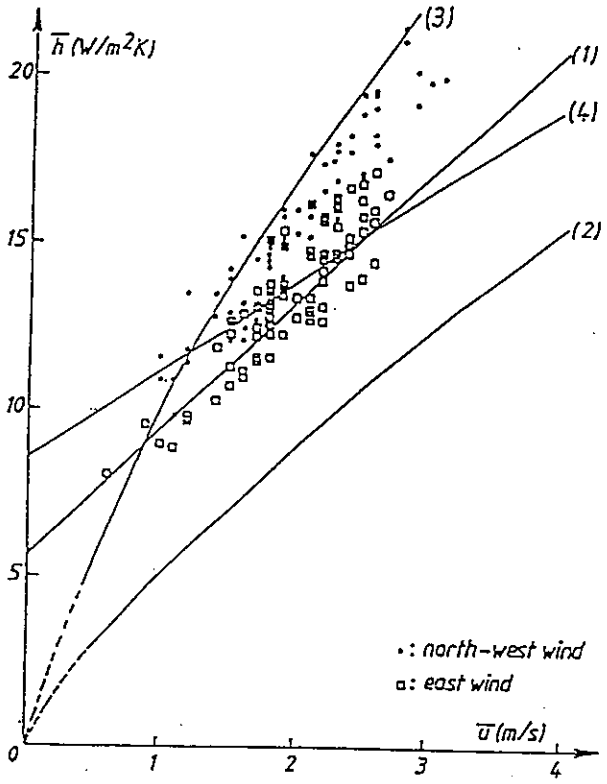

Perers linearized the radiative loss term $\varepsilon_p \sigma (T_{pm}^4 - T_e^4)$ directly, and thus introduced the radiative heat-loss coefficient

$$h_{r,p\text{-}e} = \varepsilon_p \sigma (T_{pm} + T_e)(T_{pm}^2 + T_e^2) \tag{4.7}$$

The term $h_{r,p\text{-}e}(T_{pm} - T_e)$ was then separated into two terms:

$$h_{r,p-e}(T_{pm} - T_e) = h_{r,p-e}(T_{pm} - T_a) + h_{r,p-e}(T_a - T_e) \tag{4.8}$$

the first of which was included in the overall loss coefficient U_L.

By introducing the efficiency factor F′, Perers used the mean fluid temperature as the characteristic temperature of the collector. Both U_L and F′ depend on the air speed, and in each case the dependence was taken

to first order in u. Finally, for outdoor testing Perers included a thermal capacitance term. The 'transient' model thus obtained had the form

$$\dot{q}_u = (a_1 + a_2 u)\, G_T - (b_1 + b_2 u)\, (T_{fm} - T_a) - c\,(T_a - T_e) - C\frac{dT_{fm}}{dt} \qquad (4.9)$$

Indoor and outdoor tests were used to identify the six parameters of this model for an unglazed EPDM tube-and-fin collector. The conclusion from these tests was that the model was adequate to explain both indoor and outdoor performance, with the parameters obtained by multi-linear fit corresponding closely to theoretically predicted values.

There were, however, differences between the indoor and outdoor results that reflected the difficulty of reproducing natural conditions of air flow and thermal radiation in the solar simulator. Radial fans were found to produce higher losses than natural wind at the same air speed, and closer results might have been obtained using fans with a less turbulent air flow. Also, solar simulators produce a significant amount of radiation in the region between the solar radiation detected by a pyranometer and the thermal radiation detected by a pyrgeometer. Unless this radiation can be eliminated, the long-wave radiation in a simulator should be measured with a wider-ranged instrument such as a pyradiometer.

Perers further observed that it was important in testing to measure the ambient air temperature upstream of and near to the collector. The reason for this is that the air first passes over surroundings which may be stagnating at high surface temperatures, so that outdoors there may therefore be a significant temperature difference between air streams coming from different directions. Thus an array of sensors around the collector is needed, with means of weighting the temperature readings according to wind direction.

Drawing on the experience of the individual participants, the task jointly agreed on a characterization model that could form a basis for a test method for unglazed collectors. The model is specified in the following section, and an associated test method is outlined in Appendix A.

4.3 Characterization equations

The general equation assumed for the stationary performance of an unglazed collector has the form:

$$\dot{q}_u = \alpha G_T + \varepsilon_p L_p + \varepsilon_b L_b - U_L\,(T_{pm} - T_a) \qquad (4.10)$$

where

$$\begin{aligned} L_p &= F_g \sigma\,(T_g^4 - T_a^4) + F_s \sigma\,(T_s^4 - T_a^4) \\ &= \sigma\,(T_e^4 - T_a^4) \end{aligned} \qquad (4.11)$$

and

$$U_L = U_{top} + U_{back} \tag{4.12}$$

where

$$U_{top} = h_{c,\,p-a} + h_{r,\,p-a} \tag{4.13}$$

where $h_{c,p-a}$ is dependent on wind velocity and

$$h_{r,\,p-a} = \varepsilon_p \sigma (T_{pm} + T_a)\,(T_{pm}^2 + T_a^2) \tag{4.14}$$

and, for a collector that is thermally insulated at the back,

$$L_b = 0\ W/m^2 \tag{4.15}$$

$$U_{back} = k/d \tag{4.16}$$

or, for a freestanding, rack-mounted collector with no insulation at the back,

$$L_b = \sigma (T_g^4 - T_a^4) \tag{4.17}$$

$$U_{back} = h_{c,\,b-a} + h_{r,\,b-a} \tag{4.18}$$

where $h_{c,b-a}$ is dependent on wind velocity and

$$h_{r,\,b-a} = \varepsilon_b \sigma (T_{bm} + T_a)\,(T_{bm}^2 + T_a^2) \tag{4.19}$$

Normally the front and back surfaces of the absorber have the same emittance ($\varepsilon_b = \varepsilon_p$). Therefore, in most cases, equation (4.10) takes the simple form

$$\dot{q}_u = \alpha G_T + \varepsilon_p L - U_L (T_{pm} - T_a) \tag{4.20}$$

with

$$L = L_p + L_b \tag{4.21}$$

Thus L is the total thermal irradiance received by the collector (relative to the collector ambient temperature).

4.3.1 Temperature dependence of $h_{r,p-a}$ and $h_{r,b-a}$

If we expand $h_{r,p-a}$ in equation (4.14) to first order in both $(T_{pm} - T_a)$ and variations δT_a in T_a we get

$$h_{r,\,p-a} \approx \varepsilon_p \sigma T_a^3 \left[1 + 3\frac{(T_{pm} - T_a)}{2T_a} + 3\frac{\delta T_a}{T_a} \right] \tag{4.22}$$

Hence a 10% change in $h_{r,p-a}$ results from a 20 °C change in $(T_{pm} - T_a)$ or a 10 °C change in T_a. But a 10% change in $h_{r,p-a}$ represents a change of only about 1-5% in U_{top}, since in equation (4.14) $h_{c,p-a}$ typically has a value of 20 - 60 W/(m^2 K) compared with the approximate value 6 W/(m^2 K) for $h_{r,p-a}$.

An identical argument shows that the U_{back} is also insensitive to changes in $(T_{bm} - T_a)$ and T_a.

4.3.2 Alternative models

With the use of the collector efficiency factor F′ or the collector heat-removal factor F_R we can rewrite equation (4.20) in the equivalent forms

$$\dot{q}_u = F' [\alpha G_T + \varepsilon_p L - U_L (T_{fm} - T_a)] \tag{4.23}$$

and

$$\dot{q}_u = F_R [\alpha G_T + \varepsilon_p L - U_L (T_{fi} - T_a)] \tag{4.24}$$

Since the mean plate temperature of an unglazed collector is accessible to measurement, we may use equation (4.20) directly as the basis of a thermal performance test, with measurements of $\dot{q}_u$, G_T, L and $(T_{pm} - T_a)$ used to determine values for α, ε_p, and U_L. Alternatively, (4.23) could be used, with measurements of $\dot{q}_u$, G_T, L and $(T_{fm} - T_a)$, to determine values for $F'\alpha$, $F'\varepsilon_p$, and $F'U_L$, or equation (4.24) used, with measurements of $\dot{q}_u$, G_T, L and $(T_{fi} - T_a)$, to identify the parameters $F_R\alpha$, $F_R\varepsilon_p$ and F_RU_L.

In each case, because of the practical difficulty of obtaining variability in L, it is more convenient to measure the optical constants α and ε_p separately, as recommended by Svendsen [11]. Then equations (4.20), (4.23) and (4.24) can be reduced to the simple forms

$$\dot{q}_u = \alpha G - U_L (T_{pm} - T_a) \tag{4.25}$$

$$\dot{q}_u = F'\alpha G - F'U_L (T_{fm} - T_a) \tag{4.26}$$

and

$$\dot{q}_u = F_R \alpha G - F_R U_L (T_{fi} - T_a) \tag{4.27}$$

where

$$G = G_T + \left(\frac{\varepsilon_p}{\alpha}\right) L \tag{4.28}$$

G may be treated as an effective normal irradiance appropriate for unglazed collectors.

The measurement of α and ε_p may be accomplished by standard laboratory measurement, however a portable emissometer is probably adequate. The absorptance can be measured using a small pyranometer, as described by Svendsen [11]. The pyranometer first measures the solar irradiance normal to the absorber surface, and is then turned to measure the reflected irradiance. Provided the pyranometer is sufficiently small and not too close to the surface, the shading of the absorber by the pyranometer is negligible.

For the non-selective absorber surfaces usual on unglazed collectors, however, it is observed that

$$\frac{\varepsilon_p}{\alpha} \approx 0.95 \tag{4.29}$$

and hence when evaluating G according to equation (4.28) we can in most cases simply assume the constant value 0.95 for ε_p/α.

It may be noted that equations (4.25), (4.26) and (4.27) are equivalent, and the choice between them is one of convenience. Thus, since the mean absorber-plate temperature is not easy to measure in a test and equation (4.26) is not the most convenient form for predicting the performance of the collector in a heating system, equation (4.27) is recommended.

A possible source of error when using equation (4.26) is the estimation of T_{fm} as the average of the inlet and outlet fluid temperatures. To calculate this error we eliminate G between equations (4.26) and (4.27), express $\dot{q}_u$ in the form given by

$$\dot{q}_u = \dot{m}\, Cp(T_{fe} - T_{fi})/ A_{ab} \tag{4.30}$$

and assume F_R has the form given by equation (1.5). Hence we obtain

$$\frac{(T_{fm} - T_{fi})}{(T_{fe} - T_{fi})} = \frac{1}{x} + \frac{1}{\ln(1-x)} \tag{4.31}$$

with

$$x = \frac{F_R U_L A_a}{\dot{m} C_p} \tag{4.32}$$

Hence, to first order in x, the fractional error in $(T_{fm} - T_{fi})$ obtained by estimating T_{fm} as the average of the inlet and outlet temperatures is

$$\frac{[T_{fm} - (T_{fi} + T_{fe})/2]}{(T_{fm} - T_{fi})} \approx \frac{x}{6} \tag{4.33}$$

Another approximation for this error is obtained by noting that

$$F'' = \frac{(1 - e^{-x})}{x} \approx 1 - \frac{x}{2} \tag{4.34}$$

Hence, to first order in (1-F''),

$$\frac{[T_{fm} - (T_{fi} + T_{fe})/2]}{(T_{fm} - T_{fi})} \approx \frac{(1 - F'')}{3} \tag{4.35}$$

Under normal operating conditions, with $T_{fm} > T_{fi} \geq T_a$, this gives an upper bound on the fractional error in $(T_{fm} - T_a)$. Thus we can be sure that the estimated value of $(T_{fm} - T_a)$ is accurate providing that $x/6 << 1$, i.e. that

$$\frac{\dot{m} C_p}{A_a} \gg \frac{F_R U_L}{6} \tag{4.36}$$

This means that providing the flowrate of the heat-transfer fluid per unit collector area is sufficiently high, a large value of U_L does not necessarily preclude the use of T_{fm} as the characteristic collector temperature. When we consider the airspeed dependence of the parameters, however, the use of equation (4.27) has advantages over the choice of equation (4.26). Generally $F'\alpha$ and $F'U_L$ have been observed to have a less simple dependence on u than $F_R\alpha$ and $F_R U_L$, both of which can usually be assumed linear in u [17].[3]

[3] In a recent paper Green and Cruz Costa [21], commenting on an earlier draft of the present document, claimed to show that the linear assumption was not valid for their data. However, in the range of airspeed $u \geq 0.5$ m/s for which the model is assumed valid, their plots of $F'\alpha$, $F'U_L$, $F_R\alpha$ and $F_R U_L$ are all linear to well within the uncertainties of measurement.

Hence we arrive at the model adopted by the Task as a basis for its recommended test procedure:

$$\dot{q}_u = (a_1 - a_2 u)\, G - (b_1 + b_2 u)\, \Delta T \qquad (4.37)$$

with G given by equation (4.28) and $\Delta T = (T_{fi} - T_a)$. A test procedure based on this model is given in Appendix A.

4.4 Validation of proposed test method

In reference [19] Soltau reviewed the proposed model and presented the results of testing a small array (3.5 m x 3.5 m) of unglazed collectors mounted at a slope of 45° on an insulated artificial roof. The testing was done outdoors over a period of two days and the variables were averaged over 20 minute periods. The collectors were operated at temperatures above and below the ambient temperature, with and without solar radiation, and with highly turbulent wind from both the east and the north-west. The wind-speed anemometers were placed in the free-stream region about 0.1 m above the collector absorber.

Wind-dependent collector parameters were estimated from the data and found to be consistent with values from other data. The average model error was 9 W/m^2 (5% of the mean energy yield). Hence the model was deemed valid for the data set.

In addition to the above mentioned tests, experimental test results for 7 unglazed swimming pool collectors were determined by the Solar Calorimetry Laboratory of Queen's University in the Solar Simulator of the Canadian National Solar Test Facility [22, 23]. The collectors were tested according to the method discussed in Appendix A of this document but with the use of artificially simulated wind and solar irradiance. The results of these tests indicated a significant wind dependence for the commercially available collectors tested. Application of the proposed test method was easily accomplished in the simulator facility and the performance data was found to produce a good fit to equation (4.37).

Independently, Nguyen (Laboratoire de Thermodynamique et d'Energetique, EPF-Lausanne, Switzerland) and Keller et al. (Paul Scherrer Institute, Villigen, Switzerland) [24, 25], showed that the model was also in good agreement with a large body of test data.

4.5 References

1 Havinga, J. and A.J.Th. M. Wijsman: **Characterization of Uncovered Solar Collectors I** TPD-no. 203.270 Institute of Applied Physics TN0-TH, PO Box 155, 2600 AD Delft, The Netherlands, August (1983)

2 Havinga, J. and A.J.Th.M. Wijsman, TPD-no. 203.270: **Characterization of Uncovered Solar Collectors II** Institute of Applied Physics TN0-TH,PO Box 155, 2600 AD Delft, The Netherlands (1983)

3 Havinga, J. and A.J.Th.M. Wijsman: **Characterization of Uncovered Solar Collectors III.** Institute of Applied Physics TN0-TH,PO Box 155, 2600 AD Delft, The Netherlands (1984)

4 Keizer-Boogh, E.M: **Characterization of Uncovered Solar Collectors III.** TPD-no. 203.270, Institute of Applied Physics TN0-TH,PO Box 155, 2600 AD Delft, The Netherlands (1985)

5 Keizer-Boogh, E.M: **Infrared Radiation Correction for Uncovered Collector.** Unpublished paper presented at Task III Meeting, Kingston, Canada (1987)

6 Keizer-Boogh, E.M: **Measurements of Infrared Sky Radiation.** Unpublished paper presented at Task III Meeting, Seville, Spain (1987)

7 Keizer-Boogh, E.M. and J. Havinga: **Influence of Infrared Radiation Exchange on the Performance of Unglazed Collectors.** (Translated from **Characterizing Uncovered Collectors**, TPD report no. 314.225, October 1987), Institute of Applied Physics TNO-TH, PO Box 155, 2600 AD Delft, The Netherlands (1988)

8 Keller, J., **Characterization of the thermal performance of uncovered collectors by parameters including the dependence on wind velocity, humidity and infrared sky radiation as well as on solar irradiance**, 2nd IEA SHAC Workshop on Solar Assisted Heat Pumps with Ground Coupled Storage, Vienna (1985)

9 Swiss Standard SN165001/1, **Methods of Testing to Determine the Thermal Performance of Solar Collectors, Part I: Covered Collectors using Liquids as Heat Transfer Fluids.** Swiss Association for Standardization, Zurich (1984)

10 Keller, J: **Unglazed collectors.** Unpublished paper presented at Task III Meeting, Delft, the Netherlands (1986)

11 Svendsen, S.: **Performance of uncovered collectors.** Report No. 85-17, Thermal Insulation Laboratory, Technical University of Denmark (1985)

12 Soltau, H. and G. Angermeier: **The wind related heat transfer coefficient at a rectangular plate in the natural environment**, Sektion Physik, Ludwig-Maximilians-Universität München, Munich, Germany (1987)

13 Soltau, H.: **Das Thermische Verhalten Offener Kollektoren**, Ph.D. Thesis, Ludwig-Maximilians-Universität Müchen, Munich, Germany (1988)

14 Duffie, J. A. and W.A. Beckman: **Solar Engineering of Thermal Processes**, Wiley-Interscience (1980)

15 Krischer, O.: **Die wissenschaftlichen Grundlagen der Trocknungstechnik**, Springer-Verlag, Berlin, Heidelberg, New York (1978)

16 Test, F.L., R.C. Lessmann and A. Johary: **Heat transfer during wind flow over rectangular bodies in the natural environment**, Trans. ASME J of Heat Transfer 103, pp 261-167 (1981)

17 Soltau, H.: **The thermal performance of uncovered collectors**, ISES Congress, Hamburg, Pergamon Press (1987)

18 Soltau, H. and G. Angermeier: **Modelling the Heat Transfer of a Flat Plate in the Highly Turbulent Wind Field of an Urban Environment**, Proceedings of the ITHC, Jerusalem (1990)

19 Soltau, H.: **Testing the thermal performance of uncovered flat-plate solar collectors**, Unpublished paper presented at Task III meeting, Seville, Spain (1987)

20 Perers, B.: **Performance testing of unglazed collectors: Wind and longwave radiation influence**, Unpublished paper presented at Task III meeting, Kingston, Canada (1987)

21 Green, A.A. and J. Cruz Costa: **The influence of wind on unglazed solar collectors**, Translated from- **Influencia do vento em colectores solares sem cobertura**, Comunicacoes do 4 Congresso Iberico e 2 Ibero-American de Energia Solar, Porto, Julho (1988)

22 Harrison, S.J., D. McClenahan and V.H. Nielsen: **Testing Unglazed Solar Collector Thermal Performance; Evaluation of a Method to Characterize Wind Effects**, ISES Conference Proceedings, Kobe, Japan (1989)

23 Harrison, McClenahan, Nielsen: **The Performance of Unglazed Solar Collectors**, Proceedings of SESCI Annual Conference, Canada (1989)

24 Nguyen, D.L.: **Experimental results of the thermal performance of uncovered solar collectors**, Unpublished paper presented at Task III meeting, Seville, Spain (1987)

25 Keller, J., Köllike, A., Nguyen, D.L. and Gianola, J.-Cl.: **Capteurs sans Couverture**, Ecole Polytechnique Fédérale de Lausanne/Paul Scherrer Institut, Janvier (1991)

Chapter

5

Evacuated-tubular, Heat-pipe and Boiling/condensing Collectors

5.1 Evacuated Tube Collectors

Evacuated envelopes are often placed around the absorber plate in solar collectors to minimize convection and conduction heat losses. Many configurations have been tried in the past to arrive at technically feasible and commercially viable products [1,2].

Lowering the pressure in the envelope to values below one tenth of an atmosphere is adequate to eliminate convection heat loss from the collector, (i.e. Nu = 1) but does not eliminate conduction through the remaining air [3]. To significantly reduce the conduction in the absorber to glazing gap, (i.e. to one tenth of the atmospheric value), the pressure must be further reduced to values below 0.1 Pa. At these pressures, with a good selective absorber coating, overall heat loss coefficients of the order of 1 $W/m^2\,^oC$ can be achieved.

A consequence of evacuating the space around the absorber is that the full force of atmospheric pressure ($> 10^5$ N/m^2) is applied to the cover. As a result, structural considerations have required the use of cylindrical glass tubes in virtually all cases.

A major criterion in the design of evacuated tube solar collectors is the maintenance of a high vacuum over the life of the collector. A significant technical difficulty has been the seal between the glass envelope and the metal tube carrying the heat transfer fluid. "Flow through" designs such as is the case shown in Figure 25, require that two glass to metal seals be made, one at each end of the evacuated tube, and that provision be made for the difference in thermal expansion between the absorber plate and glass cylindrical cover. In the case of the Sanyo design, shown in Figure 25, this latter problem is handled by the use of expansion bellows located at one end of the collector tube.

The operation of a vacuum tube solar collector with a flow-through design (similar to the Sanyo) is fairly simple to analyze thermally [4]. Its performance may be adequately described by the relationships presented in general heat transfer and solar engineering texts [5]. The heat loss characteristics will be very close to those described in section 3.2.2, where heat losses from the absorber to the surrounding glass envelope are dominated by radiation heat transfer. This results in a non-linear variation in heat loss coefficient with increasing plate temperature especially at high operating temperatures which may exceed 200°C. The magnitude of the heat loss is highly dependent on the emissivity of the absorber plate, with non-selective absorber surfaces approaching heat loss coefficients of 7 $W/m^2\,^oC$.

The value of the heat removal factor F_R may be calculated according to section 1.2.2 of Chapter 1, for tube and fin absorber designs. It may be shown [6] for the case of collectors with low values of heat loss coefficient, U_L, that minimal variation in the collector heat removal factor, F_R, occurs as a result of changes in the heat transfer fluid flow rate, the fluid side heat transfer coefficient, h_f, or for small variations in U_L.

Figure 25 Construction details of the Sanyo evacuated tube solar collector incorporating a "flow-through design".

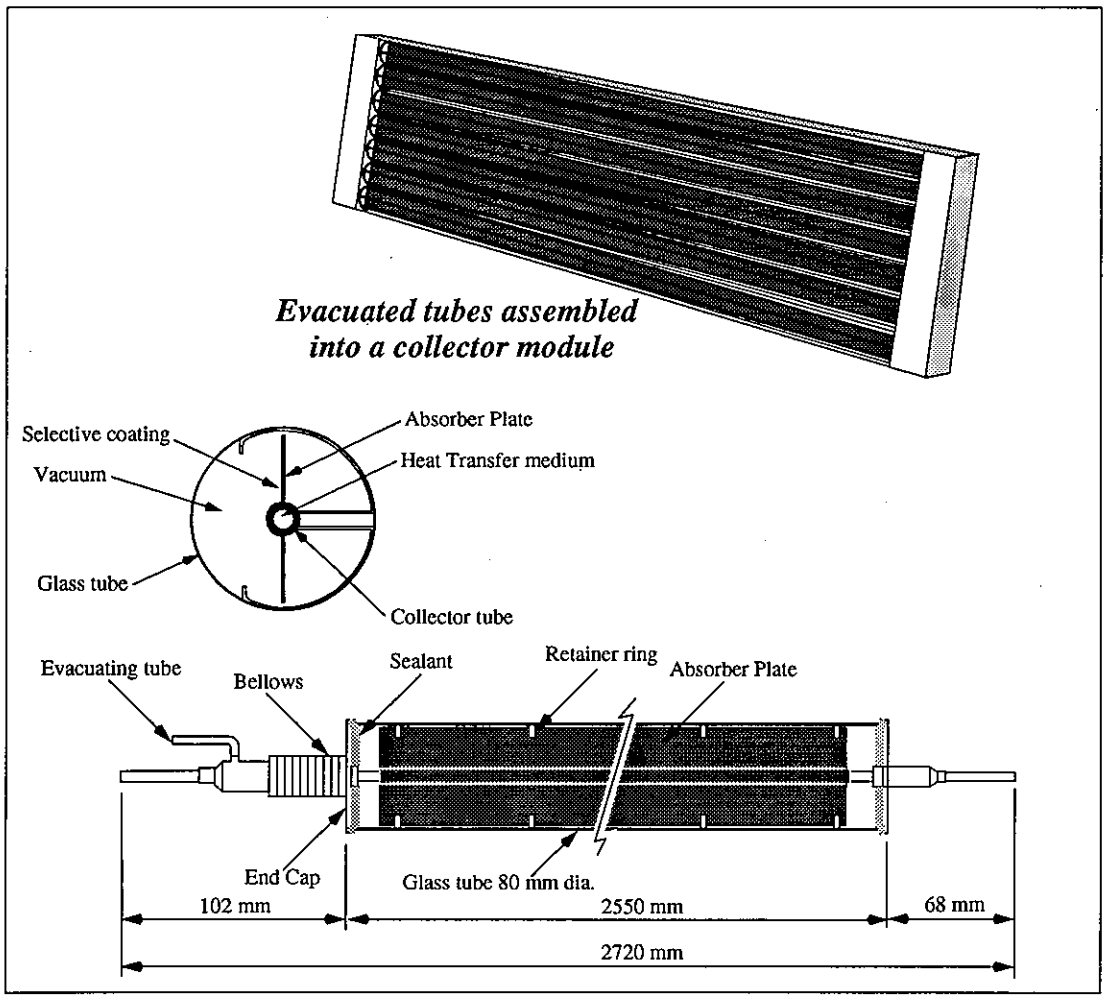

5.1.1 Thermal Performance Test Results

Experimental results as measured in a solar simulator test facility are shown in Figures 26 and 27 for the Sanyo Solar collector [7]. Of significance is the apparent dependance of performance on the irradiance level used during testing. This effect is due to the non-linear variation of the heat loss coefficient with increasing temperature as was demonstrated in section 3.3.1 of Chapter 3. A suitable characterizing equation should be able to account for the variation in U_L with temperature.

5.1.2 Thermal Performance Representation

In Chapter 3, the variability of the heat loss coefficient was illustrated for three collector types including one dominated by convection heat losses, one dominated by radiation losses, and finally, one exhibiting both radiation and convection heat losses. To account for this variability in U_L, the use of a higher order relationship to represent the value of U_L has been proposed by many researchers. A complete discussion of alternative expressions for U_L is presented in Chapter 7 and reference [6], however the relationship of Cooper [8], eq. 5.1, has been widely used.

$$U_{top} = C + D(\Delta T) \tag{5.1}$$

In most cases U_L is effectively equal to U_{top} and letting ΔT equal $(T_{fi}-T_a)$ or $(T_{fm}-T_a)$, we may substitute eq. 5.1 into eq. 1.7 and 1.8 respectively, giving

$$\eta = \frac{Q_U}{G_T \cdot A_a} = F_R\left((\tau\alpha)_e - C\frac{(T_{fi}-T_a)}{G_T} - D\frac{(T_{fi}-T_a)^2}{G_T}\right) \tag{5.2}$$

and

$$\eta = \frac{Q_U}{G_T \cdot A_a} = F'\left((\tau\alpha)_e - C\frac{(T_{fm}-T_a)}{G_T} - D\frac{(T_{fm}-T_a)^2}{G_T}\right) \tag{5.3}$$

These two expressions have been widely accepted internationally and should not be mistaken for a simple second order polynomial equation with respect to $(\Delta T/G_T)$. This mistake has often been made in an attempt to fit non-linear experimental data. Experimental results presented by Harrison [7] have shown that these equations are suitable for characterizing both flat-plate and evacuated tube collectors with selective absorber coatings, operating over a limited range of ambient air temperatures, T_a, and at low to moderate inlet fluid temperatures, i.e. $T_{fi} < 100^o$ C.

These relationships however, are not universal in their application, especially in the case of collectors with non-selective absorbers or for evacuated collectors operating at higher temperatures. In these cases, the relationships given in Chapter 7 produce better characterizations of the heat loss characteristics.

Figure.26 Experimental results for the Sanyo evacuated tube solar collector with selective absorber surface.

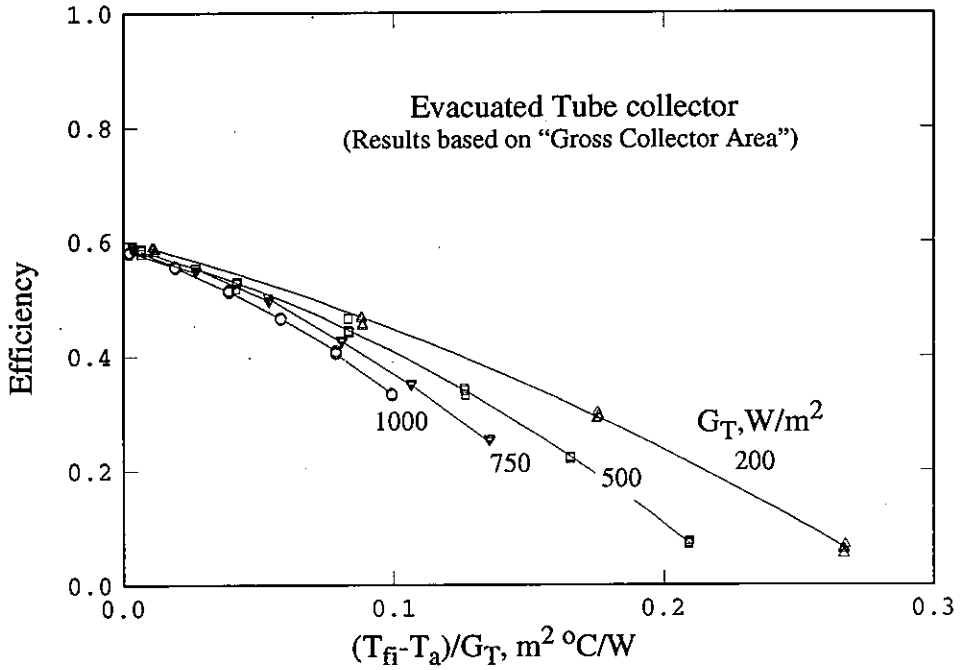

Figure 27 Data of Fig. 26 for the evacuated vacuum tube collector, plotted in "input/output" format.

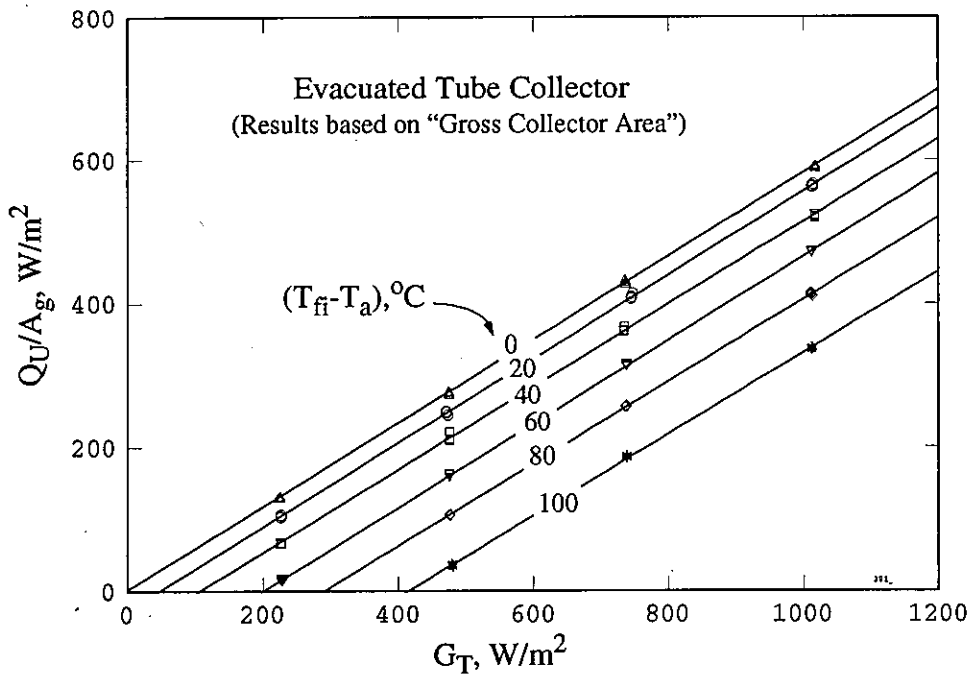

5.2 Evacuated Tube With Heat-pipe

In an effort to minimize the number of glass to metal seals, to eliminate the use of expansion bellows and to simplify the flow path of the heat transfer fluid, manufacturers have developed the use of heat-pipes [9,10,11] or two-phase thermosiphons as a means of transferring heat from the absorber plate to the heat transfer fluid, Figure 28. Commercial evacuated tube collector modules are normally attached to a common insulated header pipe to produce collector modules as shown in Figure 29.

In these designs, heat is removed from the absorber plate of the evacuated tube by the vaporization of a heat transfer fluid enclosed within a tube running through it. This tube extends through a single glass to metal seal to an external condenser [12,13].

The condenser is either immersed in the flow of a cooling fluid or mechanically clamped to a header pipe with cooling liquid flowing through it, Figure 28. Commercially available designs have largely incorporated the use of two-phase thermosiphons rather than classical heat-pipes which utilize a "wicking mate-

Figure 28 Conceptual diagram of a "heat-pipe" absorber thermally connected to a fluid circulation loop by a metal heat transfer clamping block.

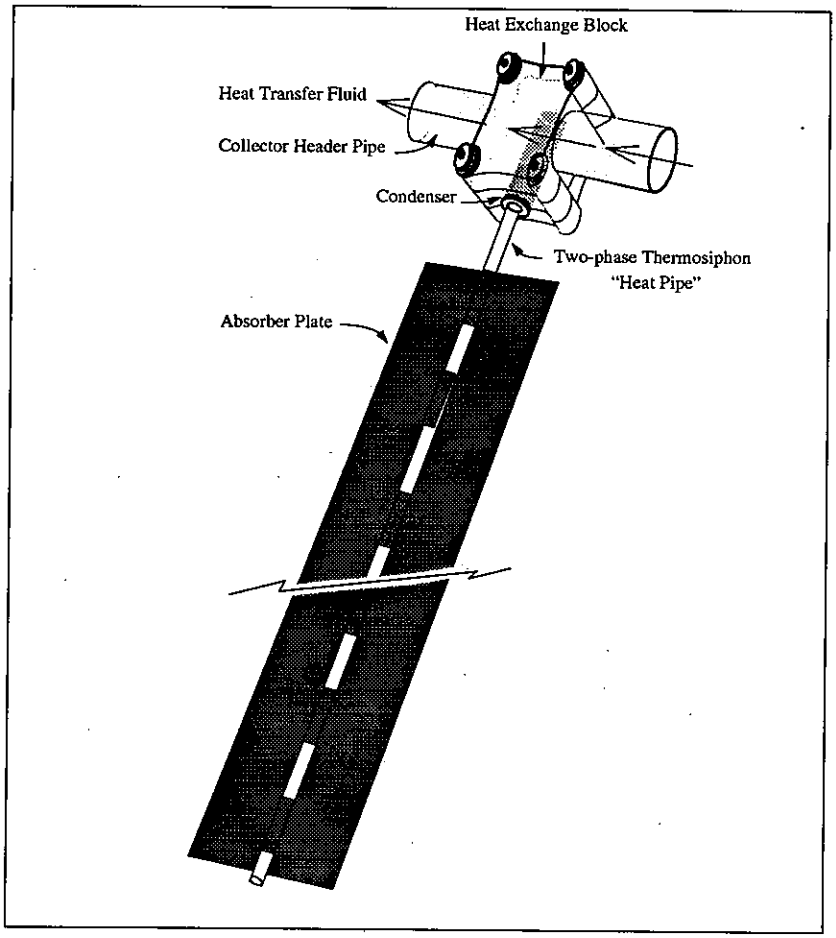

rial" to return the condensed working fluid back to the heat input section. The two-phase thermosiphon (or wickless heat-pipe) relies on gravity to return the condensate back to the bottom of the transport tube in similar fashion to the boiling condensing collector which allows thermal diode operation, (see section 5.3). These devices also have significantly less fluid (typically 1 to 2 cc. of working fluid) and may use water, or refrigerants as working fluids. Philips has produced versions using water, iso-butane or neopentane [11].

The choice of working fluid affects the start up temperature level of the heat pipe, the heat transfer rate and the upper temperature limit for operation of the heat pipe. These devices are usually characterized by high heat transfer rates [14] but have the disadvantage of requiring an additional heat exchange surface between the heat-pipe condenser and the collector header. The performance of the heat-pipe is directly related to the temperature of the condenser.

Figure 29 Construction details of the Philips evacuated tube and 19 tube version solar collector module, (dimensions shown in mm.).

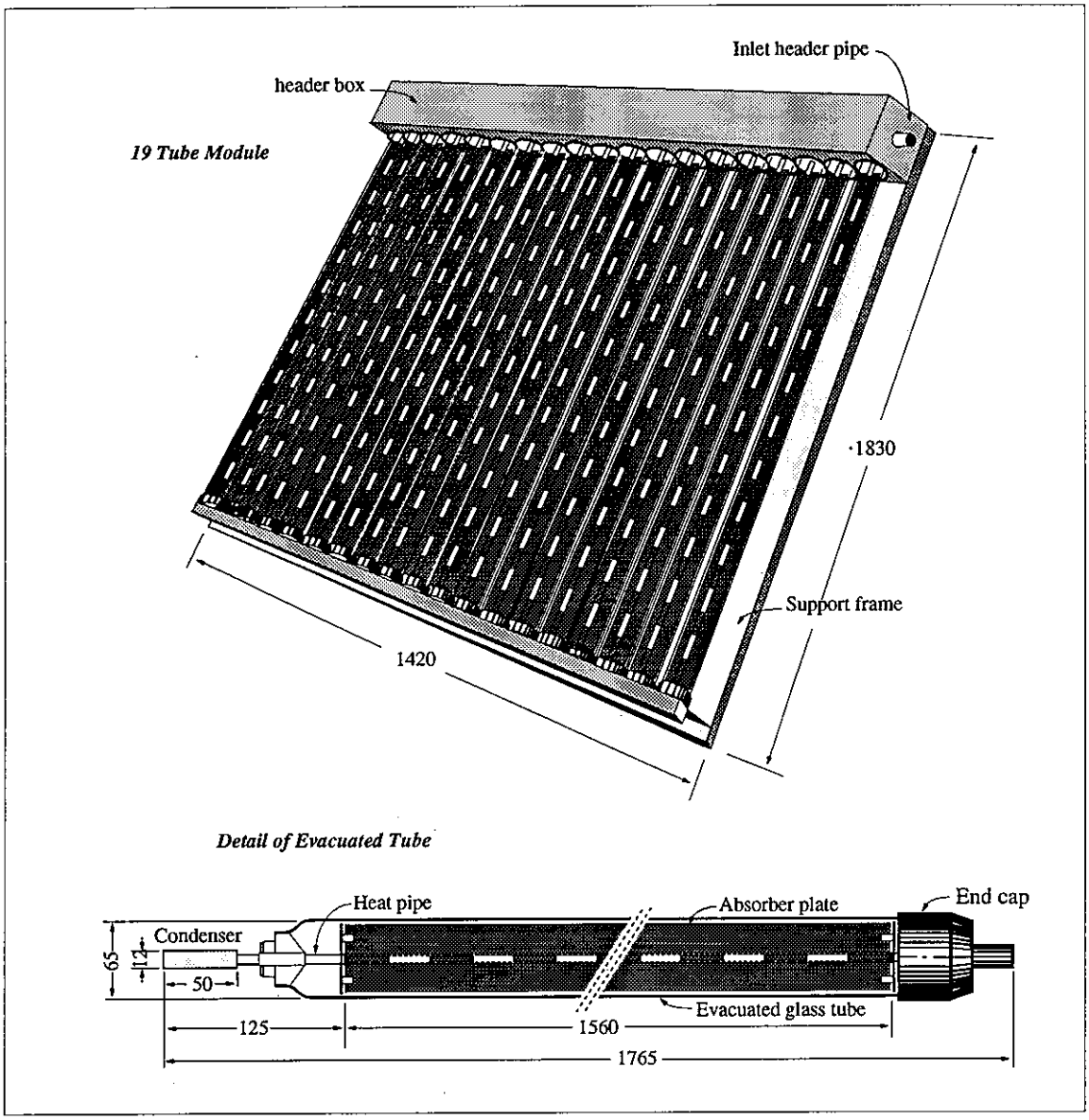

5.2.1 Thermal Performance Test Results

The measured performance of the evacuated tube collector with heat-pipe is similar to that of the conventional evacuated-tube solar collector, i.e. an apparent irradiance dependance, Figures 30 and 31. As previously stated this effect is due to the variation of the heat loss coefficient with temperature level. Another unique feature of the collector tested was the occurrence of "dryout" of the heat pipe at conditions of high solar irradiance and high temperature [11]. This condition limits the heat transfer from the absorber plate to the condenser effectively shutting down the solar collector and avoiding over-temperature conditions in the solar system. The conditions at which heat-pipe dryout occurs is highly dependant on the fluid used in the heat-pipe.

5.2.2 Thermal Performance Representation

Thermal models for evacuated tube collectors with heat-pipe absorbers have been developed [12,13,15]. It has been shown that the performance of the heat-pipe can be represented by an equivalent resistance that is a function of condenser temperature [16,17].

To account for the effect of variation in heat transfer of the absorber plate, deVaan [18] recommended fitting the value of $F_R(\tau\alpha)_e$ for the collector by an equation involving the difference between the collector fluid temperature and the ambient temperature, i.e.

$$F_R(\tau\alpha)_e = A + B\,(\Delta T) \tag{5.4}$$

Substituting eq. 5.4 into eq. 5.2 and 5.3 respectively, gives

$$\eta = \frac{Q_U}{G_T \cdot A_a} = F_R\left(A + B\,(T_{fi} - T_a) - C\frac{(T_{fi} - T_a)}{G_T} - D\frac{(T_{fi} - T_a)^2}{G_T}\right) \tag{5.5}$$

and

$$\eta = \frac{Q_U}{G_T \cdot A_a} = F'\left(A + B\,(T_{fm} - T_a) - C\frac{(T_{fm} - T_a)}{G_T} - D\frac{(T_{fm} - T_a)^2}{G_T}\right) \tag{5.6}$$

These equations are suitable for evacuated tube collectors with selective absorber coatings, operating over a limited range of ambient air temperatures and at moderate inlet fluid temperatures, i.e. $T_{fi} < 100^{\circ}$ C. As with eqs. 5.2 and 5.3, for collectors with non-selective absorbers or for collectors operating at higher temperatures, the relationships given in Chapter 7 may produce better characterizations.

Figure 30 Experimental results for the Philips evacuated tube solar collector with heat pipe absorber.

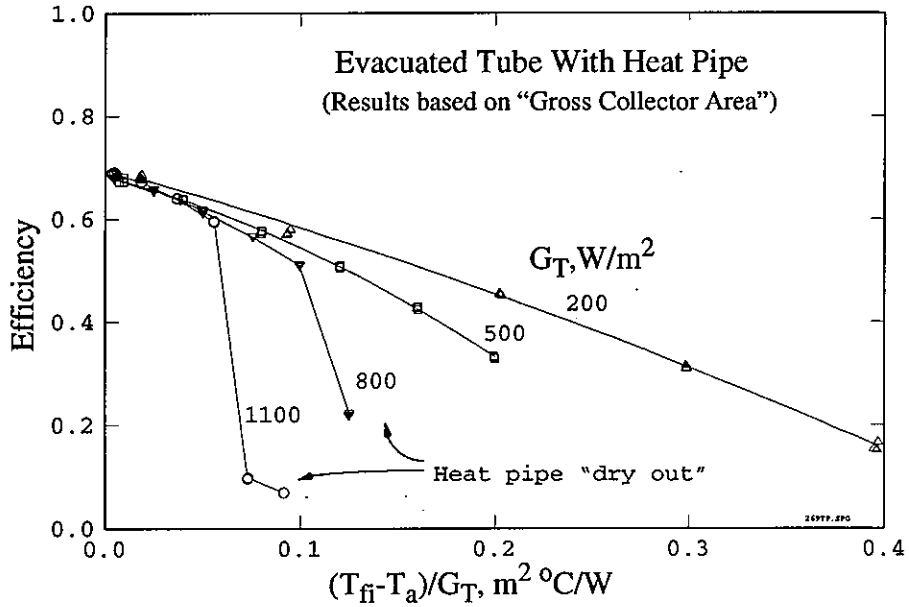

Figure 31 Data of Fig. 30 for the evacuated vacuum tube collector with heat pipe absorber, plotted in "input/output" format.

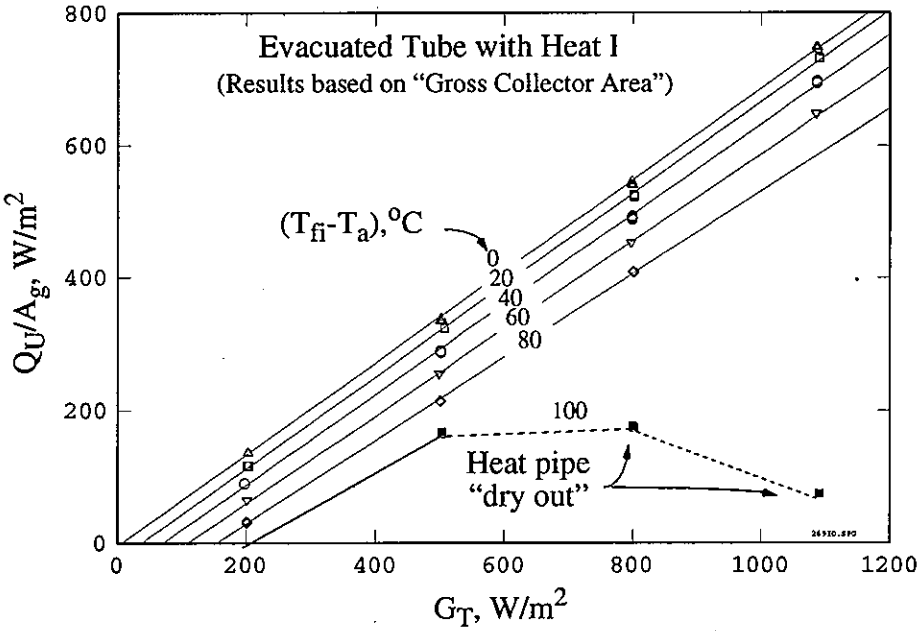

5.3 Boiling/Condensing Flat Plate Solar Collectors

Boiling/condensing collectors as originally developed by Rush [19,20,21] offer the potential for significant advantages in the design of solar heating systems including thermal "diode" operation, and simplified plumbing and control strategies. The construction of this type of collector is similar to a conventional flat-plate solar collector except for the configuration of the absorber plate.

A conceptual illustration of the absorber plate of a boiling/condensing solar collector is shown in Figure 32. It consists of finned tubes which are coupled to a splash heat exchanger at the top of the assembly and a manifold at the bottom. The absorber is partially charged with a working fluid and evacuated of air and unwanted gases. The upper and lower parts of the enclosed volume contain vapour and liquid respectively. The splash heat exchanger consists of two concentric tubes, with the liquid to be heated passing through the inner tube. When the absorber plate is heated, the liquid in the tubes boils. This boiling action produces vapour which travels up the riser tubes pushing slugs of fluid with them which splash on the condenser/heat exchanger tube giving up latent and sensible heat. This heat is absorbed by the fluid circulating through the condenser tube and is transported to the load for use or storage, i.e. domestic hot water heating or process applications.

Separate tubes located at the back of the splash heat exchanger allow liquid (condensate) to drain to the bottom horizontal manifold. The scrubbing action of the slug flow in the vapour generating tubes as well as the splashing-condensing action on the heat transfer tube are both effective means of heat transfer.

The characterization of thermal performance for boiling/condensing solar collectors presents a significant challenge. Complex patterns of boiling and condensation heat transfer occur within the absorber plate. The performance of the solar collector depends primarily on the solar energy incident on the collector, the fluid inlet temperature, the ambient temperature, and the magnitude of the heat losses from the absorber. The inlet temperature determines the temperature distribution through the condenser which, in turn, affects the vapour pressure of the working fluid within the absorber plate. At "start-up" this liquid/vapour mixture is in equilibrium at the saturation pressure corresponding to its saturation temperature. The saturation temperature is largely determined by the temperature of the condenser pipe which in turn is determined by the temperature of cooling water which flows through it.

The power level to the absorber is not only a function of the intensity of the solar irradiance striking the absorber plate but also the level of the heat losses occurring from the absorber plate. The heat losses from the absorber of a conventional solar collector are usually related to collector inlet temperature or the mean fluid temperature, (average of collector inlet and outlet temperatures).

In the boiling/condensing collector, the temperature of the absorber is in fact significantly higher than these temperatures and consequently this must be accounted for in the determination of the collector losses. It is the temperature level required for boiling that causes the operation of the boiling/condensing collector to appear significantly different from conventional collectors. To be able to fully predict the operation of this type of collector, an estimate of this temperature excursion from the collector inlet temperature must be made for a range of input power and temperature levels. Absorber plate temperatures may be 10 K to 60 K higher than the fluid inlet temperature depending on the operating mode of the collector. During quiescent periods when the working fluid is not perking, the upper part of the tube is also subjected to "dryout" with higher rates of heat loss.

Figure 32 Construction details of an absorber plate as used in a typical boiling/condensing solar collector

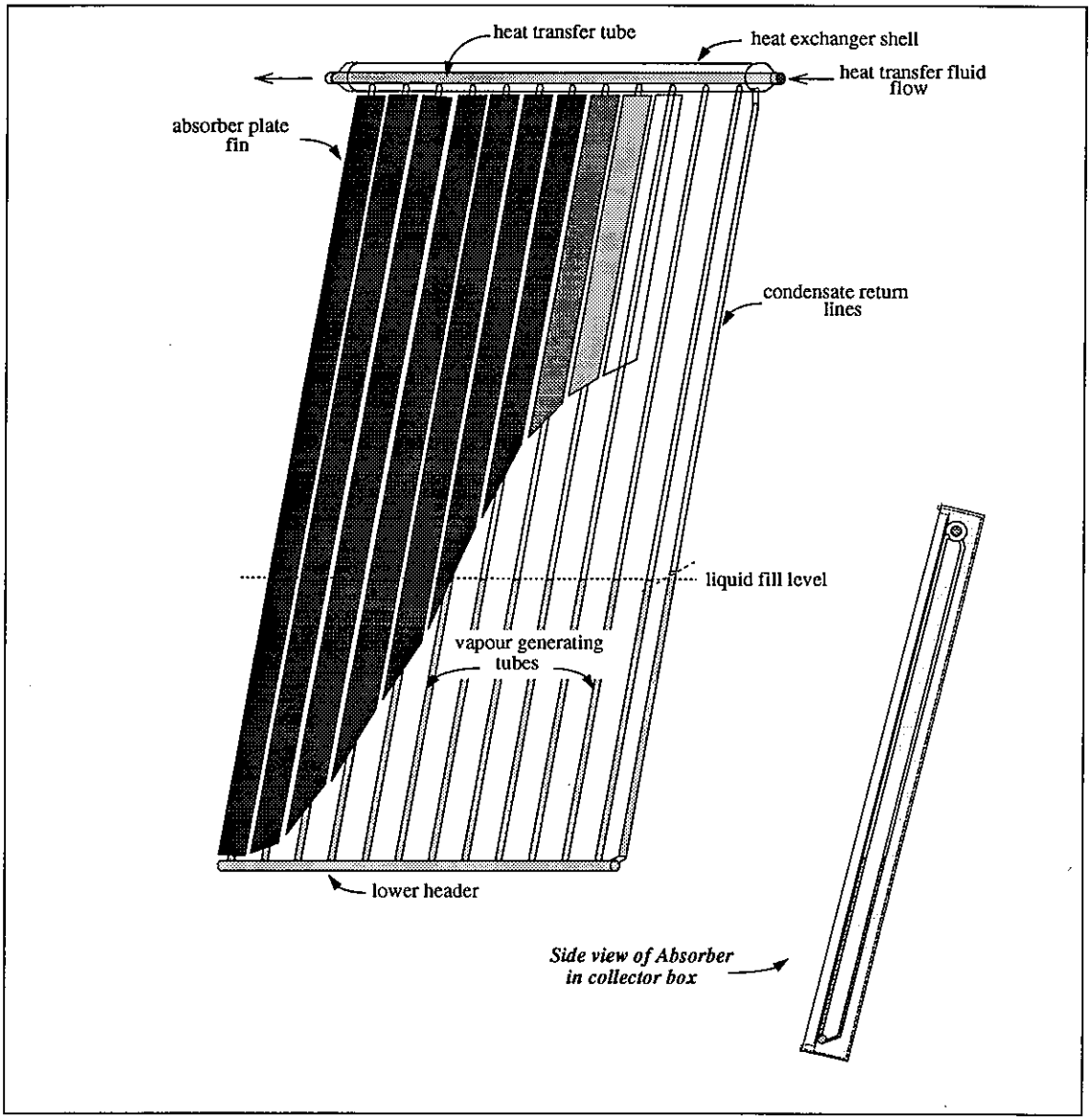

5.3.1 Thermal Performance Test Results

Thermal performance test results for a boiling/condensing collector of the type illustrated in Figure 32 are shown in Figures 33 and 34 [7]. Results shown are for data measured in a solar simulator and averaged over 100 minute test intervals. All the data was taken at a fixed ambient temperature but for a range of irradiance levels and inlet fluid temperatures. It would appear from Figure 33 that the performance of the boiling/condensing collector is very dependent on irradiance level. In actual fact it may be seen from Figure 34 that the performance is very close to that of a conventional flat-plate collector except that useful output is not obtained from the collector until a threshold irradiance level has been achieved. The level of threshold irradiance is shown in Figure 34 as $G^{\#}$ and may be thought of as the minimum irradiance level required for

boiling to start in the riser tubes. If the line for $(T_{fi}-T_a)=0$ is extended to the Q_U/A_g axis (thermal output), its intercept, E, would be negative. This effectively represents the heat loss from the solar collector that must be overcome before the net output from the collector is positive.

Figure 33 Averaged thermal performance data for the boiling/condensing collector as measured in a Solar Simulator [7].

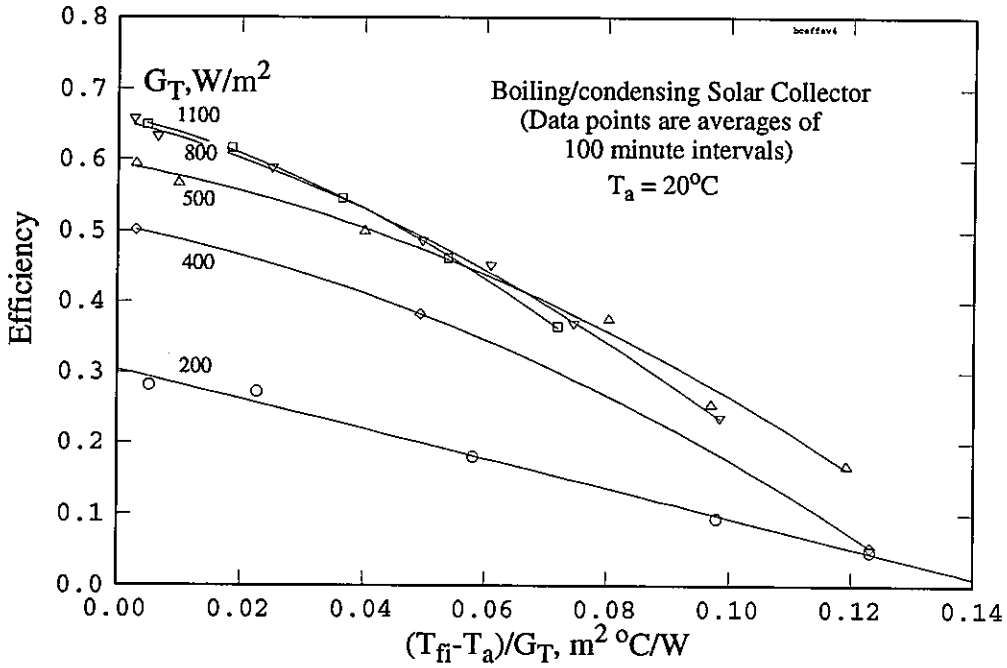

5.3.2 Thermal Performance Representations

For flat plate collectors incorporating a boiling/condensing fluid and an integral condenser, an additional term is required to account for the differences in temperature between the absorber plate and the heat transfer fluid circulating through the collector. A recent study by Price et al. [22] has investigated the performance of a solar collector with boiling fluid in the absorber (although with external condenser). The performance of the boiling collector is represented as

$$Q_U/A_a = F_R[G_T(\tau\alpha)_e - U_L(T_{boil}-T_a)] \qquad (5.7)$$

where T_{boil} is the temperature at which boiling occurs in the absorber plate.

The onset of boiling can be related to the saturation temperature of the fluid in the absorber. Assuming an equilibrium condition, this saturation pressure and temperature should be closely related to the temperature in the absorber plate's condenser. This, in turn, is very close to the mean fluid temperature of the fluid flowing into and out of the absorber, i.e. cooling the condenser. The onset of boiling requires a temperature

Figure 34 Thermal performance test data for the flat-plate boiling/condensing solar collector plotted as input/output curves, 100 min. averages .

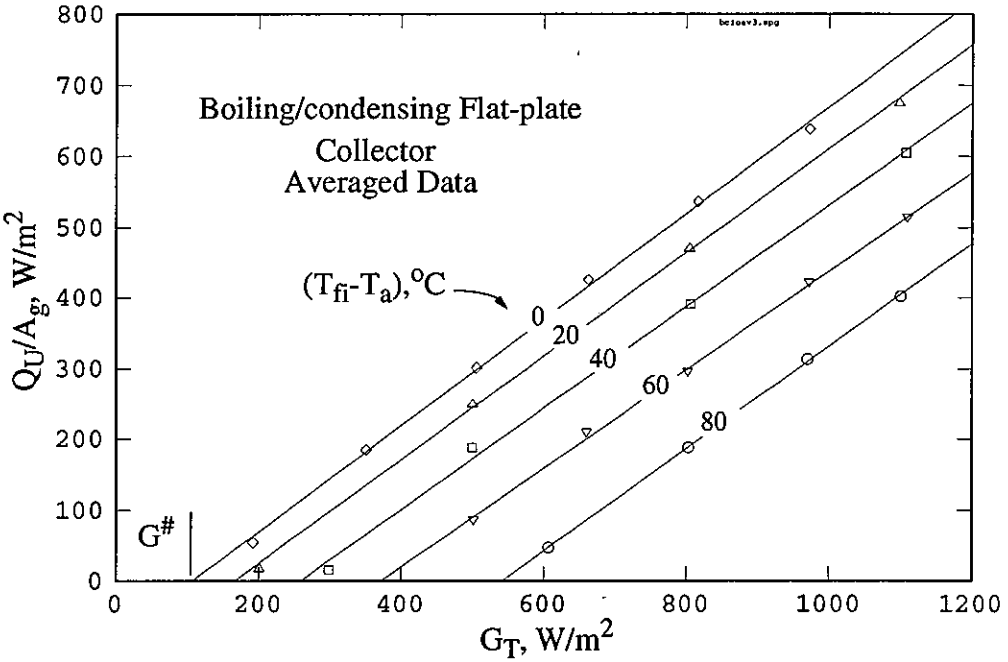

above the fluid's saturation temperature which is usually referred to as the "excess temperature". Excess temperatures can range from a couple of degrees to more than 40 K for a boiling heat flux of 2000 W/m^2. The value depends on the surface properties adjacent to the boiling surface and the local heat flux.

During start up, the boiling/condensing collector will not start boiling until the absorber has reached a level equivalent to the saturation temperature of the fluid in the absorber plus the value of "excess temperature", ΔT_{ex}, corresponding to the particular conditions. In effect

$$T_{boil} = T_{sat} + \Delta T_{ex} \tag{5.8}$$

and assuming $T_{sat} \approx T_{cm} \approx T_{fi} \approx T_{fm}$, where T_{cm} is the mean temperature of the condenser, then

$$T_{boil} = T_{fm} + \Delta T_{ex} \tag{5.9}$$

and

$$Q_U/A_a = F'[G_T(\tau\alpha)_e - U_L(T_{fm}+\Delta T_{ex}-T_a)] \tag{5.10}$$

or

$$Q_U/A_a = F_R[G_T(\tau\alpha)_e - U_L(T_{fi}+\Delta T_{ex}-T_a)] \quad (5.11)$$

which may be rearranged to give

$$Q_U/A_a = F_R[G_T(\tau\alpha)_e - U_L(T_{fi}-T_a) - U_L(\Delta T_{ex})] \quad (5.12)$$

In this form it may be seen that the effect of ΔT_{ex} is to increase the absorber plate temperature above that of the non-boiling collector. In effect the value of E is $U_L(\Delta T_{ex})$ and may be seen to be equivalent to $F_R(\tau\alpha)_e G^{\#}$, i.e.

$$E = F_R U_L(\Delta T_{ex}) = F_R(\tau\alpha)_e G^{\#} \quad (5.13)$$

This term accounts for the differences in temperature between the absorber plate and the heat transfer fluid circulating through the condenser.

Characterization equations for boiling/condensing collectors have been proposed [7] where a threshold irradiance, $G^{\#}$, has been introduced, i.e.

$$Q_U/A_a = [F_R(\tau\alpha)(G_T - G^{\#}) - F_R U_L(T_{fi}-T_a)] \quad (5.14)$$

and applying the concepts of Eqs. 5.1 and 5.13 this gives

$$Q_U/A_a = [A(G_T) - C(T_{fi}-T_a) - D(T_{fi}-T_a)^2 - E] \quad (5.15)$$

Equation 5.15 has shown to produce good results when fitted to experimental data for a boiling/condensing collector which was obtained at a fixed ambient air temperature but a later study investigating the effects of ambient air temperature on the performance of this type of collector showed that in fact the value of "E" varied for tests conducted at different values of ambient air temperature [23]. A detailed investigation of the heat transfer processes and an analysis of experimental results conducted at different ambients temperatures showed that "E" and the value of ΔT_{ex} is a non-linear function of T_{fi}, Figure 35. Values of ΔT_{ex} are plotted along with corresponding values of $F_R U_L$ as derived from experimental test results. To account for this effect, the value of "E" has been represented by

$$E = e \cdot exp(f \cdot T_{fi}) \quad (5.16)$$

The magnitude of ΔT_{ex} is seen to depend on the temperature of the integral condenser within the absorber which is directly related to the temperature of heat transfer fluid entering the collector, T_{fi}. Results taken at ambient temperatures ranging from 2 to 20°C showed that a good fit to the experimental data could be achieved by the use of eq. 5.15 with the addition of a non-linear expression to represent "E" as a function of T_{fi} [6], i.e.

$$Q_U/A_a = [A(G_T) - C(T_{fi}-T_a) - D(T_{fi}-T_a)^2 - e \cdot exp(f \cdot T_{fi})] \quad (5.17)$$

Figure 35 Plot of excess temperature and heat loss coefficient for a range of T_a and T_{fi}, [6]

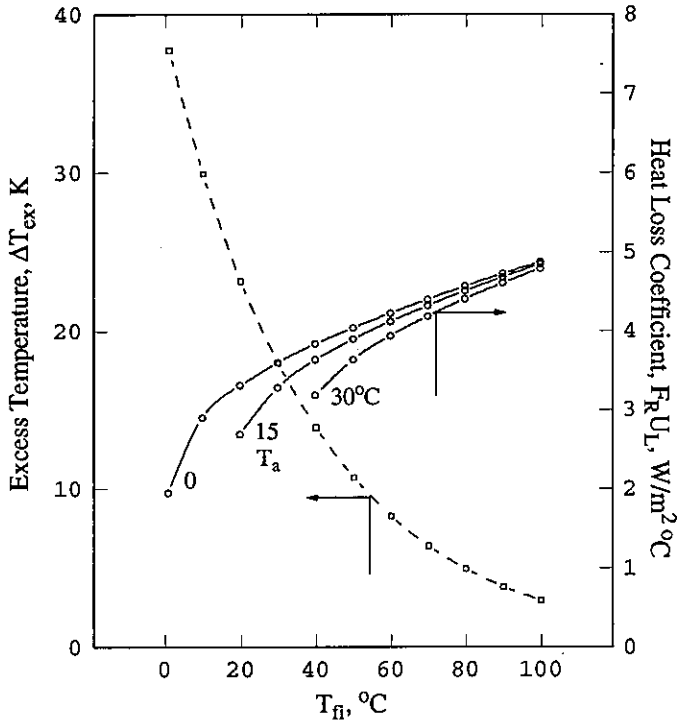

5.4 References

1. Harding, G.L., et al.: **High Performance Evacuated Solar Collectors - Design, Applications And Viability**, International Journal of Ambient Energy, Vol. 3, Number 4, (1982)

2. Graham, B.J.: A Survey of Evacuated Solar Collectors. **Proceedings of the Biennial Congress of the International Solar Energy Society**, Atlanta, Ga. (1979) and published in Solar Age (Nov. 1979)

3. **Solar Energy Conversion**, An Introductory Course, Selected Lectures from the 5th Course on Solar energy Conversion, University of Waterloo, Canada, (1978) edited by A.E. Dixon and J.D. Leslie, Pergammon Press.

4. Barrett, A.L. et al.: **Thermal Modeling of Evacuated Tubular Collectors**. Proceedings of the 1988 Annual Meeting of the American Solar Energy Society, Cambridge, MA, USA (1988)

5. Duffie, J.A., Beckman, W.A.: **Solar Engineering of Thermal Processes**. John Wiley & Sons, N.Y., (1980)

6. Harrison, S.J.: **Improved Characterization for the Thermal Performance of Solar Collectors**. Ph.D. Thesis, Department of Mechanical Engineering, Queen's University, Kingston, Canada (1992)

7. Harrison, S.J.: **The Effects of Irradiance Level on Thermal Performance Tests of Solar Collectors**. Proceedings of the Biennial Congress of the International Solar Energy Society, Montreal, P.Q., Canada (1985)

8. Cooper, P.I.: The Testing of Flat Plate Solar Collectors. **The Institution of Engineers' Annual Engineering Conference**, Townsville, Australia (1976)

9. Philips Corporation: **An Evacuated Tubular Solar Collector incorporating a Heat Pipe**. Philips Technical Review, Volume 40 (1982)

10. de Grijs, J.C., and R. J. H. Jetten: **Evacuated Tubular Collectors With Heat Pipes Simplify Module And System Design**, Proceedings of the International Solar Energy Soc., Perth, Australia, pp. 1061-1070 (1983)

11. de Grijs, J.C. et al.: **Evacuated Tubular Collector with Two Phase Heat Transfer into the System**. Proceedings of the International Solar Energy Society, Brighton, U.K., pp. 176-180 (1981)

12. Hull, J.R. et al.: **Analysis of Heat-pipe Absorbers in Evacuated-tube Solar Collectors**, Report ANL-86-16, Argonne National Laboratory, 9700 South Cass Ave., Argonne, Illinois, USA 90439 (1986)

13. Hull, J.R.: **Comparison of Heat Transfer in Solar Collectors with Heat Pipe versus Flow Through Absorbers**. Journal of Solar Energy 108, 253 (1987)

14. Kreith, F. and Bohn,: **Principles of Heat Transfer**, Harper & Row, New York (1986)

15. Tabassum, S.A.: **Heat Removal From A Solar-energy Collector With Heat Pipe**, Solar and Wind Technology, Vol. 5, No. 2., pp. 141-145 (1985)

16. Carpenter, A.M.: **Development of a Closed Loop, Preheat Solar Domestic Hot Water System**, M.Sc. Thesis, Dept. of Mech. Engineering, Queen's University at Kingston, Canada (1989)

17. Artola, J.C. and Coates, L.: **Experimental Determination of the Philips VTR-361 Heat Pipe**, B.Sc. Thesis, Queen's University at Kingston, Canada (1988)

18. de Vaan, R.L.C. (N.V. Philips' Gloeilampenfabrieken, Eindhoven, Netherlands): **Personal Communication** (1982)

19. Rush, C.K., and R.F.Sendall: **Performance of a Boiling Condensing Flat-Plate Collector**. Proceedings of 1977 SESCI National Conference, Edmonton, Canada (1977)

20. Rush, C.K.: **The Solar siphon Flat Plate Collector**, Alternate Energy Sources 3, Volume 1, Solar Energy 1, Hemisphere Publishing, Washington D.C., USA (1980)

21. Rush, C.K.: **Hot Water Heating in Remote Areas Using Solar Siphons**, Solwest 80, Proceedings of the Annual SESCI Conference,Vancouver, B.C., Canada (1980)

22. Price, H.W., Klein, S.A., Beckman, W.A.: Analysis of Boiling Flat-Plate Collectors. **Transactions of the ASME, Vol. 108**, 150 (1986)

23. Johnson, G.P., Harrison, S.J.: Characterization of a Boiling/Condensing Flat Plate Solar Collector. **Proceedings of the SESCI '89 Conference**, Penticton, B.C. , Canada (1989)

Chapter

6

Low-concentration Ratio Concentrating Collectors

Non-tracking concentrators can be treated by the standard models described in Chapter 1. For tracking concentrators the same methodology as described in Chapter 1 is applicable with only slight modifications; i.e., the characteristic equation and the incident angle modifier are somewhat different.

6.1 Characterizing equations

The Hottel-Whillier-Bliss equation can be modified as follows to characterize the thermal performance of a tracking concentrator.

$$\dot{Q}_u = A_a F_R \{ [(\tau\alpha)\rho\gamma]_e G_b - \left(\frac{A_r}{A_a}\right) U_L (T_{fi} - T_a) \} \tag{6.1}$$

Notice that the effective normal irradiance has been replaced by the direct component since only the beam solar irradiance is concentrated on the receiver. As for flat-plate collectors, the effective optical term $[(\tau\alpha)\rho\gamma]_e$ can be replaced by the value at normal incidence multiplied by the incident angle modifier i.e.

$$[(\tau\alpha)\rho\gamma]_e = [(\tau\alpha)\rho\gamma]_{e,n} K_{\alpha\tau} \tag{6.2}$$

then the Hottel-Whillier-Bliss efficiency equation for a tracking concentrator is given by

$$\eta = F_R K_{\alpha\tau} [(\tau\alpha)\rho\gamma]_{e,n} - F_R \left[\left(\frac{A_r}{A_a} \right) U_L \frac{(T_{fi} - T_a)}{G_b} \right] \tag{6.3}$$

The terms $(\tau\alpha)$, ρ and γ are often difficult to describe analytically because they are dependent on the actual concentrator geometry, concentrator optics, receiver geometry and receiver optics which may differ significantly from the original design specifications. For a single axis tracker, as the incident angle of the beam irradiance increases, these terms become more complex.

6.2 Recommendations for thermal performance testing

Concentrating collectors can be tested for thermal performance using the same procedures as described in ASHRAE Standard 93-1986 [1].

Unfortunately, most of the existing solar irradiance simulators cannot be used to test concentrating collectors because the irradiance does not meet the optical collimation requirements for the concentrator. Consequently, for the collectors with concentration ratios greater than 3:1, testing should be done outdoors.

6.2.1 Incidence Angle Modifier

If the test apparatus is adjusted to maintain the inlet fluid temperature equal to ambient temperature [i.e. $(T_{fi}-T_a) = \Delta T = 0$], the incident angle modifier can be determined from

$$K_{\alpha\tau} = \frac{\eta_{\Delta T = 0}}{F_R [(\tau\alpha)\rho\gamma]_{e,n}} \tag{6.4}$$

where $\eta_{\Delta T = 0}$ is the measured efficiency at the desired incident angle and for the inlet fluid temperature equal to the ambient temperature. The denominator in (6.4) is determined from equation (6.3) based on a regression analysis of the efficiency data measured at normal incidence.

For a one axis tracking linear concentrator the incident angle modifier consists of several separate optical loss terms, i.e.: incident angle effects for the receiver, end loss to account for the fact that part of the receiver is not illuminated during off-normal operation, screening losses to account for shadows on the reflector caused by the support structure for the receiver, changes in the projected aperture area normal to the direct solar irradiation, and the optical aberrations caused by off-normal reflection or refraction from the concentrator. The end losses are a function of the focal length and total length of the concentrator/receiver. Screening losses are directly related to the amount of shadow on the concentrator caused by support structures. The concentrator/receiver optical losses are caused by beam spreading from the concentrator and radiation properties of the receiver.

For testing at normal incidence, the collector should be mounted on the test stand in such a way that the aperture plane is maintained normal to the beam irradiance throughout the entire test.

For testing at a specified incident angle the collector should be mounted on a tracking test stand (altazimuth collector mount) so that the orientation of the collector can be arbitrarily adjusted with respect to the direction of the incident solar radiation. The collector should be oriented so that the test incident angles between it and the direct solar radiation are approximately 0°, 30°, 45° and 60°. For some collectors with unusual optical performance characteristics, other incident angles will be more appropriate. If possible, data should be taken during a single day.

6.2.1.1 Two Axis Tracking Collectors

Incident angle modifiers are not applicable to two axis tracking collectors. For these concentrators there will be data scatter, however, due to the tracking capabilities of the mounts which are an integral part of the system. Collectors of this type are normally evaluated outdoors, after minor field adjustments according to the manufacturers specification. The concentrating collector is therefore tested as received with no separate evaluation of the tracking error.

6.3 Example Test Results

Typical normal incidence test results for a parabolic trough collector with an east-west axis are given in Figure 36. Each normal efficiency test was completed within 30 minutes of solar noon. Incidence angle test results are given in Figure 37.

6.4 References

1 ANSI/ASHRAE Standard 93-1986: **Methods of testing to determine the thermal performance of solar collectors**, The American Society of Heating, Refrigerating and Air-Conditioning Engineers, Inc., 1791 Tullie Circle, NE, Atlanta, GA 30329 (1986)

Figure 36 Example normal Incidence efficiency test data for a single-axis tracking collector.

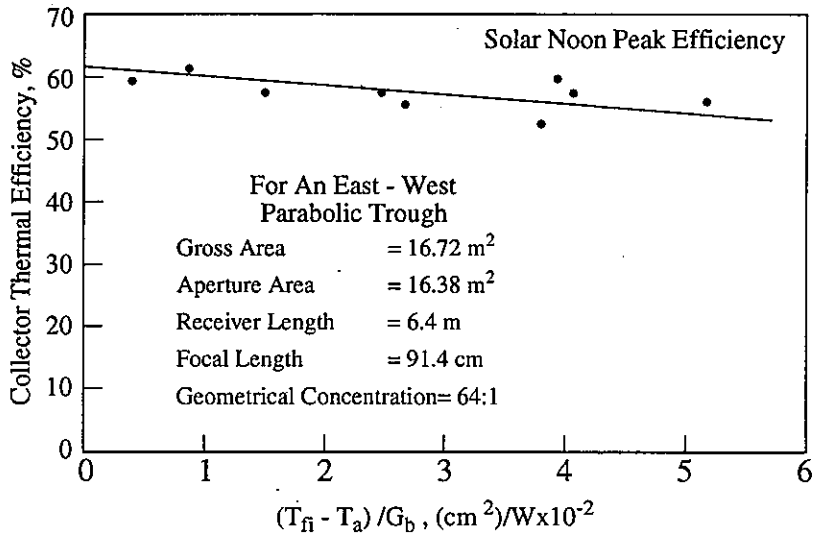

Figure 37 Typical incident angle modifier test data.

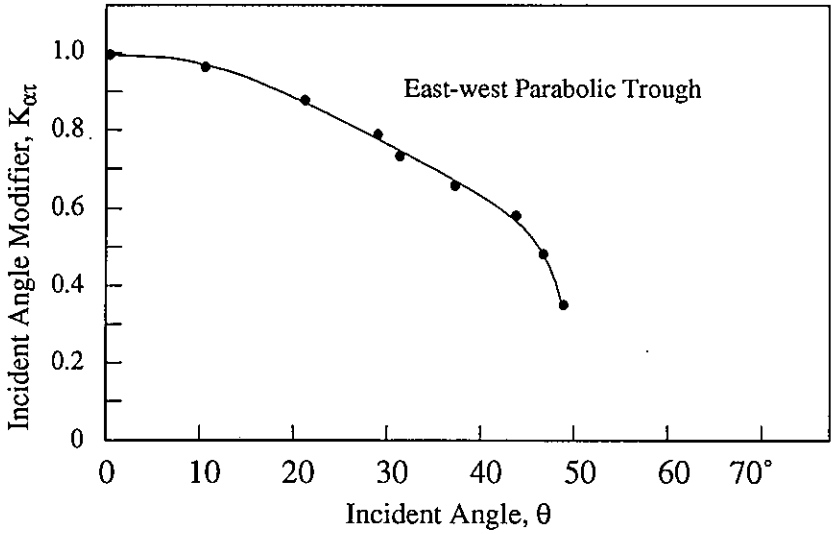

Chapter

7

Generalized Models for Solar Collector Thermal Performance

7.1 Introduction

The selection of a suitable performance characteristic for a particular solar collector type must be a compromise between testing complexity, time, and cost relative to the accuracy required. Generalized performance characteristics have been proposed [1] that account for a large number of environmental factors but require extensive testing under a full range of test conditions. In many cases the cost of such evaluations may be prohibitive.

The effects of meteorological conditions on collector performance have been shown to be significant. Dissimilar solar collectors respond differently to these varying conditions. In addition to variations in the heat loss characteristics of solar collectors caused by environmental factors, heat removal in boiling/condensing collectors has been shown to be dependent on power and temperature levels. In the case of evacuated tubes, optical effects are significantly different than those of conventional flat-plates. Unglazed collectors are sensitive to wind effects and long-wave thermal irradiance.

To arrive at generalized performance equations, relationships must be determined that will account for these effects for a wide range of collector types. This chapter will review general relationships intended to account for these effects.

7.2 Glazed Solar Collectors.

The difficulty associated with the development of a single performance equation to represent all classes of glazed solar collectors may be seen in Figure 38 where values of U_{top} for the three collectors discussed in Chapter 3 are plotted for a range of ambient air temperatures, versus T_{pm}.

It may be seen that the variation of U_{top} with these parameters is not consistent for the three collector types[4], complicating the choice of a representative equation for U_{top}. The Hottel-Whillier-Bliss representation of collector performance assumes that the heat loss coefficient from the absorber surface is effectively constant. Figure 38 illustrates that this is not true and in fact trends are not functionally consistent throughout collector types, i.e. selective or non-selective absorber and vacuum type.

7.2.1 U_{top} Correlation Equations

A number of increasingly complex equations have been developed, in an attempt to arrive at improved representations for collector performance that account for the variations in U_L due to atmospheric factors. As discussed in section 5.1.2 of Chapter 5, equation (5.1) proposed by Cooper [2] has become widely accepted to represent the heat loss coefficient for flat-plate solar collectors, i.e.

$$U_{top} = C + D(\Delta T) \tag{7.1}$$

where $\Delta T = T_{pm}-T_a$, $T_{fi}-T_a$ or $T_{fm}-T_a$.

Figure 38 Plot of "top heat loss coefficient" versus mean absorber temperature for three collector types.

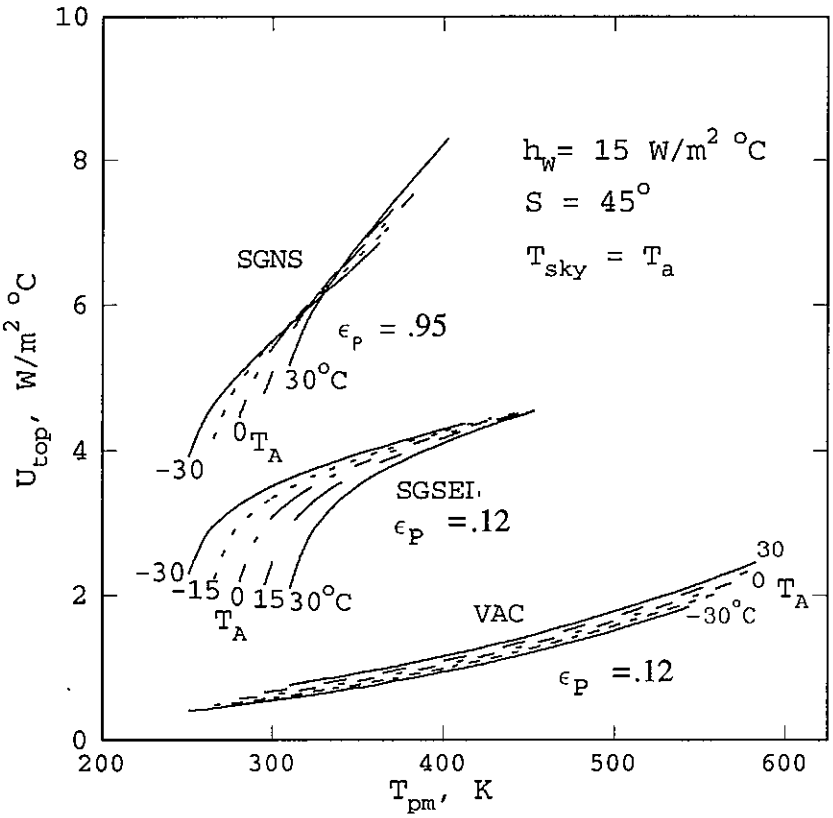

4. Collector designation: SGNS, a flat-plate solar collector with non-selective absorber; SGSEL, a collector with a selective absorber surface and; VAC, a collector with a vacuum envelope surrounding the absorber plate.

This relationship is primarily a result of the observation of experimentally derived heat loss coefficients that were measured in laboratory environments [2].

If the values of U_{top} which were shown if Figure 16 are plotted against (T_{pm}-T_a) as shown in Figures 39 and 40, it becomes apparent why this expression represents an significant improvement over the HWB assumption of constant U_{top}. However, for the SGSEL collector, Figures 39 and 40, it may be seen that a small variation in U_{top} still occurs primarily due to variation in the air properties with temperature.

The limitation of this relationship is further demonstrated in Figure 41 where values of U_{top} are plotted for a collector with non-selective surface (SGNS). In this case, the "absolute" temperature effects are larger due to the non-linear radiative heat transfer from the hot absorber plate to the cool cover glazing. The limitations of equation (7.1) are evident in its inability to adequately represent the non-linear radiative heat transfer that is dependent on the absolute temperature and not the temperature difference ΔT, Figure 42.

Tabor [3] proposed the use of a heat loss equation of the form

$$U_{top} = (\Delta T)^b \tag{7.2}$$

in order to better represent the non-linear dependence of the heat loss. This relationship, while accurately representing the post conduction regime of the heat loss, does not represent the radiative component well.

Figure 39 Values of U_{top} plotted versus T_{pm}-T_a for collector with selective absorber.

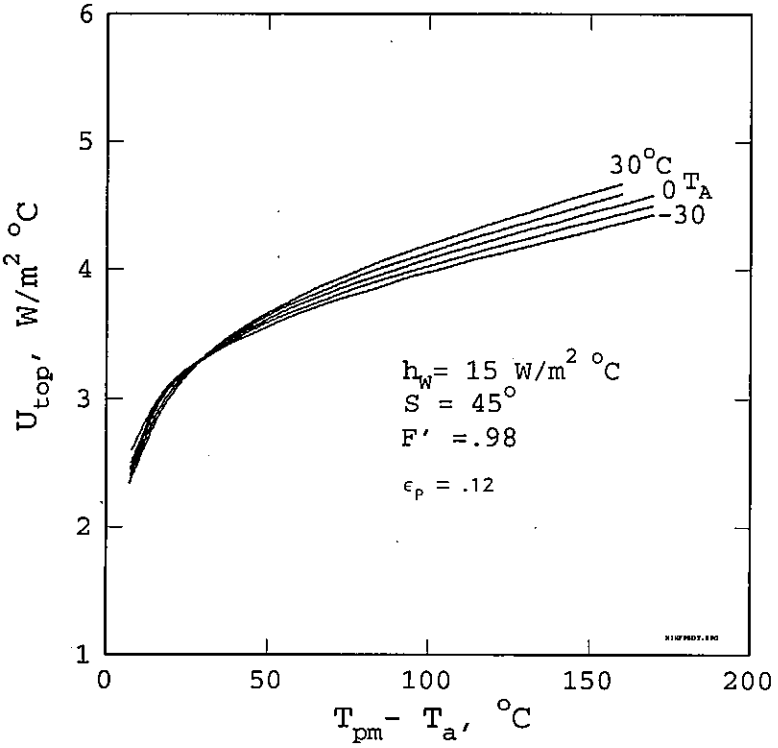

Shewan and Hollands [4] have suggested the use of

$$U_{top} = (Tm)^{b} + c(\Delta T) \tag{7.3}$$

where $Tm = (T_a + T_{fm})/2$.

This has the obvious advantage of having terms intended to represent both the radiative and convective components of the heat loss.

Proctor [1] also improved on equation (7.1) by adding convection and radiation terms explicitly, i.e.

$$U_{top} = a + bV_w + (c + dV_w)(T_{fm} - T_e) + (e + f \cdot T_{fm})\left(\frac{T_{fm}^4 - T_s^4}{T_{fm} - T_e}\right) \tag{7.4}$$

and terms to account for wind speed dependence, "b" and "d", and the variation in emissivity of the absorber plate with temperature, "f".

For the basis of comparison, and assuming that wind speed is fixed and plate emissivity does not vary, then

Figure 40 Values U_{top} plotted versus T_{pm}-T_a, showing a first order curve fit to the data.

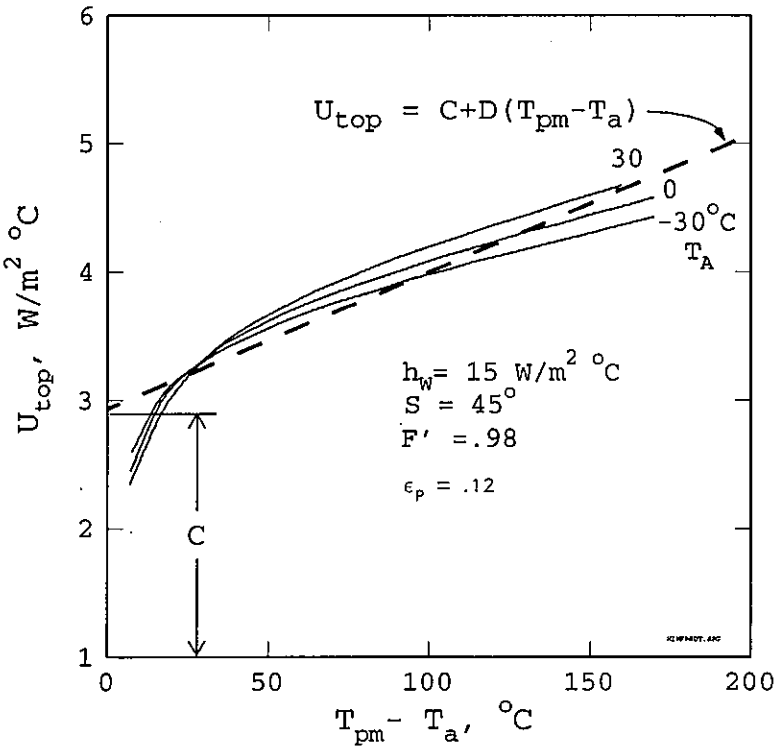

Figure 41 Values of U_{top} plotted versus T_{pm} for a collector with non-selective absorber.

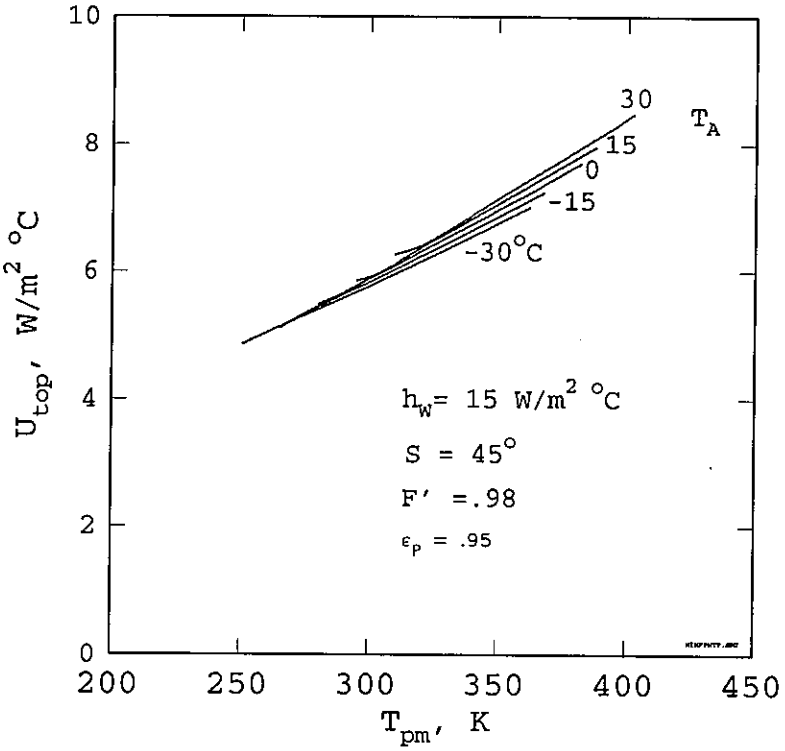

Figure 42 Values of U_{top} plotted versus T_{pm}-T_a for collector with non-selective absorber.

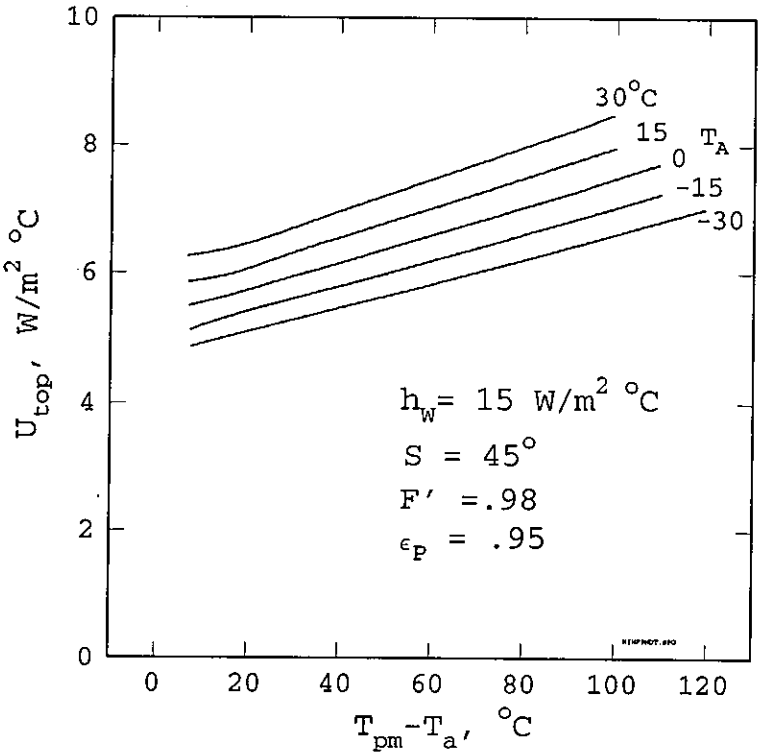

this equation reduces to

$$U_{top} = a + b\,(T_{fm} - T_e) + c\left(\frac{T_{fm}^4 - T_s^4}{T_{fm} - T_e}\right) \tag{7.5}$$

and assuming for glazed solar collectors that T_s can be treated as $T_e \approx T_a$ and noting that

$$(T_{fm}^4 - T_a^4) \cong 4\,(Tm)^3 \cdot (T_{fm} - T_a) \tag{7.6}$$

then equation (7.5) reduces to an equation of the form

$$U_{top} = a + b\,(\Delta T) + c\,(Tm)^3 \tag{7.7}$$

which represents a simplified version of equation (7.4) and should hold for cases were the difference between T_{fm} and T_a is small. A similar expression could be derived based on T_{fi}.

Phillips [5] has also recommended a product equation for the heat loss coefficient that includes both terms for conduction and radiation effects

$$U_{top} = a\,[\,(\Delta T)^b \cdot (T_m)^c] \tag{7.8}$$

Phillips has tested this equation against simulated data representing over 50 collectors of varying types and has been able to obtain good fits to the data.

In addition, an extensive evaluation of characterizing equation has been undertaken [6]. Results show that equations (7.3, 7.7) and (7.8) are significantly better than equation (7.1) at representing the full range of heat loss characteristics shown in Figure 38.

7.3 Collector models for glazed solar collectors

To arrive at a generalized collector model it is worth referring to the original relationship of Hottel and Whillier presented in Chapter 1, equation (1.2)

$$Q_U/A_a = G_T(\tau\alpha)_e - U_L(T_p - T_a) \tag{7.9}$$

It is possible to substitute higher order relationships for the heat-loss coefficient from the absorber plate to the surrounding atmosphere. Based on the results of the analysis of Chapter 3 and section 7.2.1, the relationship of Cooper [1], equation (7.1), appears suitable for collectors with highly selective absorber surfaces, e.g. convection dominated collectors.

$$U_{top} = C + D\,(\Delta T) \tag{7.10}$$

Letting U_L equal U_{top} and introducing the collector efficiency factors and corresponding reference temperatures,

$$Q_U/A_a = F'[G_T(\tau\alpha)_e - A(T_{fm}-T_a) - B(T_{fm}-T_a)^2] \tag{7.11}$$

$$Q_U/A_a = F_R[G_T(\tau\alpha)_e - A(T_{fi}-T_a) - B(T_{fi}-T_a)^2] \tag{7.12}$$

or in terms of efficiency based on T_{fi}, (eqsuations 5.2 and 5.3 of Chapter 5)

$$\eta = \frac{Q_U}{G_T \cdot A_a} = F_R\left((\tau\alpha)_e - C\frac{(T_{fi}-T_a)}{G_T} - D\frac{(T_{fi}-T_a)^2}{G_T}\right) \tag{7.13}$$

or based on T_{fm}

$$\eta = \frac{Q_U}{G_T \cdot A_a} = F'\left((\tau\alpha)_e - C\frac{(T_{fm}-T_a)}{G_T} - D\frac{(T_{fm}-T_a)^2}{G_T}\right) \tag{7.14}$$

These equations are suitable for characterizing both flat plate and evacuated tube collectors with selective absorber coatings, operating at low to moderate temperatures, i.e. $T_{fi} < 100^o$ C. For collectors with non-selective absorbers or for evacuated collectors operating at higher temperatures equations 7.3, 7.7 and 7.8 produce better characterizations of the heat loss characteristics. All these relationships include terms to account for radiation losses which are dependant on a characteristic absolute temperature level.

Depending on whether F_R or F' is used, the corresponding performance equation would be

$$\frac{Q_U}{A_a} = F\left[(\tau\alpha)_e G_T - (T_m)^b(\Delta T) - c(\Delta T)^2\right] \tag{7.15}$$

for equation (7.3), and

$$\frac{Q_U}{A_a} = F\left[(\tau\alpha)_e G_T - a(\Delta T) - b(\Delta T)^2 - c(Tm)^3(\Delta T)\right] \tag{7.16}$$

for equation (7.7), and

$$\frac{Q_U}{A_a} = F\left[(\tau\alpha)_e G_T - a\left((\Delta T)^b \cdot (Tm)^c \right) \right] \qquad (7.17)$$

for equation (7.8) where F is the corresponding value of either F_R or F' depending on whether T_{fi} or T_{fm} was used in determining ΔT and Tm. Tm is equal to $(T_a + T_{fi})/2$ or $(T_a + T_{fm})/2$, respectively.

Equation (7.17) is the form of the performance equation put forward by Phillips [5]. The above equations all still follow the form of the equation referred to as the Hottel-Whillier-Bliss equation except that higher order terms have been substituted for U_L.

7.3.1 Boiling/condensing effects

For flat plate collectors incorporating a boiling/condensing fluid and an integral condenser, an additional term is required to account for the differences in temperature between the absorber plate and the heat transfer fluid circulating through the collector. The heat transfer processes for a boiling/condensing solar collector are discussed in Chapter 5. For a limited range of ambient air temperatures equation (5.15) was proposed, i.e.

$$Q_U/A_a = [A(G_T) - C(T_{fi}-T_a) - D(T_{fi}-T_a)^2 - E] \qquad (7.18)$$

where $E = F_R U_L(\Delta T_{ex}) = F_R(\tau\alpha)_e G^{\#}$.

For a range of ambient air and fluid temperatures, "E" and the value of ΔT_{ex} was shown in Chapter 5 to be a non-linear function of T_{fi}, i.e. $E = e \cdot exp(f \cdot T_{fi})$, leading to (equation 5.17)

$$Q_U/A_a = [A(G_T) - C(T_{fi}-T_a) - D(T_{fi}-T_a)^2 - e \cdot exp(f \cdot T_{fi})] \qquad (7.19)$$

7.3.2 Evacuated tube collectors with heat pipe absorbers

In Chapter 5, evacuated tube collectors with heat pipe absorbers are described. Heat transfer models of this type of collector have been produced but detailed work related to the performance of the heat pipe or two-phase thermo-siphon has been limited. It is generally assumed that the heat transfer rates associated with this type of device are very high and consequently they are assumed to contribute only a small resistance to the heat transfer process.

There is however, every expectation that these devices should exhibit many of the same characteristics as has been described in section 5.3 for the boiling/condensing collector. The significantly reduced amount of working fluid that is used in these devices does allow the use of more expensive fluids as was the case for the Philips' evacuated tube collector. Often refrigerants or alcohols are used in place of water, and consequently the values of ΔT_{ex} may be considerably lower. In addition, the "excess temperature" effects due to the boiling working fluid are further reduced by the low value of the heat loss coefficient normally associated with an evacuated tube collector.

To account for the effects of variations in the heat transfer in the absorber plate, the value of $F_R(\tau\alpha)_e$ has been represented by an equation involving the difference between the collector fluid temperature and the ambient temperature, i.e. $F_R(\tau\alpha)_e = A + B\,(\Delta T)$ which gives (equations 5.5 and 5.6 in Chapter 5)

$$\eta = \frac{Q_U}{G_T \cdot A_a} = F_R\left(A + B\,(T_{fi} - T_a) - C\frac{(T_{fi} - T_a)}{G_T} - D\frac{(T_{fi} - T_a)^2}{G_T}\right) \qquad (7.20)$$

and

$$\eta = \frac{Q_U}{G_T \cdot A_a} = F'\left(A + B\,(T_{fm} - T_a) - C\frac{(T_{fm} - T_a)}{G_T} - D\frac{(T_{fm} - T_a)^2}{G_T}\right) \qquad (7.21)$$

These equations are suitable for evacuated tube collectors with selective absorber coatings, operating over a limited range of ambient air temperatures and at moderate inlet fluid temperatures, i.e. $T_{fi} < 100^o$ C.

7.4 Generalized Characterization Equation for Glazed Solar Collectors

Combining terms described in sections 7.3.1 and 7.3.2 and including incident angle effects, a general performance equation can be defined

$$\eta = K_{\alpha\tau}\,(A + B\,(\Delta T)) - c\frac{(\Delta T)}{G_T} - d\frac{(\Delta T)^2}{G_T} - \frac{e \cdot exp\,(f \cdot T_{fi})}{G_T} \qquad (7.22)$$

It should be noted that not all of these coefficients will apply for all collector types. Coefficient "B" has been shown to represent the case of the vacuum-tube collector with heat-pipe. This term should be very small for other collector types and therefore could be assumed equal to zero. For boiling/condensing collectors the coefficients "e" and "f" should be used to account for the effects of "excess temperature". For most other collector types, the values of "e" and "f" can be assumed equal to zero.

This results in the traditional form of the HWB equation as previously presented and should hold reasonably well for conventional flat-plate solar collectors evaluated over a limited range of environmental conditions. However, in Chapter 3 and section 7.1, the variability of the heat loss coefficient was shown for changing environmental conditions. Three collector types including one dominated by convection heat losses, one dominated by radiation losses, and one exhibiting both radiation and convection heat losses, were discussed.

The variability in U_L due to changing operational and meteorological conditions can in most cases be accounted for by the relationships given by equations 7.3, 7.7 and 7.8. All these relationships include terms to account for radiation losses which are dependant on a characteristic absolute temperature level. For

example if an equation of the same form as equation (7.8) is introduced into equation (7.22) the corresponding performance equation would be

$$\eta = K_{\alpha\tau}(A + B(\Delta T)) - (c\{(\Delta T)^d \cdot (T_m)^e\})\frac{(\Delta T)}{G_T} - \frac{f + g \cdot (T_{fi})}{G_T} \tag{7.23}$$

which includes the relationship for heat loss coefficient put forward by Phillips [5].

Generalized performance equations for a variety of solar collector types have been investigated [6]. Based on that evaluation, equation (7.23) was recommended as being suitable for a wide range of glazed solar collectors operating over a range of conditions. As previously stated, not all terms in equation (7.23) are required in all cases. To aid in the selection of suitable coefficients for the various solar collector types, Table 11 was outlined [6] to provide recommendations for the selection of suitable characterizing equation coefficients.

Alternatively, the full form of the general equation may be used and the selection of coefficients based on the fit results.

7.5 Unglazed Collectors

The performance of unglazed solar collectors has been described in detail in Chapter 4. The performance of unglazed solar collectors was found to be well represented by equation (4.37).

$$\dot{q}_u = (a_1 - a_2 u)G - (b_1 + b_2 u)\Delta T \tag{7.24}$$

for $\Delta T = (T_{fi} - T_a)$. Expressed in terms of collector efficiency

$$\eta = (a_1 - a_2 u) - (b_1 + b_2 u)\frac{(\Delta T)}{G} \tag{7.25}$$

where G is given by equation (4.28)

$$G = G_T + \left(\frac{\varepsilon_p}{\alpha}\right)L \tag{7.26}$$

Table 2 Recommended coefficients for use with various solar collector types [6].

Generalized Performance Equation:

$$\eta=(a+b(\Delta T))-c\{(\Delta T)^{d}\cdot(Tm)^{e}\}(\Delta T/G)-(f\cdot\exp(g\cdot T_{fi}))/G$$

Solar Collector Type	Fit Coefficients						
	a	b	c	d	e	f	g
Conventional, Glazed Flat-Plate, (non-selective)	●		●	●	●		
Conventional, Glazed Flat-Plate, (selective)	●		●	♦			
Conventional Vacuum Tube, (non-selective)	●		●		●		
Conventional Vacuum Tube, (selective)	●		●	●	●		
Boiling/condensing Flat-plate, (non-selective)	●		●	●	●	●	♦[1]
Boiling/condensing Flat-plate, (selective)	●		●	♦		●	♦[1]
Evacuated Tube with Heat-pipe, (non-selective)	●	♦	●	●	●	♦[1]	♦[1]
Evacuated Tube with Heat-pipe, (selective)	●	♦	●		●	♦[1]	♦[1]

Notes: [1] These terms may be set to zero if a limited ambient air temperature range is expected during use.

LEGEND: ● Required coefficients

♦ Recommended coefficients

7.6 Low-concentration Ratio Concentrating Collectors

A performance equation for low-concentration ratio concentrating collectors was described in Chapter 6. This equation represents a variation on the Hottel-Whillier-Bliss model for flat plate collectors, e.g.

$$\eta = F_R K_{\alpha\tau} [(\tau\alpha)\rho\gamma]_{e,n} - F_R \left[\left(\frac{A_r}{A_a} \right) U_L \frac{(T_{fi} - T_a)}{G_b} \right] \tag{7.27}$$

where the determination of $K_{\alpha\tau}$ depends on the tracking characteristics of the collector under consideration as described in Chapter 6.

7.7 Selection of Test Conditions

The selection of suitable conditions for conducting a characterizing test for a particular collector depends to a large degree on the range of environmental conditions anticipated during normal use of the collector and will likely be determined by the location of use and the climatic conditions. In the case of glazed collectors, the range of operating and environmental conditions may be significant. Recommendations for the testing of glazed solar collectors is given in Appendix B.

In the case of unglazed solar collectors, operation at or near the ambient air temperature is typical. Consequently, testing is usually conducted at similar temperature levels. However, as described in Chapter 4, their performance is highly dependent on wind effects and therefore testing is required at range of wind conditions. A test procedure outlining the required test conditions is included as Appendix A, based on the results of the IEA Task III research on unglazed collectors.

7.8 References

1 Proctor, D.: **A Generalized Method For Testing All Classes of Solar Collector-II, Evaluation of Collector Thermal Constants**. Solar Energy, 32, 387 (1984)

2 Cooper, P.I.: **The Testing of Flat Plate Solar Collectors**. The Institution of Engineers' Annual Engineering Conference, Townsville, Australia (1976)

3 Tabor, H.: **Testing of Solar Collectors**. Solar Energy, 20, 293 (1978)

4 Shewen, E.C. and K.G.T. Hollands: **Equations for Representing the Ul Dependence in Collector Test Procedures**. Proceedings of the International Solar Energy Society, World Solar Congress, Atlanta (1979)

5 Phillips, W.F.: **A Simplified Nonlinear Model for Solar Collectors**. Solar Energy, 29, 77 (1982)

6 Harrison, S.J.: **Improved Characterization for the Thermal Performance of Solar Collectors**. Ph.D. Thesis, Department of Mechanical Engineering, Queen's University, Kingston, Canada (1992)

Appendix

A

A Recommended Test Procedure for Determining the Thermal Performance of Unglazed Flat-Plate Liquid-Type Solar Collectors

1.0 Introduction

The purpose of this test procedure is to provide a method by which the thermal performance of an unglazed solar collector can be predicted for a range of operating conditions. A simple parametric equation is assumed to characterize the thermal performance of unglazed collectors, and an experimental means is specified to identify the values of the characteristic parameters for an individual collector module.

The proposed method of test is based on ANSI/ASHRAE Standard 96-1980 [1], and adopts essentially the same terminology and requirements for instrumentation, apparatus and test conditions. Hence the ASHRAE Standard is assumed for testing except where modified or supplemented by the following recommendations.

2.0 Scope

i) Unglazed solar collectors are defined in this test method as collectors without any cover, and capable of absorbing both solar radiation and the enthalpy of the ambient air. Solar collectors of this type are typically used for the heating of swimming pools or to supply a heat pump for domestic heating. The collectors may be insulated or uninsulated at the back and may be free-standing or integrated into roofs, walls or fences, provided that their performance is not significantly influenced by the effects listed in section (1. vi).

It is expected that with little modification the method will also be valid for compact forms of unglazed solar collector such as energy stacks or energy pillars.

ii) The test methods are applicable to single collector modules, and also to collector arrays of area up to 10 m^2 with a minimum length of connecting piping.

ii) The heat-transfer fluid may be any liquid, including water or a water-antifreeze mixture.

iv) The procedure provides for indoor or outdoor testing.

v) The procedure measures and predicts the effects on the thermal performance of:

- the absorption of shortwave solar radiation;
- the exchange of longwave radiation with the collector environment;
- wind-induced convective heat losses;
- conduction losses through thermal insulation.

vi) The procedure does *not* measure or predict the effects on the thermal performance of:

- the condensation or evaporation of ambient water vapour on the collector (which occurs when $T_{pm} < T_d$);
- heat losses by natural convection (which may be a significant part of the convective losses when the air speed over the collector is less than about 0.3 m/s);
- the collector heat capacity.

2.1 Nomenclature

The nomenclature follows the LIST OF SYMBOLS on page xi of this report.

3.0 Thermal-performance Model

3.1 Characteristic equation

The stationary thermal performance of the unglazed collectors that are included within the scope of this procedure is represented to a good degree of accuracy by a modified Hottel-Whillier-Bliss equation of the form:

$$\dot{q}_u = F_R [(\alpha G_T + \varepsilon_p L) - U_L (T_{fi} - T_a)] \quad (1)$$

where

$\dot{q}_u$ = useful output power per unit reference area, (W/m^2),
F_R = collector heat removal factor, (dimensionless),
α = absorptance of the absorber plate, (dimensionless),
G_T = rate of incident solar radiation on the solar collector per unit area, (W/m^2),
ε_p = thermal emittance of the absorber plate, (dimensionless),
L = longwave sky irradiance in the collector plane, (W/m^2),
U_L = overall heat loss coefficient for the collector, ($W/(m^2 \cdot K)$),
T_{fi} = inlet temperature of the fluid, (^oC)
T_a = ambient air temperature, (^oC).

This relationship differs from that of a glazed flat-plate solar collector in that the longwave sky irradiance is explicitly included in equation 1. The overall heat loss coefficient includes the longwave radiative heat transfer coefficient between the ambient and the collector plate, the wind induced heat transfer coefficient and the conduction losses through the back of the collector, (which may be insulated). The heat loss coefficient is dependent on the wind conditions, which in turn affects the value of F_R. The collector heat removal factor, F_R, is also dependant on fluid flow through the collector.

During testing the value of $\dot{q}_u$ is measured during testing according to

$$\dot{q}_u = \dot{m}C_p (T_{fe} - T_{fi})/A_{ab} \quad (2)$$

where

$\dot{m}$ = mass flowrate, (kg/s)
C_p = specific heat capacity of heat transfer fluid, (J/(Kg • K))
T_{fe} = exit temperature of the fluid, (^oC)
T_{fi} = inlet temperature of the fluid, (^oC)
A_{ab} = absorber plate surface area, (m^2)

3.2 Characteristic parameters

Rearranging equation (1) gives

$$\dot{q}_u = (F_R\alpha)[G_T + (\varepsilon_p/\alpha)L] - (F_RU_L)(T_{fi} - T_a) \quad (3)$$

in which the composite parameters $(F_R\alpha)$, (ε_p/α), and (F_RU_L) can be regarded as characteristic of any particular collector. The parameters $(F_R\alpha)$ and (F_RU_L) can be assumed to be linear functions of windspeed, such that

$$(F_R\alpha) = a_1 - a_2 u \quad (4)$$

and

$$(F_RU_L) = b_1 + b_2 u \quad (5)$$

where a_1, a_2, b_1, and b_2 are constants to be determined from experimentally measured calorimetric data.

The parameter (ε_p/α) is to be estimated independently, by separate measurements of the thermal emittance ε_p and solar absorptance α of the collector absorber. Since unglazed collectors are not normally given selective coatings, (ε_p/α) will in most cases have the approximate value 0.95 typical of non-selective absorbers. The values may be determined by standard photospectrometry procedures or estimated from the experimental results using a non-linear fit procedure.

The value of L is defined as

$$L = \sigma (T_s^4 - T_a^4) \quad (6)$$

where σ is the Stefan-Boltzman constant and T_s is the effective sky temperature.

In cases where high average windspeeds are encountered (u >> 3 m/s), it may be necessary to add a quadratic term to the right-hand side of equation (5), i.e.

$$(F_RU_L) = b_1 + b_2u + b_3 u^2 \quad (7)$$

in which case b_3 would also be determined from the experimental test data.

Equations 4 and 5 are recommended for the determination of collector system parameters and for predicting the energy output of unglazed solar collectors.

4.0 Instrumentation and measurement

Temperatures: temperatures (or temperature differences) should be measured with an accuracy of 0.1 °C using an instrument with a time constant not exceeding 10 s.

Flowrate of the heat-transfer fluid: the volumetric or mass flowrate of the heat-transfer fluid should be measured using a flow meter of accuracy 1% and a time constant not exceeding 60 s.

Air speed: the air speed over the collector should be measured in the free-stream region just above the boundary layer, parallel to plane of the collector absorber and in the direction of flow of the air. The instrument should have an accuracy of 0.3 m/s and a time constant not exceeding 10 s. A suitable measurement can be made using a cup anemometer fitted with a vane.

Solar irradiance: solar irradiance should be measured using a pyranometer of accuracy 10 W/m^2 and time constant not exceeding 10 s (WMO Class 1).

Thermal irradiance: Thermal irradiance should be measured to an accuracy better than 10 W/m^2 and with an instrument with a time constant not exceeding 60 s.

Outdoors, thermal irradiance can be measured directly using a pyrgeometer or can be determined by subtracting the simultaneous readings of a pyrradiometer and a pyranometer. To ensure accurate measurements it is recommended that the pyrgeometer be artificially ventilated and its body temperature measured directly.

If testing indoors under artificial conditions, it may be necessary to make measurements with a pyrradiometer and a pyranometer, as a pyrgeometer may not have sufficient sensitivity to measure the levels of net thermal irradiance experienced in a solar simulator.

Thermal emittance and solar absorptance: standard photometric methods exist to measure these optical parameters, but simple laboratory measurements are likely to be adequate.Thermal emittance can be measured using a portable emissometer such as that described by Dorman [2]. The solar absorptance of an opaque surface can be deduced from measurement of its solar reflectance ρ using real or simulated solar radiation and a pyranometer to measure the incident and reflected irradiance. The pyranometer should be sufficiently small and far from the surface that it causes negligible shading, but sufficiently close that the surface completely fills its field of view. The solar absorptance is then given by $1-\rho$.

5.0 Test conditions

5.1 Collector mounting

In normal operation, unglazed collectors may be mounted on a free-standing framework, with substantial clearance between the back of the collector and other surfaces, or they may be either incorporated into or fixed in direct contact with a surface such as a wall or roof, which thus provides an insulating backing for the collector.

Since the back losses strongly depend on the type of mounting, the collector should be mounted for testing in manner similar to that intended for normal operation. The test results should not be used to predict the performance of the collector in a significantly different mounting arrangement.

Unglazed collectors may also be operated with a number of different slopes, β:

- horizontally, as on a flat roof ($\beta = 0°$);
- tilted, as on a sloping roof ($30° < \beta < 60°$); or
- vertically, as on a wall ($\beta = 90°$).

In these cases the meteorological variables should be measured in plane of the collector.

5.2 Heat-capacity flowrate

As the heat removal factor F_R depends on the heat capacity flowrate, $\dot{m}C_p$, of the heat transfer fluid, the value of $\dot{m}C_p$ should be controlled to within 10% of the average value for all test points. If more than one collector module is tested at a time, the variation in flowrate between separate collector modules should be less that 10% of the average value for the total array.

5.3 Operating temperatures

No temperature dependence of the overall heat-loss coefficient, U_L, is assumed in the thermal performance model. To ensure the validity of this model, the fluid inlet temperature, T_{fi}, should not differ from the collector ambient temperature T_a by more than 20 ° C during the test, i.e.

$$|T_{fi} - T_a| \leq 20\ °C \tag{8}$$

The mean of the fluid inlet temperature and the ambient temperature should be restricted to

$$278\ K \leq [(T_{fi} + T_a)/2] \leq 308\ K \tag{9}$$

and to avoid condensation on the collector surface, the inlet temperature should be held to a value 0.5 K above the dew point temperature of the ambient air i.e.

$$T_{fi} \geq T_d + 0.5\ K \tag{10}$$

To ensure that $F_R U_L$ can be determined accurately, $|T_{fi} - T_a|$ should be maintained at a value > 2 K.

5.4 Meteorological variables

A variation of input variables is a required to ensure the reliable estimation of the collector parameters.

Outdoor testing: Continuous measurements taken over a two or three day period is usually suitable to provide an adequate data base. The stochastic fluctuations of the meteorology and the daily variation of solar irradiance, ambient temperature and wind speed provide a sufficient variation of the input variables. To avoid systematic errors, the inlet temperature of the fluid may be varied in an uncorrelated way with the meteorological input variables. At least 20 independent sets of data should be used for analysis.

Indoor testing: A minimum number of ten data points should taken for a range of wind speeds and inlet fluid temperatures covering the full range of operation of the collector. The wind dependence of the system parameters should be studied for at least three different values of wind speed (e.g. 1 m/s, 2 m/s and 5 m/s). Measurements conducted above as well as below the ambient temperature are preferable and the ambient temperature should be held constant such that (283 K < T_a < 293 K). At test facilities where a significant variation in solar irradiance is possible, a number of different values of G_T may be used. However, this is not required provided there is a sufficient variability in the variables (T_{fi} -T_a) and u.

Outdoor testing is characterized by a highly turbulent free-stream wind region. Test data taken at different flow conditions generally improves the reliability of the test results. Indoor testing of uncovered solar collectors requires a test facility that is designed to match the natural wind field. Preliminary experiments show that a free stream region that covers the total collector area and a turbulence intensity that exceeds 20% is required.

5.5 Collector Dynamics

The test method measures the energy output of uncovered solar collectors averaged over a time period Δt. Both outdoor and indoor testing are allowed. Consequently, arbitrary time varying meteorological conditions are to be expected over a time period Δt.

The model outlined in this test method is a zero-capacitance model and consequently does not explicitly take into account collector dynamics [2]. To limit error, the energy stored in the collector system during the time period Δt should be small compared to the measured value of the energy output of the collector under test, i.e.

$$|\Delta Q| / (\dot{q}_u \cdot A_{ab} \cdot \Delta t) < 3\% \tag{11}$$

where

$$|\Delta Q| = (C_p + C_f) \left| \left(\frac{T_{fi}(t) + T_{fe}(t)}{2} - \frac{T_{fi}(0) + T_{fe}(0)}{2} \right) \right| \tag{12}$$

and C_p and C_f are the specific heat capacity of heat transfer fluid and absorber, respectively. $|\Delta Q|$ is an approximation of the energy stored in the collector system during the time interval Δt. Data averaged over a one-hour period (Δt > 1 hr) is usually sufficient to limit the error sufficiently.

6.0 Analysis of test data

For each data point values should be determined for the three variables:

$$\dot{q}_u = \dot{m} C_p (T_{fe} - T_{fi}) / A_{ab} \tag{13}$$

$$G = G_T + (\varepsilon_p / \alpha) L \tag{14}$$

$$\Delta T = (T_{fi} - T_a) \tag{15}$$

With the set of independent values of $\dot{q}_u$, G, and ΔT and the corresponding values of u, the parameters a_1, a_2, b_1 and b_2 are obtained by standard least-squares fit to the multi-linear equation,

$$\dot{q}_u = (a_1 - a_2 u)\, G - (b_1 + b_2 u)\, \Delta T \tag{16}$$

7.0 Representation of the Test Results

A listing of the test data is required. The test data is to be supplemented by a detailed description of the tested collector system including photographs and construction drawings.

The results of the fitting process shall be represented as

$$F_R \alpha = (a_1 \pm \Delta a_1) - (a_2 \pm \Delta a_2)\, u \tag{17}$$

$$F_R U_L = (b_1 \pm \Delta b_1) + (b_2 \pm \Delta b_2)\, u \tag{18}$$

$$(\varepsilon_p/\alpha) = (\varepsilon_p/\alpha) \pm \Delta(\varepsilon_p/\alpha) \tag{19}$$

where Δa_1, Δa_2, Δb_1, Δb_2, and $\Delta(\varepsilon_p/\alpha)$ are the uncertainties resulting from the regression analysis and the method used to determine (ε_p/α), respectively. In addition, plots of $F_R\alpha$ and $F_R U_L$ versus wind speed "u" may be drawn, e.g. Figure A1.

7.1 Collector Efficiency Curve

Following the definition of the collector efficiency of covered solar collectors, a collector efficiency for uncovered collectors is defined for $\Delta T = (T_{fi} - T_a)$ as

$$\eta = (a_1 - a_2 u) - (b_1 + b_2 u)\, \frac{(\Delta T)}{G} \tag{20}$$

A typical plot of η versus $\Delta T/G$ for a range of wind velocities is shown in Figure A2. Performance data for an unglazed solar collector has been presented in reference [3].

8.0 References

1 **ANSI/ASHRAE Standard 96-1980**, Methods of testing to determine the thermal performance of unglazed flat-plate liquid-type, solar collectors, The American Society of Heating, Refrigerating and Air-Conditioning Engineers, Inc., 1791 Tullie Circle, NE, Atlanta, GA 30329

2 Dorman, G. J., **Determination of the Radiative Properties of Surfaces using Reflectance Techniques**, Joint Research Centre, Ispra, CEC Report EUR 952 EN (1984)

3 Soltau, H.: **The thermal performance of uncovered collectors**, ISES Congress, Hamburg, Pergamon Press (1987)

Figure A1 Typical plots of the variation of $F_R\alpha$ and F_RU_L with wind speed "u".

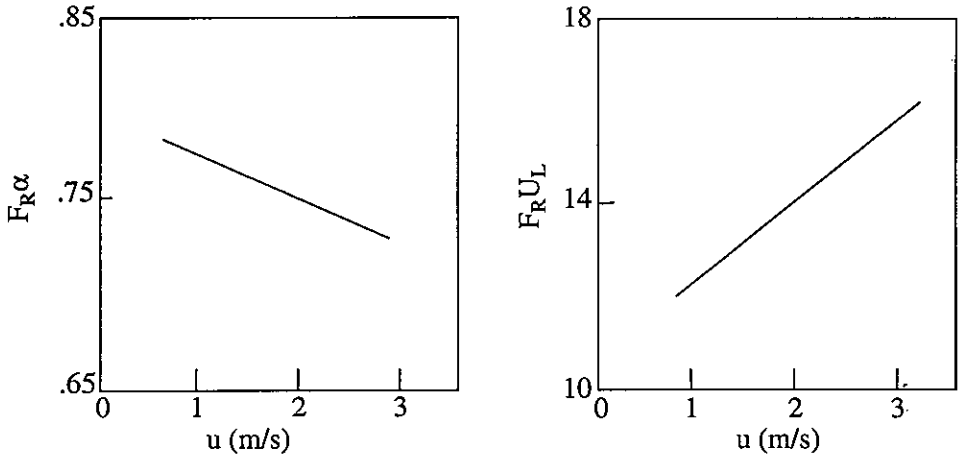

Figure A2 Typical plot of thermal efficiency, η, for an unglazed solar collector

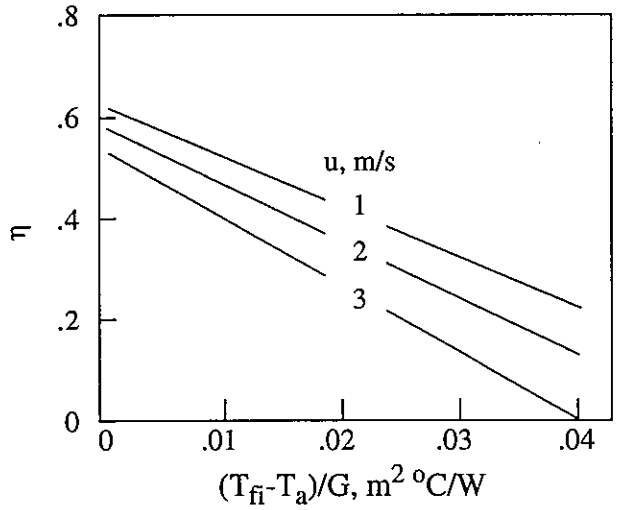

Appendix

B

Recommendations for the Testing of Glazed Solar Collectors

1.0 Introduction

If a simple parametric equation is assumed to characterize the thermal performance of a range of collector types, an experimental means must be specified to identify the values of the characteristic parameters for the specific collector module evaluated. The selection of a suitable performance characteristic for a particular solar collector type must be a compromise between testing complexity, time, and cost relative to the accuracy required.

2.0 Generalized Characterization Equation for Glazed Solar Collectors

As discussed in Chapters 5 and 7, a general performance equation (eq. 7.22) can be defined for a variety of collector types operating over a limited temperature range, i.e.

$$\eta = K_{\alpha\tau}(A + B(\Delta T)) - c\frac{(\Delta T)}{G_T} - d\frac{(\Delta T)^2}{G_T} - \frac{e \cdot exp(f \cdot T_{fi})}{G_T} \qquad (2)$$

However, in Chapters 3 and 7, the variability of the heat loss coefficient was shown for changing environmental conditions. The variability in U_L due to changing operational and meteorological conditions can in

most cases be accounted for by equations 7.23 [1].

$$\eta = K_{\alpha\tau}(A + B(\Delta T)) - (c\{(\Delta T)^d \cdot (T_m)^e\})\frac{(\Delta T)}{G_T} - \frac{f + g \cdot (T_{fi})}{G_T} \qquad (2)$$

which includes the relationship for heat loss coefficient put forward by Phillips [2].

It has been noted that not all of these coefficients will apply for all collector types. Coefficient "B" has been shown to represent the case of the vacuum-tube collector with heat-pipe. This term should be very small for other collector types and therefore could be assumed equal to zero. For boiling/condensing collectors the coefficients "e" and "f" should be used to account for the effects of "excess temperature". For most other collector types, the values of "e" and "f" can be assumed equal to zero. This results in the traditional form of the HWB equation as previously presented and should hold reasonably well for conventional flat-plate solar collectors evaluated over a limited range of environmental conditions.

3.0 Test conditions

Solar collectors to be characterized should be tested according to the experimental methods and general procedures outlined in ASHRAE Standard 93-1986 [3].

3.1 Minimum Test Conditions

As a minimum, for applicability over a limited range of ambient and fluid temperatures, the following testing sequences are recommended:

For *conventional flat-plate and evacuated-tubular collectors* that do not contain a phase-change (boiling or evaporating) heat-transfer fluid, testing should be conducted at one irradiance level under steady-state operating conditions and at a minimum of four inlet fluid temperatures spanning from ambient temperature to the maximum operational temperature expected for the collector during normal operation.

For *solar collectors with integral-condenser heat exchangers and which contain an internal fluid that changes phase*, testing should be conducted at a minimum of two irradiance levels under steady-state conditions. If the operation of the collector is intermittent (as with some boiling/condensing collectors) sufficient data will be taken and averaged over each test period at the test condition so that a representative average performance may be calculated. Values of irradiance level recommended for testing are 400 W/m^2 and 900 W/m^2. At the higher irradiance levels, testing will be conducted at a minimum of four inlet fluid temperature levels between ambient and the maximum anticipated operational temperature occurring during normal use.

3.2 Recommended test conditions

If operation is anticipated over a significant range of environmental conditions, then the collector is most likely subject to non-linear heat loss characteristics that will require the use of a charactiazation equation similar to that given by equation 2 (eq. 7.23, Chapter 7). The choice of testing conditions will be subject to

the type of solar collector under test, the anticipated range of operation and the choice of characterizing coefficients used to describe the collector's performance.

To aid in the selection of suitable coefficients for the various solar collector types, Table 2 (Chapter 7) was outlined. Alternatively, the full form of the general equation may be used and the selection of coefficients based on regression results. In effect the standard error of the coefficients may be used to determine if a variable is significant for the collector tested. If the absolute value of a coefficient is significantly larger than its standard error, then the coefficient contributes in a productive manner to the regression equation. If the standard error of the coefficient is large then it should be removed from the regression equation and the regression re-run. The selection of coefficients will however depend on the expected range of application of the characterizing equation.

In effect, the characterizing equation may be seen to be fitted over a region of space representative of the operational conditions experienced. In general this will include three variables of significance, i.e. T_{fi}, T_a, and G_T. The range of all three of these variables will influence the applicability of the proposed characterizing equation. An example would be the case of the boiling/condensing collector operating in a warm climate with very little seasonal variation in the ambient temperature conditions. In this case, the "g" term in the general characterizing equation related to the variation of the threshold irradiance may be set to zero, reducing the number of terms in the characterizing equation and the associated testing requirements.

The use of non-linear terms requires care if the results are to be extrapolated beyond the original test conditions. The fitting of non-linear regression models is an area of considerable study. One concept is to use a test sequence that ensures that a suitable range of test conditions are covered during testing. In effect the concepts of "experimental design" may be applied to the problem. One solution to the test sequence is that of a "face-centered central composite design" for three variables [4, 5] where test data is taken at the mid and extreme operational points as shown schematically in Figure B1. In this way, extrapolation of the test data is avoided.

Highly non-linear models may require even greater numbers of test points within the test "space". As previously mentioned, if one of the variables, e.g. T_a, is held constant then the experimental design may be reduced to a problem involving the fitting of a "response-surface" [5] over the range of application of the two remaining variables. In such a case, adequate results can be achieved if testing at more than one irradiance level is used in addition to a range of T_{fi},. In particular, this holds for boiling/condensing collectors and evacuated tube collectors with heat pipes.

4.0 References

1 Harrison, S.J.: **Improved Characterization for the Thermal Performance of Solar Collectors.** Ph.D. Thesis, Department of Mechanical Engineering, Queen's University, Kingston, Canada (1992)

2 Phillips, W.F.: A Simplified Nonlinear Model for Solar Collectors. **Solar Energy, Vol. 29,** 77 (1982)

3 **ANSI/ASHRAE Standard 93-1986,** Methods of testing to determine the thermal performance of solar collectors, The American Society of Heating, Refrigerating and Air-Conditioning Engineers, Inc., 1791 Tullie Circle, NE, Atlanta, GA 30329 (1986)

4 Montgomery, D.C.: **Design and Analysis of Experiments, 3rd edition.** John Wiley & Sons (1991)

5 Mason, R.L., Gunst, R.F., Hess, J.L.: **Statistical Design and Analysis of Experiments with Applications to Engineering and Science.** John Wiley & Sons (1989)

Figure B1 Diagram of "face-centered central composite design" showing possible test conditions for obtaining test data. Circles correspond to test points.